La Metallurgia Italiana
International Journal of the Italian Association for Metallurgy

n. 03 marzo 2022
Organo ufficiale
dell'Associazione Italiana
di Metallurgia.
Rivista fondata nel 1909

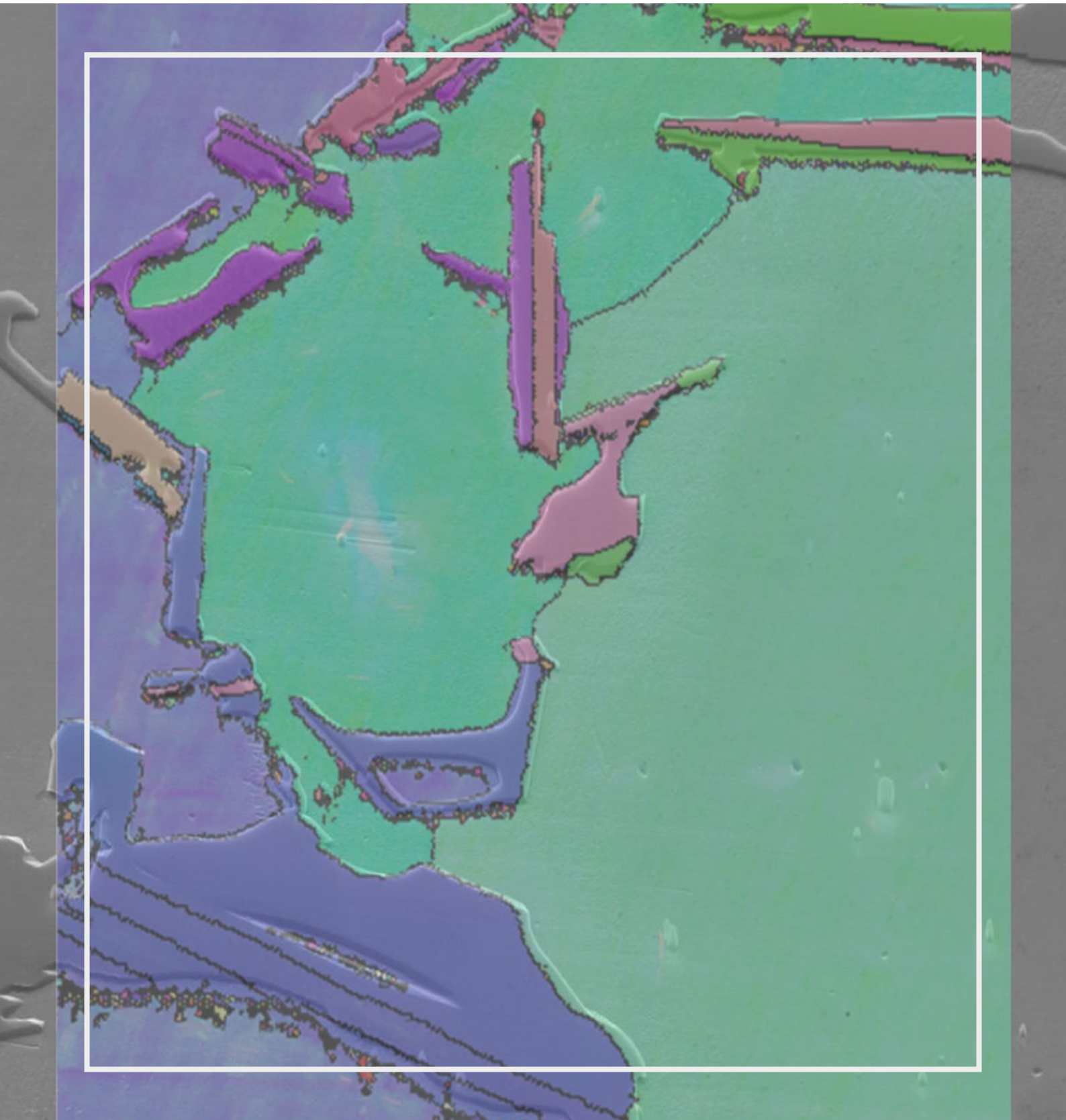

La Metallurgia Italiana

International Journal of the Italian Association for Metallurgy

Organo ufficiale dell'Associazione Italiana di Metallurgia.
House organ of AIM Italian Association for Metallurgy.
Rivista fondata nel 1909

Direzione e redazione/*Editorial and executive office:*
AIM - Via F. Turati 8 - 20121 Milano
tel. 02 76 02 11 32 - fax 02 76 02 05 51
met@aimnet.it - www.aimnet.it

Immagine in copertina: credit a Giulio Timelli

Gestione editoriale e pubblicità
Publisher and marketing office:
siderweb spa
Via Don Milani, 5 - 25020 Flero (BS)
tel. 030 25 400 06 - fax 030 25 400 41
commerciale@siderweb.com - www.siderweb.com

Reg. Trib. Milano n. 499 del 18/9/1948.
Sped. in abb. Post. - D.L.353/2003 (conv. L. 27/02/2004 n. 46) art. 1, comma 1, DCB UD

siderweb spa è iscritta al Roc con il num. 26116

n.03 marzo 2022
Anno 113 - ISSN 0026-0843

indice

Editoriale / Editorial
Editoriale
A cura di Giulio Timelli..... pag.04

Memorie scientifiche / *Scientific papers*
Metalli Leggeri / Light Metals

Formation and distribution of oxide-related defects in gravity AlSi7Cu0.5Mg alloy castings
G. Scampone, G. Timelli, R. Pirovano, S. Mascetti..... pag.07

An investigation on effect of rotary degassing-ultrasonic method on high pressure die casting products
R. Haghayeghi..... pag.13

Development of a model for the prediction of mechanical properties for Al-Si-Mg castings
C. Ransenigo, M. Tocci, A. Pola, C. Viscardi, M. Serafini..... pag.18

Simulation in support of the development of innovative and unconventional lightweight casting processes
R. Pirovano..... pag.24

Development of a new process to recover aluminium from thin complex aluminium scrap to employ for primary aluminium alloys
I.Vicario, J. Antoñanzas Gonzalez, L. Yurramendi Sarasola, J.C. Múgica Iraola, A. Abuin Ariceta..... pag.29

Eco-sustainable lightweight automotive part manufacturing: GHGs-free die casting of brake leverage prototype made of AZ91D-1.5CaO magnesium alloy
F. D'Errico, A. Gruttadauria, G. Perricone, D. Casari, M. Romeo..... pag.36

Evaluation of the use of foundry sand cores on solidification and on the characteristics of structural castings: a comparison between organic and inorganic cores and validation with simulation
A. Mantelli..... pag.42

Attualità industriale / Industry news

Design and analysis of various cooling conditions of an aluminum wheel mold
edited: by O. Özaydin, Y. Çatal, A.Y. Kaya..... pag.56

The new biocide regulation - their impact and innovative sustainable solutions for casting lubricants
edited by: U. Schmidt-Freytag, A. Kelly..... pag.61

Applications of automotive lean production tools on casting industry
edited by: Ü. Ayyildiz..... pag.65

Suction system from the self-induced mold cavity (Venturi)
F. Tonolli..... pag.73

Atti e notizie / AIM news

Eventi AIM / AIM events..... pag.80
Comitati tecnici / Study groups..... pag.82
Normativa / Standards..... pag.86

"la fonderia high tech delle leghe leggere rimane viva e in continua evoluzione, essenziale nello sviluppo industriale del paese"

F. Bonollo, G. Timelli

"the high-tech light alloy foundry remains alive and well, and is essential to the country's industrial development"

F. Bonollo, G. Timelli

Prof. Franco Bonollo
Università degli studi di Padova

Prof. Giulio Timelli
Università di Padova - DTG, Vicenza

LA FONDERIA HIGH TECH DELLE LEGHE LEGGERE

I lavori che vengono pubblicati in questo numero rappresentano una selezione di memorie presentate alla 7a edizione del Convegno Internazionale High Tech Die Casting 2021, che si è tenuta in modalità virtuale dal 22 al 25 giugno 2021. Il successo del Convegno che ha visto un'ampia partecipazione sia del mondo industriale che del mondo accademico sta a dimostrare che le tematiche relative alla fonderia delle leghe leggere sono di grande attualità. La sfida per la fonderia delle leghe leggere è stata, e così sarà nel prossimo futuro, il raggiungimento di un miglioramento continuo in termini di qualità del prodotto ed efficienza del processo; in definitiva, abbandonare gli approcci più convenzionali per raggiungere metodologie di processo "high tech". High Tech Die Casting significa quindi:

- Leghe con composizioni chimiche ottimizzate;
- Impianti di colata volti a massimizzare i vantaggi del processo stesso;
- Ampio uso di modelli di simulazione numerica e di me-

HIGH-TECH LIGHT ALLOY FOUNDRY

The papers published in this issue represent a selection of the papers presented at the 7th International High Tech Die Casting 2021 Conference, which was held in virtual mode from 22 to 25 June 2021. The success of the conference, which was well attended by both industry and the scientific community, shows that the issues surrounding light alloy foundry are highly topical. The challenge for light alloy foundry has been, and will be for the foreseeable future, to achieve continuous improvement in terms of product quality and process efficiency; in short, to move away from more conventional approaches towards "high tech" process methods. High Tech Die Casting therefore means:

- Alloys with optimised chemical compositions;
- Casting equipment designed to maximise the benefits of the process itself;
- Extensive use of numerical simulation models and virtual methods;
- Optimisation of the work cycle;

todi virtuali;
- Ottimizzazione del ciclo di lavoro;
- Processi innovativi.

Nuovi scenari, legati alla transizione energetica, alla sostenibilità e all'economia circolare, e nuove sfide, quindi, si stanno affacciando al mondo della fonderia delle leghe leggere. Solo un approccio trasversale e interdisciplinare permetterà alle fonderie high tech di interpretare ed elaborare quantità crescenti di informazioni e di individuare, proporre, validare soluzioni sostenibili e affidabili.

Questo è quanto traspare anche dalla selezione di memorie raccolte in questo numero dove da tematiche inerenti ai sistemi innovativi per il trattamento del metallo liquido si è guidati verso nuovi modelli e strumenti di simulazione numerica per la previsione dell'integrità dei getti; dai metodi di lean economy nel comparto fonderia all'utilizzo di materiali e leghe leggere eco-sostenibili.

Diverse, inoltre, le memorie con impatto in ambito industriale. Dai recenti lubro-distaccanti biocompatibili utilizzabili nella fonderia di pressocolata all'ottimizzazione del processo di termoregolazione/raffreddamento degli stampi fino alle recenti tecnologie di tranciatura dei getti pressocolati.

Nonostante le recenti flessioni del mercato, la fonderia high tech delle leghe leggere rimane viva e in continua evoluzione, essenziale nello sviluppo industriale del paese.

- Innovative processes.

New scenarios, linked to the energy transition, sustainability and circular economy, and new challenges, therefore, are facing the world of light alloy foundry. Only a transversal and interdisciplinary approach will enable high-tech foundries to interpret and process increasing amounts of information and to identify, propose and validate sustainable and reliable solutions.

This is also reflected in the selection of articles collected in this issue, where the topics include innovative systems for the treatment of liquid metal, new models and numerical simulation tools for predicting the integrity of castings, lean economy methods in the foundry sector and the use of eco-sustainable materials and light alloys.

There are also a number of memoirs with an impact on industry. From the recent biocompatible lubricants that can be used in the diecasting foundry to the optimisation of the thermoregulation/cooling process of moulds and the recent technologies for stamping diecast parts.

Despite recent market downturns, the high-tech light alloy foundry remains alive and well, and is essential to the country's industrial development.

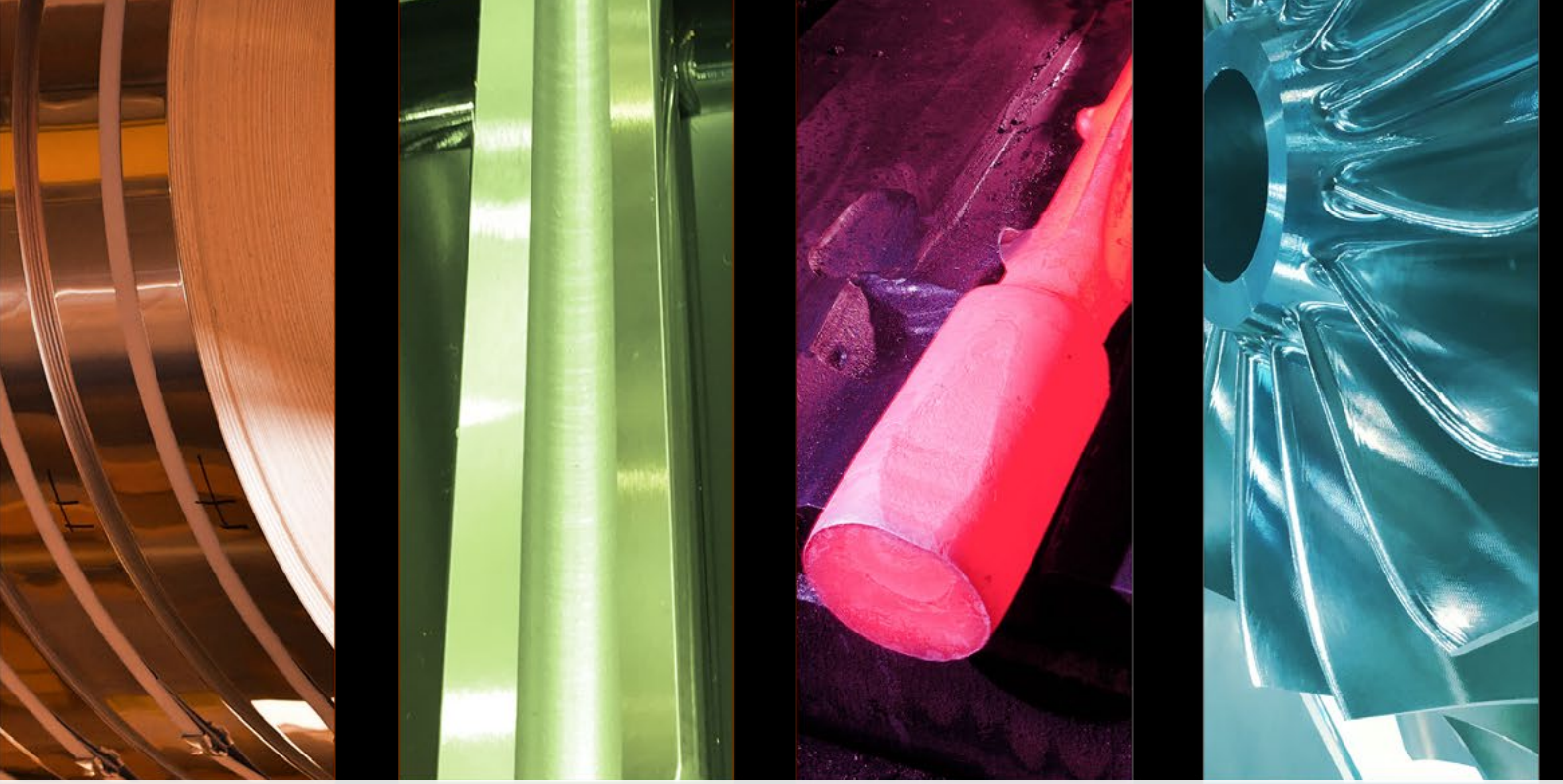

ESSC &DUPLEX

Bardolino · Verona · Italy, 15-17 June 2022

AIM is glad to announce the **11th European Stainless Steel Conference Science & Market** and the **7th European Duplex Stainless Steel Conference & Exhibition**, that will be jointly organized, as a single event in Bardolino (Verona) on 15th-17th June 2022.

The Conference will focus on all the aspects of development, production technology (hot and cold rolling, heat treatment, etc.), welding, corrosion and applications of stainless steels and duplex stainless steels and it addresses delegates with both academic and industrial backgrounds.

The results shall contribute to the advancement of existing and potential applications and will help to guide future development.

The event will bring together developers, designers, manufacturers and users of stainless steel from industry and academia and will compare the present and future needs to satisfy these demands now or in the future.

Short and medium term perspectives of European stainless steel flat, long products, forgings and castings will be widely discussed during the Stainless Steel Market Outlook session.

It is expected the presence of speakers representing the most important European stainless steel associations and reports coming from the big stainless steel companies.

Organized by

ASSOCIAZIONE ITALIANA DI METALLURGIA

In cooperation with

siderweb
THE ITALIAN STEEL COMMUNITY

Sponsored by

Arvedi

www.aimnet.it/essc.htm

La Metallurgia Italiana
International Journal of the Italian Association for Metallurgy

Formation and distribution of entrainment defects in gravity AlSi7Cu0.5Mg alloy castings

G. Scampone, G. Timelli, R. Pirovano, S. Mascetti

In this study, the formation of entrainment defects in gravity permanent mould casting process was experimentally and numerically investigated. The distribution of oxide inclusions was mapped at the microscopic scale using metallographic and image analysis techniques. A fluid-dynamic simulation commercial software was used to predict the formation of defects and air entrapment during the casting process. The results showed that the typical casting defects detected throughout the castings were generated by the entrainment of bifilms. Moreover, the good agreement between the numerical results and the experimental findings proved that the numerical models had successfully predicted the entrainment phenomena, especially the formation of oxide inclusions and the entrapment of air bubbles.

KEYWORDS: ALUMINIUM ALLOYS, ENTRAINED AIR, BIFILM, MICROSTRUCTURE, NUMERICAL SIMULATION;

INTRODUCTION

The careful control of the casting process plays a key role in the final properties of aluminium (Al) alloy castings. The appropriately monitoring of the molten metal preparation, the pouring and the filling stages allow to produce high-performance components [1,2]. During these steps, due to the action of turbulence, the metal oxide surface can be easily entrained inside the liquid metal, resulting in filling defects called bifilms. These defects promote the formation of several solidification defects, such as gas and shrinkage porosity and hot tearing, which drastically decrease the performances of casting [2]. The use of numerical process simulation able to predict the damage caused by oxide inclusions can lead to the rapid optimisation of the process parameters and casting design, and to improve the final quality of the component.

In many papers from the literature, the characterization of oxide inclusions on the fracture surface and their impact on the mechanical properties have been investigated [3,4]. Other studies have correlated the numerical results of commercial simulation software with the experimental data related to the formation of macro-porosity

Giulia Scampone, Giulio Timelli
University of Padova, DTG, Italy

Raul Pirovano, Stefano Mascetti
XC Engineering Srl, Italy

[5]. However, to the best of the authors' knowledge, few works have been conducted to map the experimental distribution of entrainment defects at the microscopic scale and evaluate the severity of damage due to air and surface entrainment. This work aimed to compensate for this gap in the literature by studying the experimental and numerical distribution of oxide inclusions.

EXPERIMENTAL PROCEDURE

A primary AlSi7Cu0.5Mg cast alloy (EN AC-45500) was manually poured into a pre-heated permanent steel mould at 330 ± 3 °C. The pouring time and the molten metal temperature were 3 s and 735 ± 3 °C, respectively. The die, shown in Figure 1, was made of AISI H11 tool steel and it allowed the casting of flat tensile test specimens with a rectangular cross-section of 10 x 6 mm^2. A 30-minute argon degassing treatment was conducted to improve the quality of molten metal and remove impurities and old oxides. Before each casting, the bath was manually skimmed with a coated paddle. No filtering operations, chemical eutectic modification or grain refinement were performed. During the experimental procedure, a batch of 6 castings was produced and 3 samples were separately poured for chemical composition analysis. Table 1 reports the average chemical composition of the alloy, measured by optical emission spectroscopy.

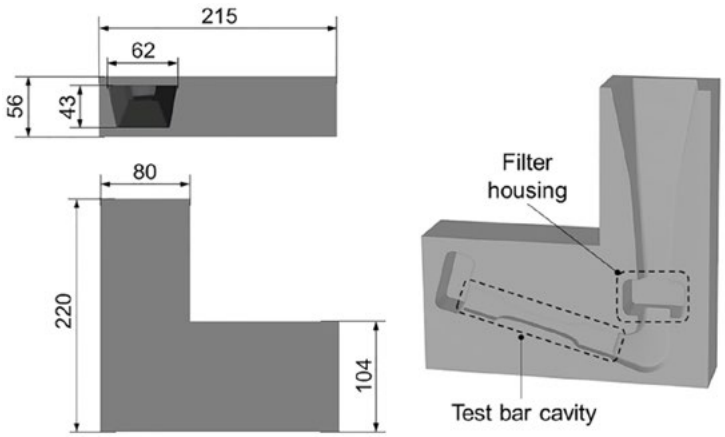

Fig.1 - Design of the permanent mould with overall dimensions (in mm).

Tab.1 - Chemical composition (wt.%) of the experimental AlSi7Cu0.5Mg alloy.

SI	FE	CU	MN	MG	NI	ZN	CR	TI	AL
6.50	0.089	0.652	0.012	0.431	0.005	0.004	0.014	0.121	bal.

The longitudinal section at half of the thickness of the tensile test specimen was selected for the metallographic investigation. The samples were drawn from each casting in correspondence of the filter zone and the test bar, and then they were mechanically prepared to a 3-μm finish with diamond paste and polished with a commercial 0.04-μm silica colloidal suspension.

An optical microscope was used to map the distribution of entrainment defects throughout the polished samples. Contiguous micrographs, each with an area of 1.2 x 0.9 mm^2, were automatically collected by exploiting the automatic handling of the microscope stage. To identify the oxide inclusions, a chemical etching was performed in a 5 vol% HF and 95 vol% H_2O solution.

Five severity grades (SGs) were identified to assess the severity of the oxide inclusions in the survey area. Each SG was defined according to the area of defects, which was quantitatively analysed using an image analyser. The area fraction covered by entrainment defects (A_D) was determined by dividing the total defect area measured in the micrograph by the entire area of the micrograph. Table 2 reports the different colours and ranges of A_D values as-

sociated with each SG. The A_D ranges were defined to emphasise low damage conditions. In general, SG equals to 1 corresponds to a region showing few closed bifilms or porosity with a maximum size of about 20 μm. The regions containing porosities with a maximum size of 300 μm and coarser unfurled bifilms were classified as SG 4. The definition of these five SGs allowed to obtain a good resolution in the mapping of the casting damage.

Tab.2 - Ranges of area fraction covered by entrainment defects (A_D) used to assess the severity grades (SGs) caused by the entrainment of bifilms. For each SG, the associated colour is also reported.

Severity grade (SG)	Area fraction covered by entrainment defect	Associated colour
0	$A_D = 0\%$	
1	$0\% < A_D \leq 0.2\%$	
2	$0.2\% < A_D \leq 0.8\%$	
3	$0.8\% < A_D \leq 1.6\%$	
4	$1.6\% < A_D \leq 5\%$	

CASTING SIMULATION

The gravity die-casting workspace of FLOW-3D CAST v5.1 (2020) commercial software [6] was used to simulate the filling and solidification stages of the casting process. The three-dimensional (3D) computer-aided design model of the mould was imported into the simulation software. The physical properties of the die and the alloy were defined as linear functions of temperature within their respective operating temperature ranges. The process parameters were set using the empirical data collected during the experimental procedure. The gravity, adiabatic gas regions [7], k-ω turbulence [8] and surface tension [9] models were used during the casting simulation.

The air leakage from the two halves of the die was simulated by inserting virtual vents along the parting plane. Two probes were inserted at the beginning of the pouring channel to regulate the end of the pouring phase and avoid that the metal overflowed from the die.

A mesh of 747,000 cubic cells with a grid size of 1.5 mm was automatically generated by the software for the whole system (die and casting). The mesh was refined in correspondence with the interface between the mould halves, generating 572,000 cells for the die cavity.

The distribution of entrainment defects was numerically investigated by analysing the outputs of free surface defect concentration [10] and entrained air volume fraction [6].

RESULTS AND DISCUSSION

The typical casting defects detected throughout the microstructure were generated by the entrainment of bi-films. As shown in Figure 2, porosities were contoured by a thin oxide layer with a thickness in the range of 0.1 to 0.6 μm. The formation of solidification defects close to bifilms is consistent with many results reported in the literature [1-4]. As described by Campbell [2], the double oxide films acts like points for the growth of defects, because the unbounded oxide surfaces can be easily separated with minimal gas pressure or minimal stress, forming pores or cracks. The reduced film thickness here detected suggests that the formation of entrainment defects can be primarily associated to the pouring and filling stages. No thick oxides (i.e. old oxides) were observed, indicating the high quality of the metal before pouring and the efficiency of the degassing phase used in the present work.

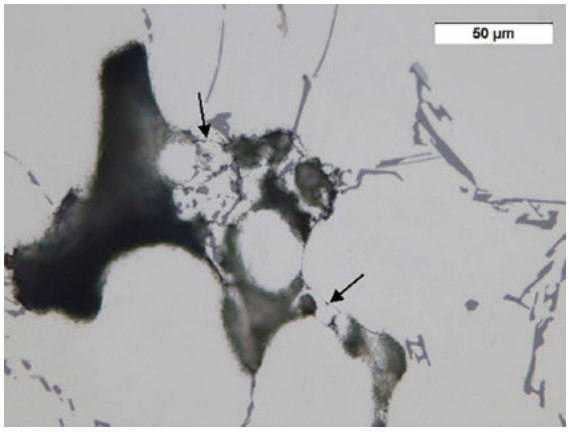

Fig.2 - A pore formed due to bifilm entrainment. The oxide layer contouring the pore is indicated by arrows.

Figure 3 shows the SG mapping related to oxide inclusions in the survey areas (filter zone and test bar). These two regions were hardly affected by entrainment defects: the average severity grade was lower than 0.8 (Table 3). The filter zone showed higher A_D values than the test bar, especially in the upper central area of the filter housing. The maximum SG value in the tensile stress test was equal to 2 and it was observed in 22 micro-graphs (~23.8 mm^2), while, in 74 fields (~79.9 mm^2) of the filter zone, the A_D values ranged between 0.2% and 5% (SG=2÷4). This is in agreement with good foundry practice, where the mould design is optimized to avoid the accumulation of defects in the test bar [2].

In Table 3, a statistical analysis of the SG distribution is reported. About 60% of the investigated micrographs (~1783 mm^2) showed SG equal to 1, and 36.6% of the survey area was defect-free. Moreover, only 6 fields (~6.5 mm^2) had A_D higher than 0.8% (SG=3 or 4). The average SG in the test bar and the filter zone was equal to 0.6 and 0.8, respectively. These low values were related to the lack of old thick oxides and a large number of small a thin bifilms.

During the pouring and filling stages, the massive formation of young and fine bifilms may be caused by two main reasons: the height of the pouring channel and the short pouring time. The pouring height was about 210 mm, greater than 12.5 mm, which is the maximum height from which an Al alloy can fall without generating surface turbulence [2]. Tiryakioğlu et al. [10] proved that, due to the high kinetic energy of the metal flow that tears the surface oxide films, a filling velocity higher than 1 m/s increases the number density of porosities and reduces their size. In the current work, the filling velocity at the bottom of the sprue was higher than 1.5 m/s (Figure 4a), so during the impact with the die, the molten metal may have easily entrained oxide layers and bubbles, reducing its quality since the beginning of the casting. Moreover, the reduced pouring time (equal to 3 seconds) promoted high-speed flow and the generation of turbulence inside the die cavity.

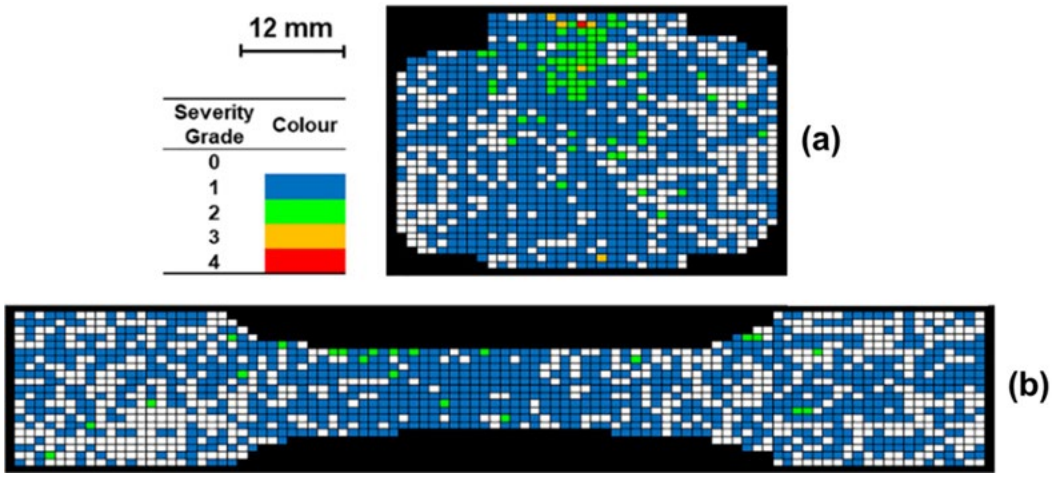

Fig.3 - Experimental distribution of the severity grade associated with entrainment defects (a) in the filter zone and (b) in the test bar.

Tab.3 - Statistical analysis of the distribution of oxide related-defects. The number of fields for each SG was evaluated in the two survey areas.

Survey area	Severity grade					
	0	1	2	3	4	Mean
Filter zone	368	756	68	5	1	0.8
Test bar	639	895	22	0	0	0.6
Total number of fields	1007	1651	90	5	1	
Percentage on total	36.56%	59.95%	3.27%	0.18%	0.04%	

Figure 4b shows the numerical distribution of the free surface defect concentration and the entrained air volume fraction in the section at half the thickness of the tensile test specimen. The first parameter is mainly related to the formation of oxide inclusions that promote crack propagation, while the second output is more representative of bubble damage or gas porosity. Both these outputs were analysed to study the numerical distribution of defects generated by entrainment phenomena. The higher values of these two parameters were detected in the upper central area of the filter and in the gauge length of the tensile test bar, as shown in Figure 4b. These results were consistent with the experimental findings and proved the reliability of the simulations performed.

It should be noted that the free-surface defect model, used to predict the formation of oxide inclusions, is based on some approximations in the modelling of the oxide film. In particular, the strength effect of the superficial oxide skin, the buoyancy of a bifilm, and its adhesion to the mould wall are not modelled [11]. However, in the current study, these approximations do not seriously affect the numerical distribution of oxide-related defects, as shown by the good agreement with the experimental results.

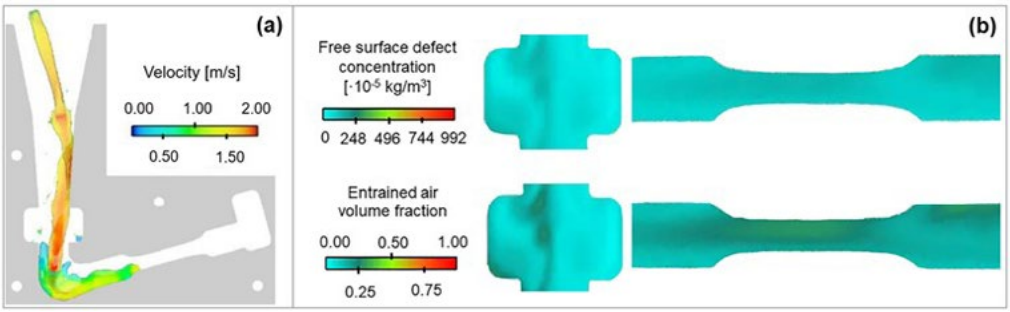

Fig.4 - (a) Numerical distribution of filling velocity at 20 s from the beginning of the pouring. (b) Numerical outputs concerning the entrainment phenomena in the filter zone and the test bar at the end of the filling, when the liquid metal is at rest.

CONCLUSIONS

In the current work, the numerical and experimental distributions of entrainment defects in AlSi7Cu0.5Mg cast alloy were analysed. The experimental mapping of the severity grade related to entrainment phenomena was investigated, and the numerical outputs related to oxide formation and air entrainment were studied. The following conclusions can be drawn.

- The generally low level of damage caused by entrainment defects is related to the molten metal velocity, higher than 1 m/s since the beginning of the filling. The high kinetic energy at the bottom of the

pouring basin promotes the tearing of the oxide film surface and the formation of a large number of reduced-in-size defects.

• The good agreement between the numerical results and the experimental findings indicates that the defect-prediction model has successfully predicted the entrainment phenomena, especially the entrapment of bubbles and oxide surfaces.

ACKNOWLEDGEMENTS

This research was developed with the financial support of Fondazione Cassa di Risparmio di Padova e Rovigo (CariPaRo). The Authors would like to thank Prof. M. Tiryakioğlu for the helpful tips and the stimulating reflections.

REFERENCES

[1] Dispinar D., Campbell J. Effect of casting conditions on aluminium metal quality. J. Mater. Process. Tech. 2007; 182:405-410.
[2] Campell J. Complete Casting Handbook: Metal Casting Processes, Metallurgy, Techniques and Design. Oxford-Waltham, MA: Butterworth-Heinemannpp; 2011. 11-13, 17-50, 67-72, 776, 833-852, 899-901 p.
[3] Uludağ M., Çetin R., Dispinar D., Tiryakioğlu M. The effects of degassing, grain refinement & Sr-addition on melt quality-hot tear sensitivity relationships in cast A380 aluminum alloy. Eng. Fail. Anal. 2018; 90: 90–102.
[4] El-Sayed M.A., Salem H.A., Kandeil A.Y. et al. Effect of Holding Time Before Solidification on Double-Oxide Film Defects and Mechanical Properties of Aluminum Alloys. Metall. Mater. Trans. B 2011; 42:1104–1109.
[5] Cao H., Shen C., Wang C., Xu H., Zhu J. Direct Observation of Filling Process and Porosity Prediction in High Pressure Die Casting. Materials. 2019; 12:1099.
[6] FLOW-3D® Version 12.0.2 Users Manual. 2020. FLOW-3D [Computer software]. Santa Fe, NM: Flow Science, Inc.
[7] Hirt C.W., Barkhudarov M.R. Void Regions and Bubble Models in FLOW-3D. Flow Science Report 01-13. 2013; Flow Science, Inc., Santa Fe, NM.
[8] Wilcox D.C. Formulation of the k–ω Turbulence Model Revisited. AIAA Journal. 2008; 46: 2823-2838.
[9] Hirt C.W. Surface tension modeling. Flow Science Report 01-14, 2003; Flow Science, Inc., Santa Fe, NM.
[10] Tiryakioğlu M., Yousefian P., Eason P.D. Quantification of Entrainment Damage in A356 Aluminum Alloy Castings. Metall. Mater. Trans. A 2018; 49:5815–5822.
[11] Barkhudarov M.R., Hirt C.W. Tracking defects, in: 1st International Aluminium Casting Technology Symposium. 1998; Rosemont, IL.

La Metallurgia Italiana
International Journal of the Italian Association for Metallurgy

An investigation on effect of rotary degassing-ultrasonic method on high pressure die casting products

R. Haghayeghi

A new rotary degassing-ultrasound system was implemented and compared with Impeller+N_2. The results suggest an enhanced hydrogen removal from the melt with a one third of required time for degassing by Impeller+N_2. The gas removal increased by 20% in comparison with rotary impeller. Inclusions reduced significantly by 3 and 6 times compared to impeller+N_2 and non-treated melt, respectively. Better cavitation dispersion, increased bubble surface area, less dross formation and better floatation rate contributed to better degassing and inclusion removal. For the first time, the ultrasonic melt treatment was performed on 400 Kg melt whereas the maximum volume ever been treated was 200 Kg.

KEYWORDS: DIE CASTING, ROTARY DEGASSING-ULTRASONIC, CAVITATION;

INTRODUCTION

Al-Si-Cu alloys are appropriate candidates for automotive applications. Many components such as ladder frame or engine block are produced from this group of aluminum alloys. A major problem in these alloys is porosity formation. This is related to various factors like the obstruction of feeding channels by β-Al_5FeSi phase as well as the segregation of copper by formation of constitutional undercooling ahead of the eutectic/liquid interface and establishment of eutectic mushy zone [1]. In addition, intermetallic compounds precipitate at last stages of solidification, that is when feeding is critical and permeability is the lowest [1]. This further could contribute to porosity formation. Alloying elements would have an effect on porosity formation. Previous researches [1-3] have shown the deleterious effect of Fe-Cu interaction on increasing the porosity content in Al-Si-Cu alloys. Hence, finding a solution to the above is required. In this research, the effect of rotary degassing ultrasonic process in a large pool of melt respecting previous researches [4,5] has been analyzed. It was compared with impeller degassing and its effects on porosity formation in a high pressure die casting (HPDC) process were discussed.

Experiment

About 400 kg of molten metal of Al-9 wt.%Si-3 wt.%Cu-1.3

R. Haghayeghi
Volvo Truck North America, 13302 Pennsylvania Avenue,
Hagerstown, MD 21742, USA

wt.%Fe ($T_{LIQUIDUS}$=620 oC) melted in an electrical furnace. It was transferred to degassing vessel at 700±5 oC. Two separate processes were implemented to degas the melt, namely a rotary furnace-sonication system and an impeller degassing where N_2 was blown from the bottom of the impeller (Figure 1). The sonication was applied by an air-cooled piezoelectric transducer at frequency of 25 kHz, amplitude vibration of 25 μm and an input power of 1 KW for 3 minutes. Simultaneously, the vessel was rotating (2 rpm) with a circular plate underneath where the ultrasonic horn was located at 2/3 of the radius of degassing tank (Figure 1a). This position was determined based on preliminary experiments which have evidenced how the sonotrode's position affects the acoustic streaming and the grain morphology of the solidified material [6]. In the other approach, the impeller was applied at a rotation speed of 750 rpm for 10 min where the N_2 was inserted at 5 Lit/min during the degassing process (Figure 1b). In each process, the treated melt was transferred to a cold chamber die casting machine with a locking force of 22 MN for producing a shock tower (10 Kg) with minimum thickness of 1.6 mm. The plunger speed changed from 0.3 m/s to 4.3 m/s with the intensification pressure of 97 MPa. The vacuum was applied after 110 mm of the plunger movement and the casting temperature was 680 oC.

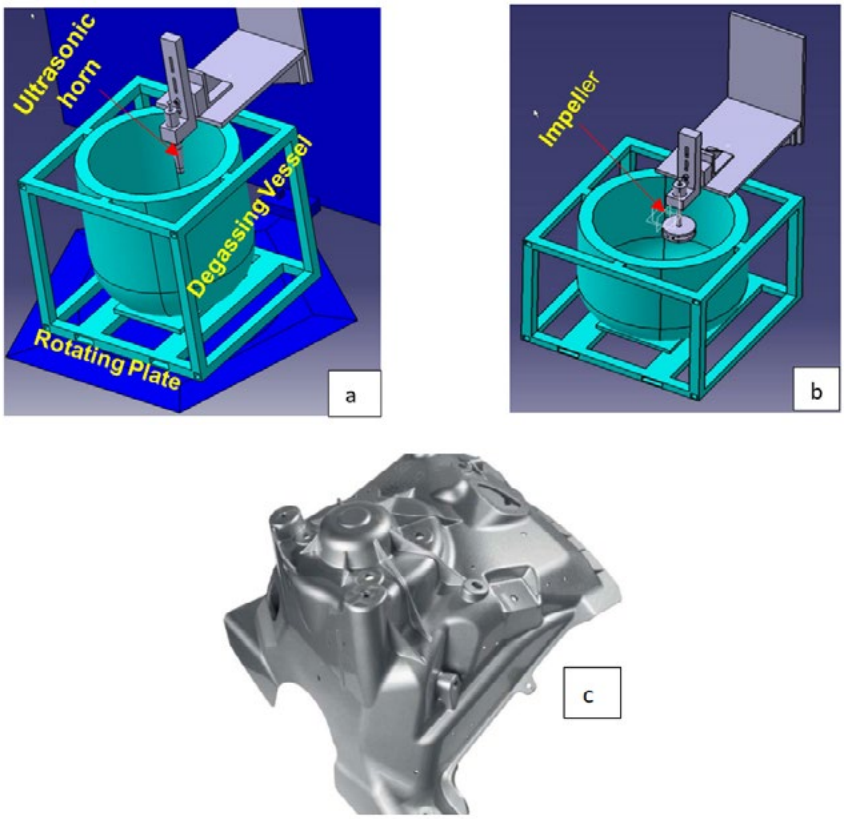

Fig.1 – (a) The rotating furnace-sonication system; (b) Impeller with nitrogen degassing, (c) Shock tower.

The quality of molten bath was measured via reduced pressure test (RPT) [7] and an image analyzer software examined several pictures (100×100 μm^2) on RPT samples. The density (D) of each RPT specimen was measured by Archimedean method defined by the equation: $D=W_a/(W_a-W_w)$, where W_a and W_w are the specimen's weights in air and in water, respectively. Measurement of inclusions was carried out by PoDFA on 3 kg samples for each degassing method. Tensile tests were performed according to ISO 6892-1 A standard on sub-size specimens drawn from the castings at defined locations based on ASTM B557 M-15.

RESULTS AND DISCUSSION

The RPT results and the comparison between the degassing methods are shown in Figure (2). As observed, both melts had a similar quality before degassing. The rotary vessel-ultrasound resulted in better degassing efficiency compared with the impeller+N_2.

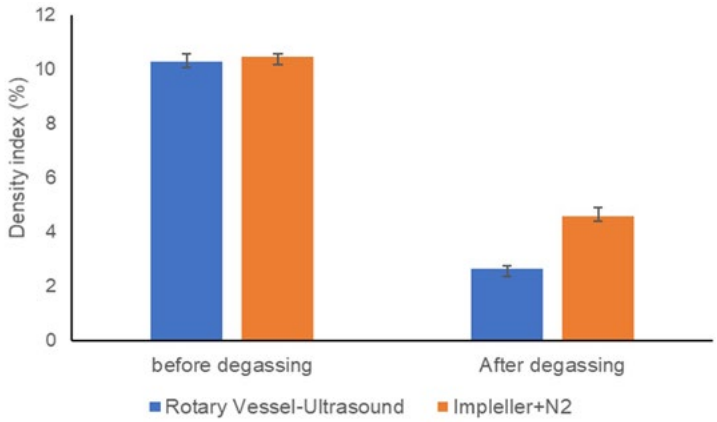

Fig.2 – Density index of molten metal before and after degassing with two different methods.

By rotary Vessel-Ultrasound, the density index decreased from 10.3% to 2.6% whereas by performing degassing with the impeller+N_2, the value decreased from 10.5% to 4.6%. This indicates that rotary ultrasound has performed nearly 20% higher in degassing efficiency in comparison with the rotary impeller in one third of the time. It is known that in both impeller and ultrasonic techniques, cavitation degases and clean the melt. The reason of better degassing by ultrasound is based on the bubble density. An investigation by Eskin et al. [8] suggests a bubble density of 1×10^{11} m^{-3} with initial radii of 1 μm is produced by using a frequency of 17.7 kHz [8]. Such a high density of bubbles with increased surface area would improve the gas diffusion and further gas removal. The rotary system causes better spread of the bubbles throughout the melt to minimize shielding and attenuation effects where the frequency of 25 KHz is applied. In addition, in every acoustic cycle, the Bjerknes force attempts to bring the bubbles together whilst each of the bubbles creates a strong velocity field in the surrounding that gives rise to bubble spacing. These alternate attempts provide a steady state condition in which the distance between the bubbles remains nearly constant [9]. Therefore, more bubbles are available for hydrogen diffusion and further gas removal. Another reason of better degassing by ultrasonic is due to higher dross formation by impeller where the dross acts as an accumulator of hydrogen by adsorption of hydrogen molecules which is significant at above 600oC [10]. The dross level by rotary vessel-sonication system was 245 gr whereas for rotary impeller was 1300 gr. The rotary system competes with new design which was offered by ref [11] where 25% increment was observed on degassing efficiency.

Furthermore, the rotary vessel-ultrasound system could help for removal of the inclusions. By variation in the acoustic pressure, the cavitation bubbles are exploded and split into two smaller bubbles where a jet stream releases. The inclusions collide with the jet stream and the local variation of the acoustic pressure ruptures the oxide films and inclusions. Therefore, they are attached to the bubbles and float to the melt surface. Smaller bubbles with higher surface tension would contribute in removal of fine Al oxides. Kang et al. [12] has demonstrated the floatation rate of inclusions would increase by 6 times through the cavitation bubbles. Comparatively, the impeller by N_2 process inclusion reduction is a win/lose process. The forced convection helps the agglomeration of the inclusions and their sedimentation whereas at the same time gas blow increases the probability of the attachment of inclusions to a bubble and its floatation. The PoDFA analysis (Figure 3) suggests the rotary vessel-ultrasonic method is more effective in comparison with impeller+N_2 to remove inclusions. This could be attributed to the small velocity of forced convection in impeller system and poor wettability of inclusions. Nevertheless, in comparison with untreated melt the values have improved for impeller+N_2. The significant amount of carbides is due to graphite impeller whereas for ultrasonic treatment the amount of carbon decreased to 0.09 mm^2/kg. With respect to the initial content, the amount of aluminium oxides was decreased by 6 and 3 times by using ultrasonic treatment and impeller+N_2, respectively.

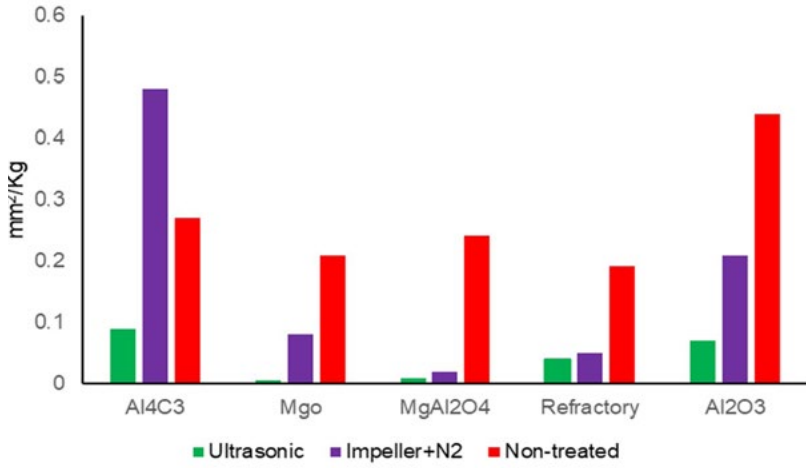

Fig.3 – PoDFA analysis of untreated, impeller+N_2 and ultrasonically treated melts.

The microstructure of the diecast alloy at untreated, treated by impeller+N_2 and rotary system is shown in Figure (4). More porosity are seen close to the intermetallic particles (e.g. $Al_{15}(Fe,Mn)_3Si_2$). The β-phase particles are potential sites for porosity formation regardless of the alloy composition and the type or size of the β particles [13]. By application of rotary process, the intermetallic size has decreased considerably. The rotary vessel-ultrasonic system presented YS and UTS of 210 and 303 MPa and elevated elongation to 6% due to primary/eutectic Si refinement/modification as described in ref [14]. Impeller+N_2 and untreated melt presented value of 180 and 165 for YS and 288 and 273 MPa for UTS, respectively. However, the elongation was not higher than 3% and 1% for impeller process and untreated melt, sequentially.

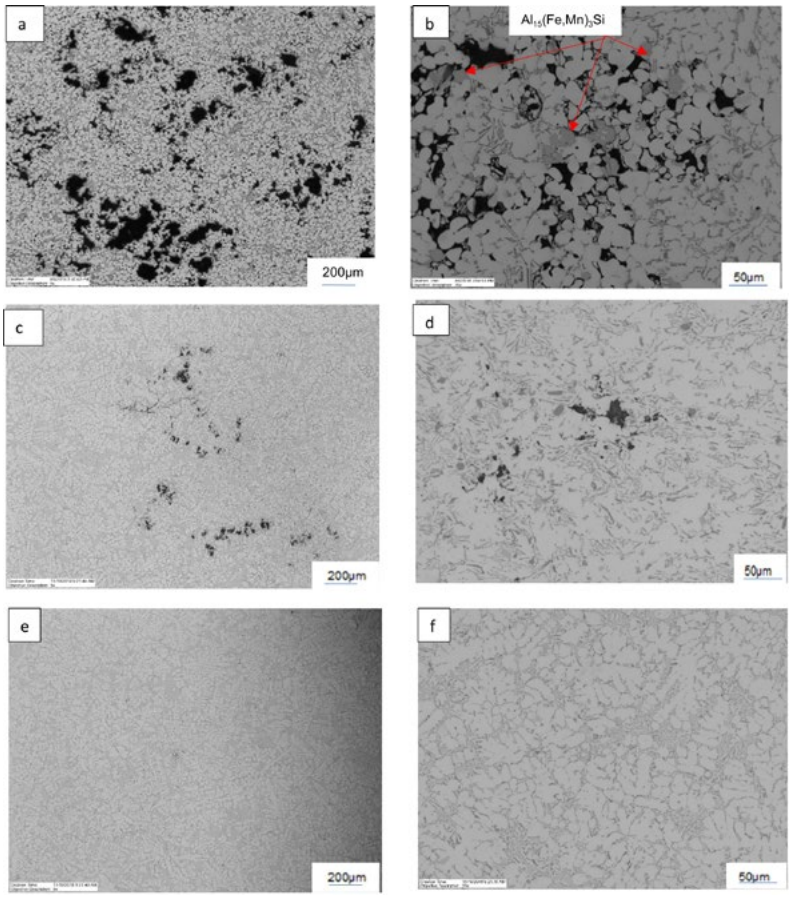

Fig.4 – Microstructure of diecast $AlSi_9Cu_3(Fe)$ alloy: (a,b) untreated; degassed with (c,d) impeller+N_2 and (e,f) rotary vessel-sonication.

CONCLUSION

A rotary sonication-ultrasonic technique was offered for degassing and inclusion removal. The results suggest 20% improvement for degassing and 2 times enhancement in oxide removal compared with impeller+N_2. The YS, UTS and elongation was increased considerably. Moreover, 400 Kg of molten metal was treated whereas the maximum ever reported was 200 Kg. By the suggested technique the formation of undesired composition from the impeller decreases significantly and melt quality improves accordingly.

ACKNOWLEDGEMENT

The authors appreciate George Fischer-Linamar company for their profound support.

REFERENCES

[1] Dinnis C.M, Taylor J.A, Dahle, A.K. Iron-related porosity in Al–Si–(Cu) foundry alloys. Mater. Sci. Eng. 2006; 425: 286-296.
[2] Roy N., Samuel A.M. and Samuel F.H. Porosity formation in AI-9 Wt Pct Si-3 Wt Pct Cu alloy systems: Metallographic observations. Met Mater Trans A.1996; 27: 415-429.
[3] Heiberg G., Nogita K., Dahle A.K., Arnberg L. Columnar to equiaxed transition of eutectic in hypoeutectic aluminium-silicon alloys. Acta Mater. 2002; 50:2537–46.
[4] Haghayeghi R., Kapranos P. The Effect of Processing Parameters on Ultrasonic Degassing Efficiency. Mater Lett. 2014;116: 399-401.
[5] Haghayeghi R., Heydari A., Kapranos P. Effect of ultrasonic vibrations prior to high pressure die-casting of AA7075. Mater Lett. 2015;153:175-8.
[6] Lebon G.S.B, Abou-Jaoud G.S., Eskin D., Tzanakis I., Pericleous K., Jarry P. Numerical modelling of acoustic streaming during the ultrasonic melt treatment of direct-chill (DC) casting. Ultrason Sonochem. 2019; 54:171-182.
[7] Samuel A.M., Samuel F.H. Various aspects involved in the production of low-hydrogen aluminium castings. J Mater Sci, 1992; 27: 6533–63
[8] Eskin D.G., Tzanakis I., Wang F., Lebon G.S.B, Subroto T., Pericleous K., Mi J. Fundamental studies of ultrasonic melt processing. Ultra Sonochem. 2019; 52:455-467.
[9] Doinikov A.A., Translational motion of two interacting bubbles in a strong acoustic field. Phys. Rev. E, 64 (2001), Article 026301.
[10] Eskin D., Alba-Baena N., Pabel T. and Da Silva M. Ultrasonic degassing of aluminium alloys: basic studies and practical implementation. Mater Sci Techno. 2015; 31: 79-84
[11] Eskin D.G, Al-Helal K., Tzanakis I. Application of a plate sonotrode to ultrasonic degassing of aluminum melt: Acoustic measurements and feasibility study. J. Mater. Process. Technol. 2015;222: 148-154.
[12] Kang S., Shen M., Li C., Cold Model Experiments and Mechanism on Inclusion Removal by Ultrasonic Horn. Adv Mater Res, 2013; 750-752: 404-7.
[13] Khalifa W., Samuel A.M., Samuel F.H., Doty H.W. & Valtierra S., Metallographic observations of β-AlFeSi phase and its role in porosity formation in Al–7%Si alloys. Int. J Cast Metal Res. 2006; 19:156-166.
[14] Haghayeghi R., Depaula L.C, Zoqui E.J. Comparison of Si Refinement Efficiency of Electromagnetic Stirring and Ultrasonic Treatment for a Hypereutectic Al-Si Alloy. J Mater Eng Per. 2016; 29:1900-7.

Development of a model for the prediction of mechanical properties for Al-Si-Mg castings

C. Ransenigo, M. Tocci, C. Viscardi, M. Serafini, A. Pola

A356 alloy is widely used to produce structural components by means of Low Pressure Die Casting (LPDC) process. Generally, a T6 heat treatment (solution, quenching and aging treatment) is carried out to improve the strength of the casting. Nowadays, software simulation of casting processes and solidification phenomena is a common practice for designing sound components even if mechanical strength values and their correlation with microstructure parameters are not given. However, the possibility to predict material behaviour before producing the castings would represent an additional precious tool for exploiting material properties. In the present study, a model for the estimation of tensile as-cast properties based on casting simulation was validated on a 22'' wheel obtained by LPDC. Microstructural and mechanical properties were investigated on the component both in as-cast and T6 condition. First, areas with different thicknesses and cooling conditions were analysed and secondary dendrite arm spacing (SDAS) measurements were carried out. Subsequently, tensile tests were performed on specimens from rim and spokes. Experimental data were used to verify the reliability of simulation results and to validate the as-cast model. Based on additional information provided by simulation software and experimental data, a mathematical model to predict the mechanical properties after T6 heat treatment was also proposed.

KEYWORDS: ALUMINUM, HEAT TREATMENT, SIMULATION, MODEL, CASTING;

NTRODUCTION

A356 is an aluminum casting alloy widely used because of its good castability, corrosion resistance and mechanical properties, in particular high strength-to-weight ratio, which make it suitable for various applications in the automotive industry [1]. In order to allow its use in structural application, generally a T6 heat treatment is carried out to further increase the strength of the castings [2]. Nowadays the quality of castings is constantly improving, also thanks to casting simulation software that provide results in terms of microstructure, defects like shrinkage porosity, solidification time, fraction solid and residual stresses [3] by modelling both mold filling and solidification phenomena. For instance, Sadeghi et al. [4] used simulation to predict fluid flow and solidification steps of the castings while Aloe et al. [5] focused their attention on the development of numerical tools to successfully predict stresses, microstructures and defects. Commercial casting software are not able to provide mechanical

C. Ransenigo, M. Tocci, A. Pola
Department of Mechanical and Industrial Engineering, University of Brescia, via Branze 38, 25123, Brescia, Italy

Cristian Viscardi
Ecotre Valente srl, Via S. Orsola 145, 25135, Brescia, Italy

Marco Serafini
Maxion Wheels Italia srl, Via Roma 20, 25020, Dello (Bs), Italy

strength values before and after heat treatment. However, the possibility to predict the material behavior would represent a precious tool for exploiting material properties and simplifying production processes.

The aim of the work is to develop a mathematical model to successfully predict the local mechanical strength of the casting from the main microstructural parameters. In particular, specific equations to predict yield strength and ultimate tensile strength for the as-cast and T6 conditions were studied using the commercial software ProCAST®. First, microstructural and mechanical properties were investigated on a 22'' wheel obtained by LPDC process both in as-cast and T6 conditions. In parallel, using casting and geometrical parameters given by the foundry, a complete simulation was set up and a predictive model for as-cast condition was developed by exploiting the results. Experimental data were used for two main reasons: first, microstructural properties were used to verify the reliability of results from the casting simulation and then the validation of the predictive models for as-cast condition was carried out based on experimental tensile properties. Finally, a T6 model was proposed by extending the as-cast model previously validated.

EXPERIMENTAL PROCEDURE

The experimental tests were performed on two 22'' wheels obtained by LPDC using A356 alloy, one in as-cast condition, the other one after T6 treatment. The T6 heat treatment performed by the foundry consisted of solution treatment at 530 °C, quenching and then aging at 146 °C for 3 hours. A preliminary analysis was carried out in different positions of the as-cast wheel in order to analyze the influence of geometry and cooling rate on microstructure and to identify relevant sections for further characterization.

Five samples from the main spoke (letter A) and three from the minor one (letter B) were taken from the as-cast component in order to investigate different thicknesses: A1 and B1 from the rim, A2 at the root of the spoke, A3, A4, B3, B4 from the spokes and A5 close to the hub (Fig. 1). Fewer samples were examined on the second spoke because, after a preliminary analysis on the main one, it was found that they described the evolution of SDAS through the entire wheel in the most representative way.

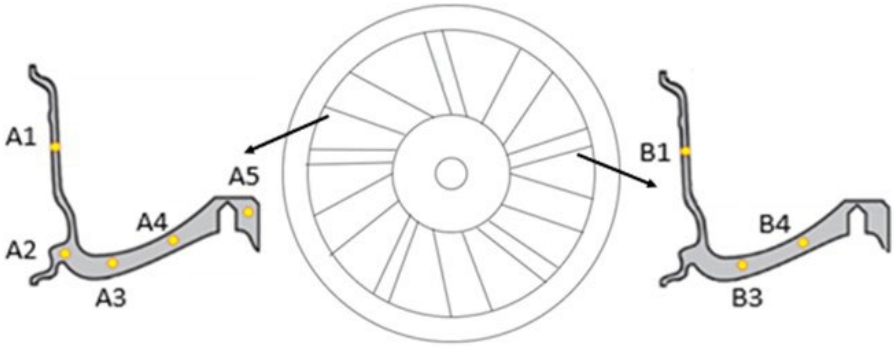

Fig.1 - Schematic representation of samples drawn from the two different spokes. For confidentiality reasons, the real wheel cannot be shown so a schematic representation is given.

The microstructure of the as-cast samples was observed via optical microscope Leica DMI 5000M after metallographic samples preparation. Average SDAS values were obtained for each sample using the linear intercept method. Several measurements were performed in order to obtain reliable mean values. Brinell hardness was measured on the as-cast and on the T6 samples in order to verify the increased resistance due to heat-treatment. More than 25 hardness tests were carried out with a load of 613 N and holding time of 15 seconds. Tensile tests were performed on cylindrical specimens with gauge length of 25 mm and average gauge diameter of 5 mm machined from the as-cast and T6 wheels. Samples position was chosen according to results from previous characterization: 3 coming from the rim (A1), 3 from the main spoke (A3) and 3 from the minor one (B3) for both the as cast and T6 component. An Instron 3369 testing

machine with a load cell of 50 kN was used and a cross head speed of 1 mm/min was applied in the elastic field, while it was increased to 2 mm/min in the plastic field.
In parallel, using casting and geometrical parameters given by the foundry, a casting simulation was set up using a software widely used by foundries: ProCAST®. Subsequently, values of SDAS coming from the simulation were compared to experimental data in order to guarantee the reliability of simulation results. Based on information provided by simulation software, a mathematical model to predict yield strength and ultimate tensile strength for as-cast conditions was developed and validated using the experimental results coming from tensile tests, as described in the following section. A first predictive model for mechanical properties after heat treatment was also proposed.

RESULTS

Microstructural analysis

Microstructure of each as-cast sample, observed by optical microscope, is reported in Fig 2. A356 is a hypoeutectic aluminum-silicon casting alloy characterized by a primary dendritic phase, α-Al solid solution, and a eutectic mixture of aluminum and silicon, as indicated in the central in-set in Fig. 2. Intermetallic compounds, such as Fe-rich intermetallics, were seldom observed. As expected, a finer microstructure can be found at the rim, while it becomes coarser in the spoke and hub because of the reduction of cooling rate due to the increase of thicknesses. Analogous micrographs for the minor spoke and the T6 samples are not shown for brevity sake.

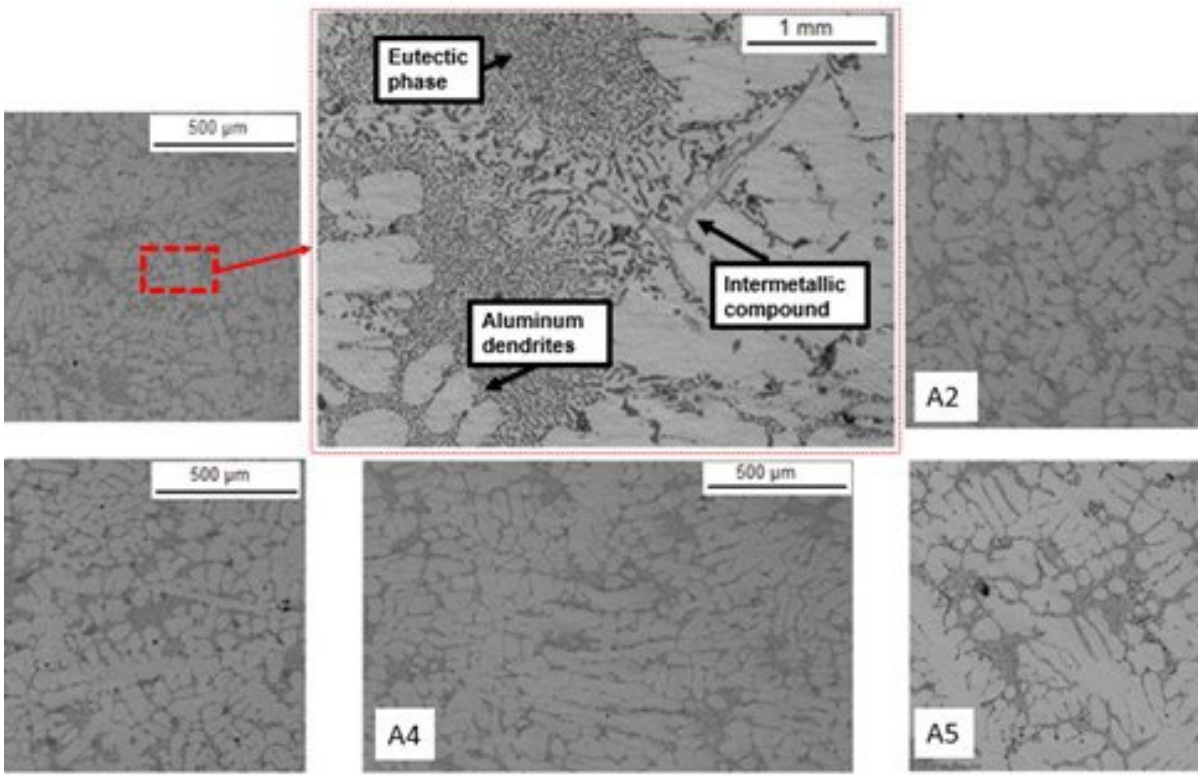

Fig.2 - Microstructure of each as cast sample. The central in-set shows the main microstructural constituents.

Simulation results

Simulation results in terms of microstructure, shrinkage porosity, solidification time, fraction solid and cooling rates are usually provided by the software. Among these, SDAS and level of shrinkage porosity were used in the present study. First, the values of SDAS coming from simulation were compared to experimental data and summarized in Tab. 1. The good agreement between them showed the reliability of simulation results and allowed them to be used in the development of the predictive models. Shrinkage porosity appears in one of the predictive models since it is known to affect the quality of the product and, consequently, its mechanical performances especially for those casting used in high-level request components [6]. Simulation values are reported in Tab.1.

Tab.1 - Simulation data and experimental values of SDAS and level of shrinkage porosity.

	A1	A2	A3	A4	A5	B1	B3	B4
Simulation SDAS [μm]	30	43	48	54	55	30.5	46	55
Experimental SDAS [μm]	31 ± 5	45 ± 6	48 ± 6	49 ± 6	59 ± 8	28 ± 3	45 ± 5	54 ± 5
Shrinkage porosity [-]	0.058	0.01	0.015	0.14	0.02	0.03	0.01	0.02

Tensile tests

Values of yield strength, ultimate tensile strength and elongation both in as-cast and T6 conditions are shown in Fig. 3.

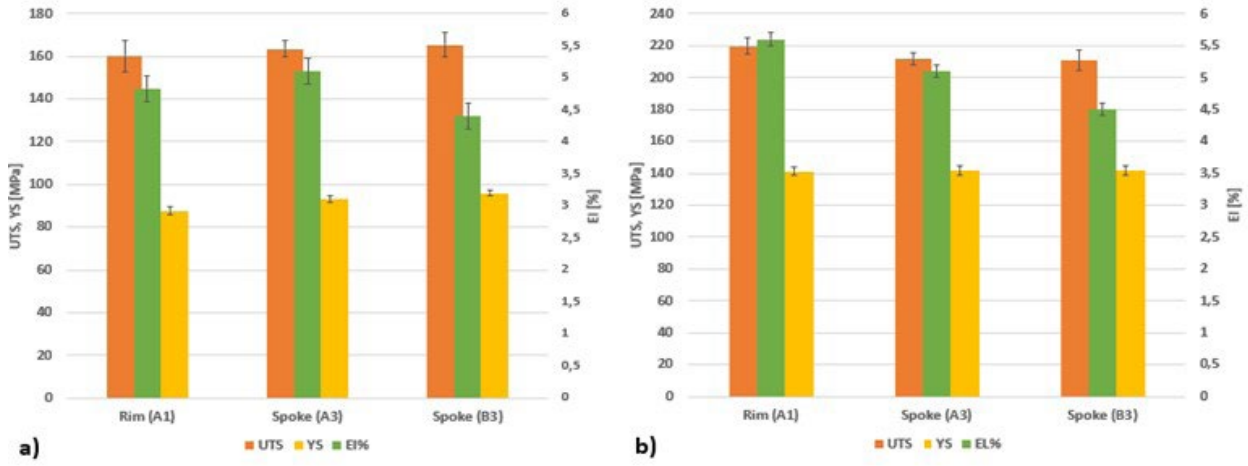

Fig.3 - Tensile properties from as-cast (a) and T6 (b) wheels.

For as cast condition, a uniform distribution of mechanical properties is displayed except for a slight reduction of elongation for the minor spoke (B3). No direct correlation between SDAS and tensile properties can be observed, suggesting that this point deserves to be better explored.

After T6, as expected, there is a marked increase of YS and UTS while elongation rises in a less remarkable way.

YIELD STRENGTH MODEL

As reported in literature [7], yield strength is mainly affected by microstructure following this general equation:

$$YS = A - B * ln\ ln\ (SDAS) \quad (1)$$

Simulation software provides YS values for as-cast conditions, obtained from interpolation of experimental data corresponding to different cooling rates, and SDAS values, which came from the casting simulation previously set up. Using YS and SDAS values provided by the software, unknown elements (A, B) of the general equation (1) were found. YS as well as SDAS values from three different positions were used (A1, A3, B3). Finally, an equation to predict the local tensile property was developed for the as-cast condition:

$$YS = 31.6 + 16.4 * ln\ ln\ (SDAS) \quad (2)$$

Tensile tests were used to validate the predictive model for as-cast condition (Tab.2): YS values coming from the application of the equation (2) are sufficiently close to the experimental ones. A comparison between predicted and

experimental values showed that the mean error in the property prediction was about 2% of the actual measured value. The validation of this model ensured the possibility to implement the equation into the software in order to obtain reliable values of YS in any position of the casting, characterized by different thicknesses and solidification conditions, without performing any tensile tests. The simplicity of the equation is positive for its use at industrial level.

Tab.2 - Validation of as cast model.

	YS from the model [MPa]	Experimental YS [MPa]
A1	86.9	87.7 ± 2.1
A3	94.8	92.8 ± 1.9
B3	94.6	96 ± 1.4

A model for the estimation of YS for T6 condition was also developed, based on SDAS values, as an extension of the as cast model previously validated. Coefficients were defined following the same procedure as the as cast condition by exploiting experimental values of YS coming from tensile tests. The following equation is proposed:

$$YS = 135.6 + 1.67 * ln\ ln\ (SDAS) \quad (3)$$

ULTIMATE TENSILE STRENGTH MODEL

After a study of literature [8], it was found that Ludwig model represents the most reliable equation to predict UTS:

$$UTS = YS + K * \varepsilon^{\alpha} \quad (4)$$

where K is a function of SDAS while ε depends on tensile parameters. However, also casting defects, such as porosity level, are known to affect tensile strength, while they are not considered in Ludwig model. As expecting, after analyzing the correlation between the level of casting defects given by the software and UTS values, it was found that the higher the shrinkage porosity, the lower the mechanical strength value. Therefore, also the level of shrinkage porosities was taken into account for a more accurate estimation of UTS values. The possibility to analyze the strength reduction due to casting defects would represent an additional precious tool for predicting how solidification phenomena can affect material properties. The level of casting defects, together with the other input variables of equation, came from simulation results. A model to predict UTS both for as-cast and T6 conditions was developed:

(5)

$$UTS = YS * (1 - 0.5 * \%SHR.POROSITY) + \left(280 * 3 * e^{\frac{3.5}{SDAS}}\right) * (ln\ ln\ \left(1 + \frac{El\%}{100}\right))^{0.5}$$

It is revealed that predictions from Eq. 5 are consistent with the experimental measurements of this property, thus the validation of the as-cast model is achieved (Tab. 3). In fact, the maximum error between the predicted UTS values and the experimental ones was about 5 MPa, which is lower than the experimental standard deviation. Thus, the validity of this metallurgical model is demonstrated. In this study, the most innovative contribution lies in the development of a new predictive model characterized by the appearance of shrinkage porosity. T6 model was developed by extending the as-cast model previously validated and by exploiting experimental results coming from tensile tests.

Tab.3 - Validation of as cast model.

	UTS from the model [MPa]	Experimental UTS [MPa]
A1	159.2	160.4 ± 7.3
A3	168.1	163.6 ± 6.1
B3	163.3	165.5 ± 5.9

CONCLUSIONS

In this study, a mathematical model to predict tensile behavior of A356 both for as-cast and T6 conditions as a function of microstructural parameters is proposed.

First, the yield strength was found to depend on SDAS and experimental values ensured the validation of the model for the as-cast condition. The same model was extended to predict the material behavior after heat treatment and new coefficients were found.

The ultimate tensile strength of the alloy was found to depend on SDAS, defects content and tensile parameters. After the validation of this model for the as-cast conditions, a new predictive equation was developed also for T6 conditions by exploiting experimental values. The two equations result to be the same since the difference lies in the value of each variable involved.

The good results obtained suggest that the proposed models could be integrated in the casting simulation software to obtain the local distribution of mechanical properties to be used during the re-design step of a new component. In this way, a reduction of thicknesses, where possible, can be achieved, and the always more restricted criteria for the lightening of vehicles can be met.

REFERENCES

[1] Kaufman J. G., Rooy E. L. Aluminium alloy castings, Properties, Processes and applications, ASM International; 2004.

[2] Morri A. Correlations among microstructure, effect of thermal exposure and mechanical properties, in heat treated Al-Si-Mg and Al-Cu aluminium alloys. 2012; 1-2.

[3] Abdullin A. D. New Capabilities of the ProCAST 2017 Software in Simulating Casting Processes. Metallurgist volume 61. 2017;433–438.

[4] Ravi, B. Computer aided design and analysis for zero defects. International Conference on Aluminum. 2000; 1-6.

[5] Aloe M., Lefebvre D., Mackenbrock A., Sholopurwalla A., Scott A. Advanced casting simulations. ESI Group, paper 30.

[6] Chudasama B. J. Solidification Analysis and Optimization Using Pro-Cast. International Journal of Research in Modern Engineering and Emerging Technology, Vol. 1, Issue: 4. 2013

[7] Shabani M. O., Mazaheri A. Prediction of Mechanical Properties of Cast A356 Alloy as a function of microstructure and cooling rate. Archives of Metallurgy and Materials, 2011; volume 56, issue 3.

[8] Brusethaug S., Langsrud Y. Aluminum properties, a model for calculating mechanical properties in AlSiMgFe-foundry alloys. Metallurgical Science and Technology, Volume 18; 2000.

Simulation in support of the development of innovative and unconventional lightweight casting processes

R.Pirovano, M. Todte

Nowadays, foundry process simulations play a fundamental role to achieve a reduction of casting defects, an increase of the quality of the casting parts, an optimization of process stability and finally an improvement of the mechanical properties of the casting.
To reach the highest quality levels new foundry processes have been proposed, to overcome the limits of the well-known classical approaches. Even if the advantages of a new method can be relevant, all its details must be carefully studied in a very preliminary stage, being the process itself, in its details, not completely known. For this reason, it is important to be able to study how to optimize the system to reach the desired performances, but also to highlight the challenges and the limitations of the new approach.
A flexible simulation software allows to do it in a very effective way, analysing in detail the variation of the sensible variables in space and time and allowing to understand how to control and to calibrate the process parameters without the costs of an experimental evaluation.
This presentation introduces application examples for four innovative casting and casting related processes where CFD simulations played an important role in their development and optimization: injector casting, laminar HPDC, salt cores and double plunger HPDC.

KEYWORDS: SIMULATION, CFD, INNOVATION, UNCONVENTIONAL PROCESSES, LIGHTWEIGHT CASTING;

INTRODUCTION: UNCONVENTIONAL APPROACHES

Recently several innovations in the foundry industry have been shown, in the wake of the continuous research of increasing the product quality and reducing the scrap. In this direction a great work is done in optimizing, also using numerical optimization software, the existing processes, trying to find better and more controlled process parameters which minimize or maximize the desired performance, such as the amount of porosity and other defects or the mechanical properties of the casted part.
Another, maybe more difficult, way to go towards a better result is through a more radical innovation, trying to develop and bring on the market new und unconventional approaches which can overcome the intrinsic limitations of the classical processes: the present work wants to focus on this last line, showing some of the most recent developments proposed in the lightweight casting industry.

Raul Pirovano
XC Engineering Srl, Italy

Matthias Todte
Flow Science Deutschland, Germany

In the developing phase of new technologies, it is critical to be able to forecast in detail advantages, limitations, and challenges that the implementation of the idea will bring. In order to do it in the most efficient way, reducing the time and the costs related to an experimental phase, the intensive use of simulation software has been widely diffused in the last year: in fact, they allow to test easily different configurations, calibrate the process and analyze the outputs in detail in a very fast and effective way. The present work will show how a flexible CFD process simulation software was helpful in the development of four different innovative technologies.

INJECTOR CASTING

Many engine components are produced with a gravity casting process. As for most of the casting part, the aim of the process is to reduce casting defects and increase the quality of the casting part and its mechanical properties, optimizing at the same time the process stability.
Traditionally, different casting processes have been proposed: for instance, a top pouring method, where the feeders are filled with hot metal with consequent advantages for the shrinkage porosity location and the possibility to cool down the bottom plate. On the other hand, in this case there is a high risk for entraining air and oxides, du to the high velocities and the turbulence. On the opposite, a bottom pouring method minimize this risk, but the metal in the feeders is colder and it is not possible to cool down the bottom plate. Again, there is the possibility to make a tilt pouring, which improve these limitations but has high costs due to the machine used and additional risk of air entrainment due to the rotation.
In order to combine the advantages of traditional processes and avoids their disadvantages, an innovative casting process with a moving feeding system has been developed: the metal is poured in the cast directly through thin injectors connected to a moving basin placed at the top of the casting part: the injectors at the beginning of the process are near the bottom of the part, reducing turbulence levels, air entrainment and oxides, but moving in the vertical direction they are able to fill directly the feeders with hot metal at the end of the filling phase. The bottom plate can be cooled, and there is no need to model pouring basin and gating system. The only limitation is that this process is not suitable for all casting parts, because of the placement of the injectors.

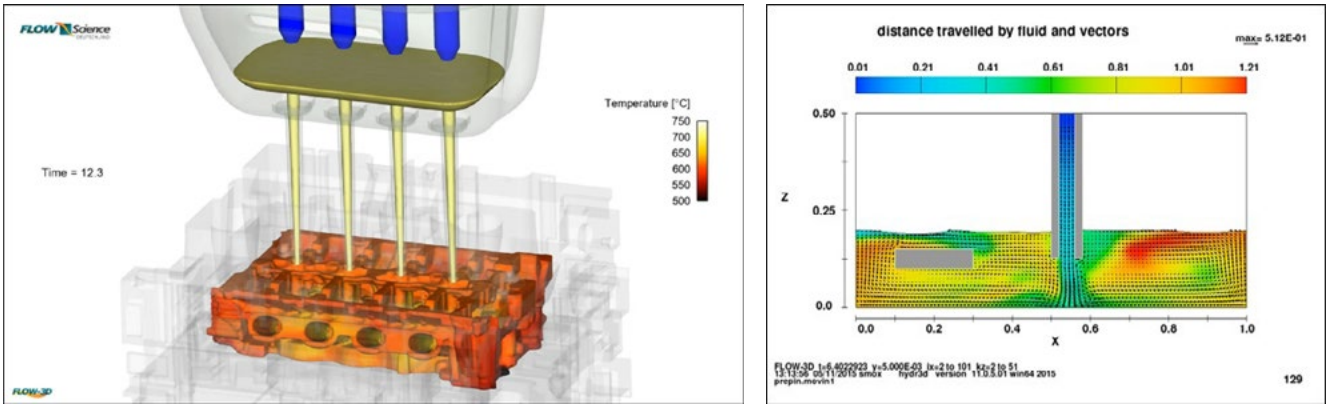

Fig.1 - Injector casting, global view and detail of the velocity field at the exit of one injector.

In the design of this system the simulation played a crucial role to understand the filling behavior and design the best shape and movement of the injectors, to get an optimal metal flow during the whole filling process, monitoring velocities, turbulence, temperature distribution and casting defects. Moreover, being able to move basin and injectors directly into the simulation, allowed to perfectly calibrate the process parameters such us the initial temperatures, the timings and the movement of basin and stopper, with a great reduction of the experimental effort.

LAMINAR HPDC

Nowadays, the OEMs in the automotive industry, receive strong requirements for increased mechanical properties,

for instance for structural parts, and at the same time for weight reduction, associated to the production of high volumes in aluminum alloys, where HPDC is the most important process. One of the issues of achieve these requirements is that HPDC castings are often not suitable for heat treatment or welding, because of the presence of pores containing entrapped gas which would form blisters. To overcome this limitation an innovative "laminar HPDC" process, which is an HPDC done with a very low plunger velocity, has been tuned. The advantages are several: first, the process can be run on conventional HPDC machines, but obtaining a filling with basically no turbulence and a considerable reduction of air inclusions, allowing a longer intensification pressure phase due to the compact gating system, with a consequent reduction of shrink holes. Finally, the castings can be welded and undergo heat treatment.

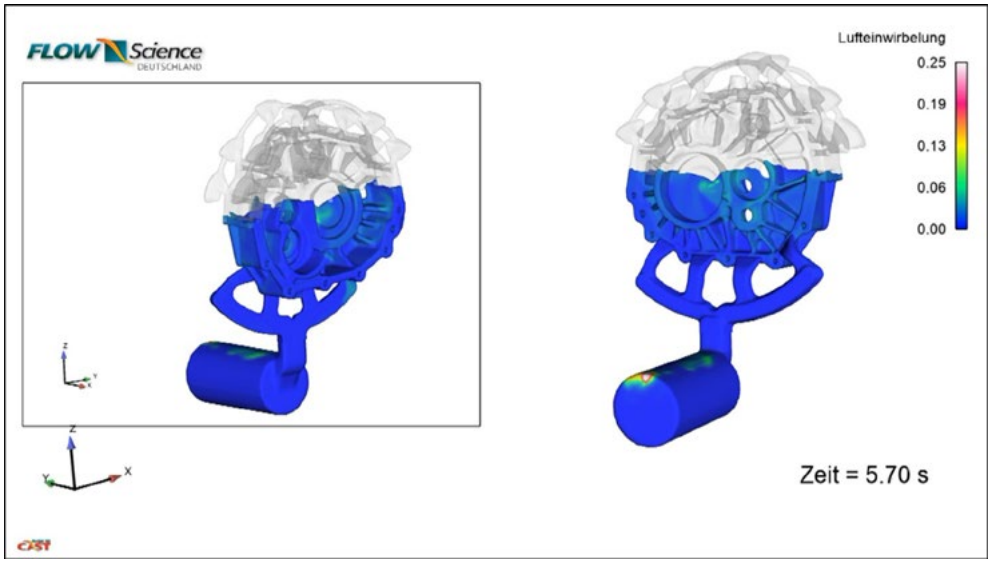

Fig.2 - Gas porosity entrained during the filling during a laminar HPDC process.

Conversely, there are several challenges that need to be addressed. The gating system needs to be adapted, as well as the venting system, and there is a high risk for cold run due to long filling time. Then, an heavy heating of the die must be expected, with the adaptation of the thermal control system and the development of a dedicated spraying methodology. In setting up this new method, process simulations had a great importance, being able to provide to the engineer prior to go the real machine, with all the consequent risks, all the information regarding both the casting quality and the mold temperatures, allowing the precise calibration of all the process parameters.

SALT CORES

To produce casting parts with a complex shape, often removable cores are adopted. Commonly sand cores are used but they have different limitations, for example in terms of surface finish and gas development. In the last years salt cores have been studied and brought to mass production because of the several advantages that they guarantee compared to the conventional sand cores. In fact, they can be removed without residues and risk of damage due to water solubility; there is no core gas development, so no porosity generation in an emission-free process; they produce high quality surface finishing, due to the very smooth core surface; they have a high stability against mechanical and thermal loads and they can increase the process robustness the casting quality. For these reasons, today they are used not only for the standard gravity casting applications, but also in HPDC.

To use salt cores in a such demanding process as HPDC, several considerations must be done prior to go in production. First of all, it is important to understand if the core, once in the mold and subject to the high mechanical and thermal loads typical of the process, will be able to resist. Process simulation software can help, being able

to detect precisely stress and deformations on the core during the whole filling phase.
Then, the production of salt core itself must be carefully investigated. There are various options: pressing, in gravity casting, in LPDC, in HPDC. Even in this case simulation software have been greatly helpful to understand the critical aspects of this new process. In fact, they can show in detail the filling and the solidification behaviour and allow to design and adapt gating and overflow system. Moreover, it is possible to optimize the process parameters and to keep in the correct consideration peculiar aspects, such as the residual stress and the high risk of shrink holes due to the very high density variation across the solidification.

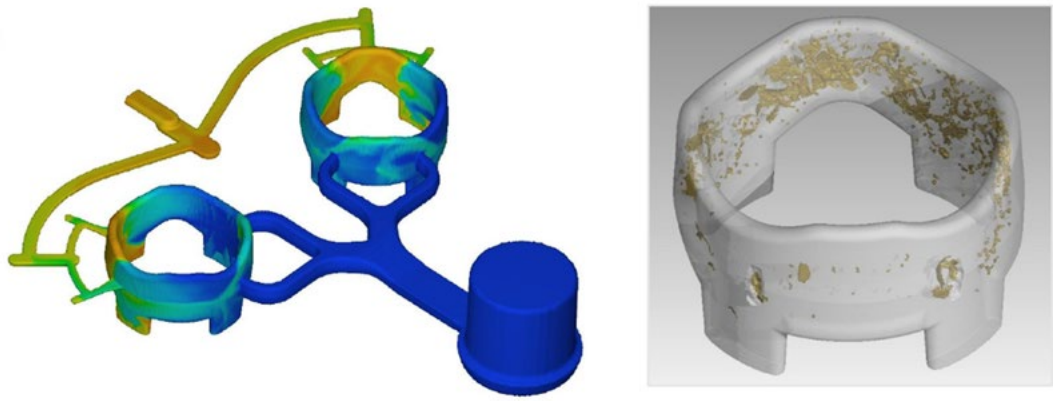

Fig.3 - Salt core production with an HPDC process and porosity prediction.

DOUBLE PLUNGER HPDC

To improve performances without increase excessively costs different techniques have been evaluated across the years. Among them, the idea of using two plungers during the same HPDC process has aroused a lot of interest and has been thoroughly investigated in order to grasp all its potential and criticalities.
The idea of this innovative process is to put in series two plungers in the same vertical shot sleeve, which move in opposite directions. First, the bottom plunger is moved near the top of the shot sleeve, to reduce the drop height during the pouring of the metal in the sleeve itself, slowly moving downwards to increase the available space in the sleeve. Then, both plungers move downwards, and the top plunger reaches and block the open surface of the metal. When the bottom plunger reaches the gating system, a fast and well-coordinated motion of the two plungers injects at a high pressure the metal in the mold.

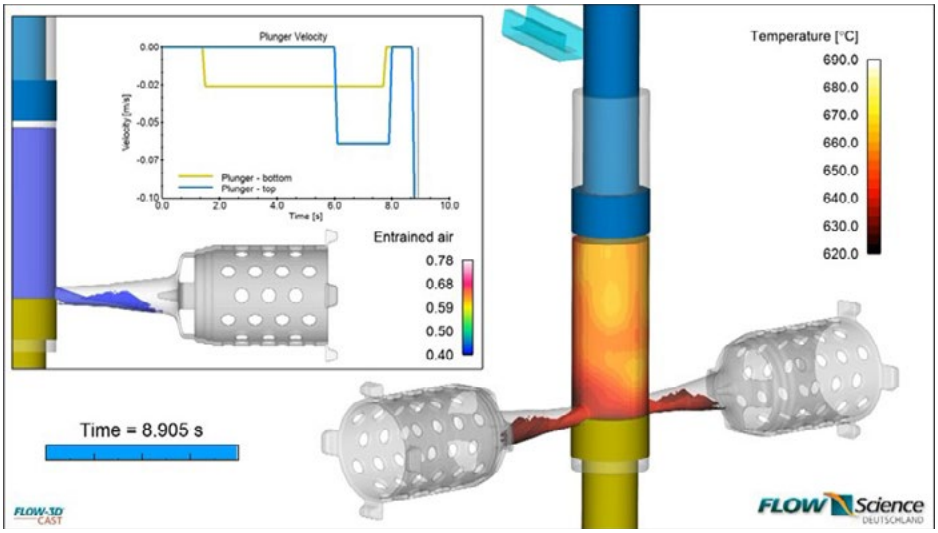

Fig.4 -Double plunger HPDC, beginning of the fast shot.

The possibility to work with a flexible simulate software, which allows to study several general moving objects at the same time, permitted to the developers of this concept to study the improvement in terms of casting quality of this process. Moreover, it allowed to perfectly calibrate the motion of the pistons, avoiding a premature compression of the metal and determining the perfect moment in which apply the fast shot.

CONCLUSIONS

Process simulation software are more and more common in the foundry industry, and they become even more useful when the development of a new process is investigated, allowing, with their accuracy, reliability, velocity and flexibility, to develop every detail of a concept highlighting both advantages and limitations in a very preliminary phase.

REFERENCES

[1] Todte M., Fent A., Lang H., Simulation in support of the development of innovative processes in the casting industry. Duesseldorf: GIFA Technical Forum 2015
[2] Wei G., A fixed-mesh method for general moving objects. Technical note FSI-05-TN73, August 2005, Flow Science ed.
[3] FLOW-3D CAST v5.1 User's manual. June 2020, Flow Science, ed.

La Metallurgia Italiana
International Journal of the Italian Association for Metallurgy

Development of a new process to recover aluminium from thin complex aluminium scrap to employ for primary aluminium alloys

I. Vicario, J. Antoñanzas, L. Yurramendi, J. C. Múgica, A. Abuin

Current thermal processes for the treatment of metals contaminated with impurities, especially with high contents of organic compounds, present problems in obtaining the metal fraction: the metal fraction oxidises with increasing process temperature and the contact with organic compounds. Often, the quality of aluminium obtained from "dirty" raw materials does not allow using it for applications requiring high metal purity or low metal oxidation (alloying tablets, aluminium shots, ...), or for HPDC structural parts. Some aluminium scrap streams cannot be recovered with existing processes and new developments are needed.

A new two-step continuous process has been developed. It consists of a heating process at 300°C in a controlled oxidising atmosphere furnace, followed by a second heating process at 400-550°C in an inert atmosphere, which results in a combined thermo-mechanical action. The obtained clean material can be continuously sintered under pressure, obtaining a product with a density close to 2.7 g/cc. Several "dirty" materials with initial contents up to 15% wt. C and up to 1.5% wt. O have been studied, reaching to final products containing as low as 0.15% wt. C and 0.3% wt. O. An example with a filter dust from shredding of aluminium profiles is described. The final composition of the product obtained after the treatment allows using the recycled aluminium as a high quality secondary raw material for aluminium alloying tablets, aluminium powder and high-performance aluminium casting alloys.

KEYWORDS: ALUMINIUM RECYCLING, COMPLEX ALUMINIUM SCRAPS;

INTRODUCTION

Aluminium processing residues, in the form of fine particles, sheets and chips, are difficult to recycle due to their high surface/volume ratio, small size with a high oxidising capacity and the presence of contaminants. Recycling aluminium leads to significant savings in energy and greenhouse gas emissions, with only a 5% of the energy required compared with the conventional molten salt electrolysis [1]. Aluminium is a critical raw material and multi-objective design approaches have been proposed to evaluate the environmental impact and the criticality issues linked to raw materials [2]. Aluminium scrap from aluminium profiles contains not only lacquers, but also plastic insulation materials. These profiles are shredded, and aluminium and plastic are separated. Fine particles are sent to a filter with a metal content between 80 and 90% wt. When melting aluminium scrap in a furnace, an

Iban Vicario, Javier Antoñanzas, Lourdes Yurramendi, Juan Carlos Múgica, Alberto Abuin
Tecnalia Research & Innovation, Basque research & technology alliance (BRTA), Spain

oxide layer forms on the surface, which results in metal loss and metal yield can be low (loss of material as high as 20%, with the thinner the scrap, the higher the losses). Conventional aluminium recovery methods based on scrap melting are the most widely used by secondary metal recyclers, involving high energy consumption and CO_2 emissions. Induction melting with protective atmosphere can also be used, but due to the higher cost of electricity compared to natural gas, induction furnaces are less used [3]. In Vortex melting system, which consists of a vortex that is generated by a stirring mechanical or electromagnetic device chips are added to the vortex and due to the speed and movement produced in the vortex, chips are immersed in the molten metal and they are melted in a short period of time. This system presents problems for melting lacquered aluminium or aluminium containing plastics, unless a protective atmosphere is employed. The study of a method combined vacuum pyrolysis with dilute sulfuric acid leaching to delacquer pyrolysis shows that the higher the pyrolysis temperatures, the less carbon presents in the solid residue, while the aluminium yield remains [4]. Direct hot extrusion technique in recycling of aluminium chips shows that properties of the extrudates depend on the process parameters and the alloying elements. High shear strain is required to disperse the oxide layer on the surfaces of the chip [5]. Friction Stir Extrusion recycling process based on the plastic deformation generated by the heat from the friction of the rotation and the chips was employed to obtain extruded products. The energy required is lower, but cracks were detected [6]. A procedure of cold compaction for chips and powder using uniaxial cold compaction followed by a sintering process allows obtaining a sintered product with a high density [7]. Though these processes represent a reduction in energy consumption, they are not industrialized.

MATERIALS AND METHODS

Materials

Filter dust from shredding of aluminium profiles and aluminium parts with high percentage of plastics was tested for organics removal with the developed process. The bulk density was only 0.3 kg/dm3. Particles were long and fines, and they contained organic plastics (PVC, PU...), wood, lacquers, paints... as shown in Fig. 1.

Fig.1 - Filter dust from shredding aluminium profiles.

Methods

Thermal Gravimetric Analyzer (TGA), model SETSYS Evolution, (SETARAM, France) was employed to determinate the variation in mass of the samples subjected to a temperature gradient. Samples were heated in air from 20 to 300°C (5°C/min) with a residence time of 1 hour at 300°C with a subsequent heating in an argon atmosphere (99.998% pure) from 300 to 550°C (5°C/min) and a residence time of 1 hour at 550°C. Tests were performed also in a laboratory muffle, model L9/C6, (EHRET, Germany) with 200 gr of every sample, combining a first process at 300°C in an oxidant atmosphere and a second one in an argon atmosphere at 500°C. To sieve the raw material an industrial circular sieve shaker, model FTI-0550, (Fil-

tra Vibración SL, Spain) was employed. Carbon wt.% was determined with an Automatic Analyzer, model CS-400, (LECO, USA) and Oxygen wt.% with a N, O, H Automatic Analyzer, model TCH-600, (LECO, USA). To simulate at the semi-industrial scale a continuous recycling process, 2 rotatory drum type furnaces were designed and constructed by TECNALIA. Both were equipped with an external electrical heating cover of 200 KW, vibratory feeders and fume extractions systems connected with a filter. The rotation speed of the furnace was adjustable from 1 to 80 r.p.m., with a calculated residence time for the material from 4 to 60 minutes. Temperature thermocouples were installed to automatically control by a PID system to maintain the objective temperature of the furnace camera and of the exhaust gases. Thermocouples were added to control temperatures. To avoid explosions, a continuous CO and O_2 gas concentration measurement system was employed. The inert furnace atmosphere was held inert by a continuous addition of N_2 gas, at a rate of about 60 l/min. The first drum furnace with an oxidizing atmosphere was constructed with internal helixes to allow a good mixing and movement of aluminium particles and swarf inside the furnace, avoiding particles agglomeration and a regular distribution of the heat. The second furnace was constructed in a similar way, but with a gas inlet and a near sealed vessel.

RESULTS AND DISCUSSION

The average wt.% composition and the standard deviation of as received sample have a C wt.% of 5.0±0.5 and O wt.% of 2.1±0.6. For employing the obtained material for alloying tablets / aluminium powder 0.5-1 %wt. for C and 0.3-0.5 %wt. for O are the acceptable values. TGA analysis showed a clearly defined peak in the oxidizing and in the inert atmosphere. Mass loss starts at approximately 200-250°C with a maximum at 289°C. Mass loss during this stage is a 3%. The second peak occurs in an inert atmosphere starting at 330°C. Mass loss in this case is a 4.5%. The total mass loss attributable to organics is 7.5%, in line with the C obtained by LECO and it would indicate that C present in the initial material is susceptible to being eliminated. Based on these results, seven different tests were performed in a laboratory muffle, combining a stage in an oxidant atmosphere (air) and in an inert atmosphere, as shown on Tab. 1:

Tab.1 - Laboratory tests at different temperatures with loss weights (LW).

Sample	Temp. (°C)	Time (Min)	% C	% O	LW (wt. %)	Temp. (°C)	Time (Min)	% C (wt.%)	%O (wt. %)	LW (wt. 5)
	Oxidant					Inert				
Test 1	300	0	-	-	-	550	120	0.19	1.13	4.5
Test 2-3	300	15	3.66	1.98	3.9	550	120	0.77	2.15	4.2
Test 4-5	300	30	3.11	1.73	4.1	550	120	0.59	1.70	4.3
Test 6-7	300	60	3.01	1.60	4.3	550	120	1.00	1.63	4.4

When a pre-treatment in an oxidising atmosphere it's performed at 300°C, partial C content is reduced in about 1.5-2%. During the subsequent treatment in an inert atmosphere, about a 2.5% of C% is eliminated. A possible explanation is that test material has a large helicoidal shape, so the dilatation of the chips could lead to an easier elimination of carbonaceous depositions from the chip surface. The minimum obtained O wt.% is 1.1% in the inert atmosphere. When a previous oxidising stage is introduced, there is an increase in the final O content, but the values obtained after the inert stage are similar to those obtained in the oxidising phase. It can be deduced that oxidation takes place during the first phase. The original oxidation cannot be reduced by only thermal treatments.

At 300°C an oxidation process starts, since it is not possible to reduce the value reached afterwards. It was so defined a maximum treatment temperature at the oxidant stage of 300°C.

Seven tests were performed to determine the maximum treatment capacity of the furnace in its oxidising at-mosphere treatment stage and the effect of the inert atmosphere treatment stage in the designed pilot plant. Different feeding rates and process parameters were defined at the semi-industrial trials, as shown in Tab. 2.

Tab.2 - Process parameters used at the semi-industrial scale tests.

Parameter / Sample	Test 8	Test 9	Test 10	Test 11	Test 12	Test 13	Test 14
Feeding rate (Kg/h)	30	60	90	120	90	120	120
Oxidant furnace temp. (°C)	450	450	450	450	300	300	300
Residence time at oxidant furnace (min)	10	5	5	5	15	30	30
Product temp. at the exit of oxidant furnace (°C)	265	380	440	480	135	135	135
Inert furnace temp. (°C)	20	20	20	20	-	-	450
Residence time at the inert furnace (min)	4	4	4	4	-	-	15
C (wt.%)	0.28±0.0	0.46±0.2	0.34±0.1	0.39±0.1	4.77±0.4	4.33±0.9	1.03±0.1
O (wt.%)	1.11±0.3	1.48±0.3	1.60±0.5	1.58±0.4	2.33±0.4	2.75±0.7	1.12±0.3

In Test 8, an oxidising stage with flame has been obtained inside the furnace, with a small reduction in the O wt.% in comparison with the original sample. The obtained O wt.% value was 1.1%, a value that coincides with that obtained in the laboratory in an inert atmosphere, and which could be interpreted as the percentage as-sociated with the intrinsic oxidation of the aluminium in the original product. When the feed flow rate increases, the oxidation of the obtained product increases. This may be due to the higher temperature that the aluminium reaches when the material feed to the furnace is increased, containing a higher organic charge per time unit. Temperature of the material at the exit of the oxidising furnace rises from 265°C with 30 kg/h of feed to 380°C at 60 kg/h, with values that reach 440°C and 480°C with feeds of 90 and 120 kg/h respectively. In Test 11 material, a flameless oxidising stage was followed by an inert stage. The feed was progressively increased up to 120 kg/h. Under these conditions, a very small reduction of C occurred in the oxidising. Further treatment in an inert atmosphere reduced the carbon content to 1 wt.%. With regard to O, it has been observed that the final value obtained (1.1%), after the inert stage, is similar to that obtained in the previous test (with flame inside the furnace) and in the laboratory test in the muffle furnace with inert atmosphere. On this basis, it is possible to confirm the existence of a limiting value for oxygen, which is approximately a 1% and which corre-sponds to an intrinsic oxidation of the aluminium fed to the furnace. Under these working conditions, the exit temperature of the product from the oxidising furnace was 135°C, which is far from the upper limit of 300°C established for the process. For a more adequate opera-

tion, this value should reach at least 200-250°C, which is the range where the first important mass reduction peak occurs according to thermogravimetry.
To continue with the study, a new lot of the studied material was employed. A reduction in the average of C wt.% was observed with C 1.4±0.5 wt.% and O 2.9±0.6 wt.%. These variations are very common in the recov-ery industry. The aim of these new tests trials was to work at a product outlet temperature of the oxidising furnace close to 300°C. Two setpoint temperatures were tested in the oxidising furnace (375 and 400°C). The process was carried out without flames inside the furnace. Process parameters are summarized in Tab. 3.

Tab.3 - Process parameters at the semi-industrial scale tests.

Parameter / Sample	Test 15	Test 16	Test 17	Test 18	Test 19	Test 20	Test 21	Test 22	Test 23
Feeding rate (Kg/h)	90	90	90	90	53	53	70	53	53
Oxidant furnace temp. (°C)	400	375	375	375	375	400	400	375	400
Residence time at oxidant furnace (min)	10	10	10	10	13	13	10	13	13
Product temp. at the exit of oxidant furnace (°C)	397	183	215	206	220	270	270	220	270
Inert furnace temp. (°C)	-	-	450	500	-	-	-	500	500
Residence time at the inert furnace (min)	-	-	15	30	-	-	-	30	30
C (wt.%)	1.6±0.4	2.1±0.1	0.3±0.1	0.2±0.0	1.6±0.1	2.0±0.2	1.7±0.1	0.4±0.1	0.6±0.1
O (wt.%)	1.1±0.3	1.1±0.1	0.8±0.2	0.4±0.2	1.4±0.2	1.0±0.2	1.3±0.1	0.7±0.0	0.9±0.1

The best results have been obtained in test 18, with a C of 0.24 wt.% and O of 0.45 wt.%. The oxidizing furnace remains in operation for a 24% of the operating time, with the temperature of the furnace oscillating between 371 and 390°C, for a set point of 375°C. The inert furnace remains in operation for a 29% of the operating time, with the furnace temperature ranging from 496 to 510°C, for a set point of 500°C. In the case of C wt.%, there is a clear reduction in the inert treatment, decreasing the final C wt.% by increasing resident time with the same operating parameters. A near 2% wt. of reduction in the O wt.% was obtained in the oxidizing furnace, probably due to the liberation of the aluminum oxide in the surface of the material by the induced dilatation of the increase of the temperature and by the mechanical attrition induced over the treated material. It can be observed a higher decrease in the final O wt.% by increasing the treatment tem-perature and the residence time.

The low C wt.% could be explained because when the material rotates in the interior of the drum, there is a combined thermo-mechanical effect over the treated material, promoting the collection of fines (inorganics and C) in the filter. This effect promotes a reduction in inorganics and C wt.% in the material treated, espe-cially in the inert furnace. Comparing the results obtained between the sample treated in the muffle furnace and the tests carried out at a semi-industrial level, C wt.% variates from 0.19-1.00

% in the muffle to an in-terval between 0.28-0.46 in the semi-industrial process with the same lot, and therefore there is a consid-erable reduction in C %wt. This is due to the fact that in the semi-industrial process, aluminium particles rotate inside the rotary furnaces, with friction between the aluminium particles and falling from the interior wall of the furnace when the material rises inside the furnace during the rotation, allowing part of the fine C particles to be extracted by the filtering system. In the case of the O wt.% with the first lot, the obtained values variated from 1.13-2.15 in the muffle to a range of 1.11-1.59 in the semi-industrial process. The val-ue obtained in the muffle is slighter higher because in the semi-industrial process some of the oxides are collected by the filter.

CONCLUSIONS

The use of a continuous recycling process involving a first oxidizing furnace combined with a second furnace, where the remining organics are pyrolyzed under an inert atmosphere, allows recycling complex aluminium scraps. The waste known as filter dust from shredding of aluminium profiles has very different levels of organic contamination depending on where it comes from. This fact, demonstrated in the analysis of the two lots, makes difficult to establish optimum general conditions for the treatment of this type of waste. The capacity and process parameters to be used in the treatment of a waste in the furnace is influenced by its organic matter content:

- If the organic content is medium-high, it is possible to work with flame or without flame inside the furnace. When working with flame, the treatment capacity for the defined composition interval de-creases, as the product overheats and tends to oxidise. If operating without visible flame, the treatment conditions can be wider, but unburned gases are generated, and they will need to be treated.
- If the organic content is very low, it is not possible to cause a self-ignition of the gases. Under these conditions, the treatment capacity can be increased but the generation of unburned gases that need to be treated is also increased.

In the second furnace with the inert atmosphere a final pyrolysis of the remaining carbonaceous is produced. A thermo-mechanical effect takes part in the furnace, combining an attrition of the aluminium particles among them and the surface of the rotating furnace at high temperatures. This mechanical effect allows removing carbonaceous particles from aluminium scrap and these fine particles are collected in the baghouse filter. This mechanical effect allows reducing the content of C in the final material.

The final quality of the product obtained depends on the initial quality of the product. If there is oxidised aluminium in the original waste, it will not be possible to reduce all the oxygen content. The technology can only reduce some of the oxygen liberated by the thermo-mechanical processing and liberated as fine particles.

The obtained final composition of the tested filter dust particles shows a best C %wt. less than 0.25 %wt., below the optimum of a 0.5 %wt. target. In the case of O, the best obtained values are below the maximum of a 0.5%wt. target. Thus, the semi-industrial trials confirmed the researched process as a valid technology for the obtention of aluminium material with compositions fulfilling the severe requirements to be used for aluminium alloying tablets and for high valuable aluminium alloys.

REFERENCES

[1] Capuzzi, S.; Timelli, G. Preparation and Melting of Scrap in Aluminum Recycling: A Review. Metals 2018, 8, 249. https://doi.org/10.3390/met8040249.

[2] Ferro, P., Bonollo, F., Cruz, S. Product design from an environmental and critical raw materials perspective. International Journal of Sustainable Engineering. 14. (2020). 1-11.

[3] Brough D., Jouhara H. "The aluminium industry: A review on state-of-the-art technologies, environmental impacts and possibilities for waste heat recovery". International Journal of Thermofluids. 1-2. (2020) 1-38.

[4] Li, N. & Qiu, K.. Study on De lacquer Used Beverage Cans by Vacuum Pyrolysis for Recycle. Environmental science & technology. 47. (2013)10.1021/es4022552.

[5] Wagiman, A., Mustapa, M.S., Asmawi, R. et al. A review on direct hot extrusion technique in recycling of aluminium chips. Int J Adv Manuf Technol 106, 641–653 (2020).

[6] Abdi R.; Mahdavinejad R.; Yavari A. et al. Production of Wire From AA7277 Aluminum Chips via Friction-Stir Extrusion (FSE). Metallurgical and Materials Transactions B. 45. (2014)10.1007/s11663-014-0067-2.

[7] Kadir M.; Mustapa, M. S.; Latif N. et al. Microstructural Analysis and Mechanical Properties of Direct Recycling Aluminium Chips AA6061/Al Powder Fabricated by Uniaxial Cold Compaction Technique. Procedia Engineering. 184. 687-694. (2017). 10.1016/j.proeng.2017.04.141.

Eco-sustainable lightweight automotive part manufacturing: GHGs-free die casting of brake leverage prototype made of AZ91D-1.5CaO magnesium alloy

F. D'Errico, D. Casari

Employing non-flammable AZ91D-1.5CaO Eco-Magnesium® (Eco-Mg) alloy in the European project CRAL provides the lowest carbon footprint for the magnesium cast process. Non-flammable magnesium AZ91D alloyed with Ca (in the form of CaO) was successfully processed by experimenting specific casting process window to melt the non-flammable magnesium alloy in a stationary furnace with no SF6 cover gas and then poured in the air into a vertical short-injection displacement press machinery specifically developed in EU CRAL project.
Brake leverage made of AZ91-1.5CaO Eco-Mg series alloy was successfully manufactured at Brembo Spa premise, as a real example of Mg cast component alternative to the current component made of forged aluminium alloy. As discussed in the experimental part, a preliminary computer-aided simulation test campaign reduced uncertainty in cast trials. The CRAL EU project with the realization of Mg-SF6 free cast part for brake systems has promoted the drastic reduction of Global Warming Potential (GWP) of the Mg cast process route. The Eco-Mg series is a feasible and affordable casting solution for introducing non-flammable Mg alloys in the automobile sector; today struggled for researching cost-driven lightweight components due to forthcoming CO2 emissions restrictions.

KEYWORDS: MAGNESIUM, CALCIUM OXIDE, SUSTAINABLE METALLURGY;

INTRODUCTION

Led in the last century by the aerospace industry, the development of magnesium alloys has historically occurred to meet the needs of the transport industry, which sought to find advantages on additional strategies related to weight reduction. Compared to aluminum alloys, magnesium has a high castability and reduced chemical compatibility with the steel used in constructing the molds. This property makes it possible to realize part geometry at very high complexity (similar to those realized with plastics), extending steel molds' lifespan.
Although these are great promising features, safety is still a concern due to high flammability when magnesium is treated in the air. Once ignited, magnesium proceeds with its self-combustion sustained by an exothermic reaction forming magnesium oxide, releasing heat. As a result, the combustion flame rapidly reaches temperatures between 2,000 ° K and 4,000 ° K. For this problem, magnesium

F. D'Errico
Politecnico di Milano, Department of Mechanical Engineering, Milan, Italy

D. Casari
Brembo Braking Systems, Stezzano, Italy

alloys require unique melting plants and expert personnel, increasing the production cost of cast parts. To safely control Mg alloys in the molten state, it is necessary to eliminate the presence of O2 in contact with the metal bath; that is to say, it is necessary to eliminate the primary trigger source of the Mg combustion reaction. Removing oxygen is possible by creating inert atmospheres towards the molten Mg. Various techniques are used in Mg foundries divided into a) vacuum melting plants, b) melting plants equipped with inert and protective atmospheres of the Mg bath. The inert atmospheres usually used are mixed SF6 and CO2, based on freon gas R-134a and SO2. Both SF6 and freon gas R-134a are greenhouse gases with very high global warming potential (GWP).

In contrast, SO2 gas, despite being a valid alternative to greenhouse gases SF6 and R-134a from an environmental point of view, requires stringent application protocols due to its high toxicity for operators. The SO2 gas would be a green solution against SF6, but it is highly corrosive to the equipment made of steel; it reacts readily with water to form H2SO3, thus provoking health risks for workers, especially for the skin and lungs. Compared with SO2, SF6 is non-toxic, non-corrosive, but

due to the negative impact on the greenhouse effect, by 1 January 2018 in the European Union, SF6 has been prohibited in magnesium die-casting in the recycling of magnesium die-casting alloys [1].

Today it is common knowledge that the choice of lighter materials for manufacturing combustion engine-powered vehicles plays a crucial role in reducing emissions. For automakers, the weight saving is not only a key strategy to be compliant with a green-consciousness market pushed by demand more and more aware of the environmental and social impact that comes with eco-responsible purchases. The new stringent targets set in the EU for the fleet-wide average emissions of new cars and vans include, together with penalty payments for excess emissions, a mechanism to incentivize the uptake of zero- and low-emission vehicles. However, cleaning up vehicle emissions at the tailpipe is an effective but partial measure if we refer to an enlarged green-manufacturing view.

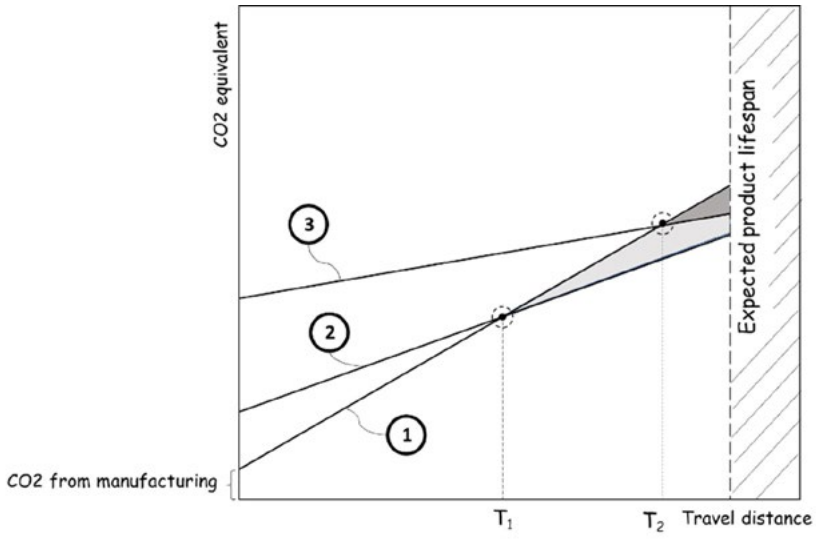

Fig.1 - Three qualitative scenarios for addressing at-a-whole the environmental impact over the product lifespan of using light metals (2) and (3) to substitute the heavy solution (1).

If we point out the linear function emissions over travel distance as it is depicted in Fig.1, we can just consider two scenarios: the baseline scenario of part made of heavy ferrous alloy (1), and two different lightweight solutions, capable of answering the same functional property of the steel-made part. Depending on the "slope" and the initial carbon footprint "stored" in early alloy manufacturing and part shaping, even though the direct CO2 emissions are lowered (look at the slope of (1) and (2) solutions), the break-even point could be reached after long-distance traveled. The problem depicted by (3) in Figure 1 is typical of magnesium alloy fabricated starting from primary magnesium ingots obtained by small—scale Pidgeon processes based on thermal reduction of magnesium-be-

aring ores (like dolomite) with silicon (usually supplied in from of ferrosilicon) conducted in coal-fired retorts [2]. Furthermore, due to its high reactivity, magnesium needs to be cast for product shaping using protective gases. In the past, SF6, the preferred cover gas, was replaced by mixtures of CO2 and SO2 by HFC-134a. Recently the Novec 612 fluid registered by the 3M Company promises a very low GWP of 1, equivalent to CO2. Several studies have shown that magnesium auto part produced by raw material fabricated by Pidgeon process and secondly shaped by casting using pollutant cover gases could not save CO2 within the car's lifespan [3].

The high Mg reactivity with oxygen is the low density of the magnesium oxide layer formed during melting in the presence of oxygen. Although various metals form a thick, dense, and non-porous oxide layer, this does not apply to magnesium [5-9]. The volume change between molten metal and the oxide layer formed on the top surface is responsible for surface stresses (Fig.2).

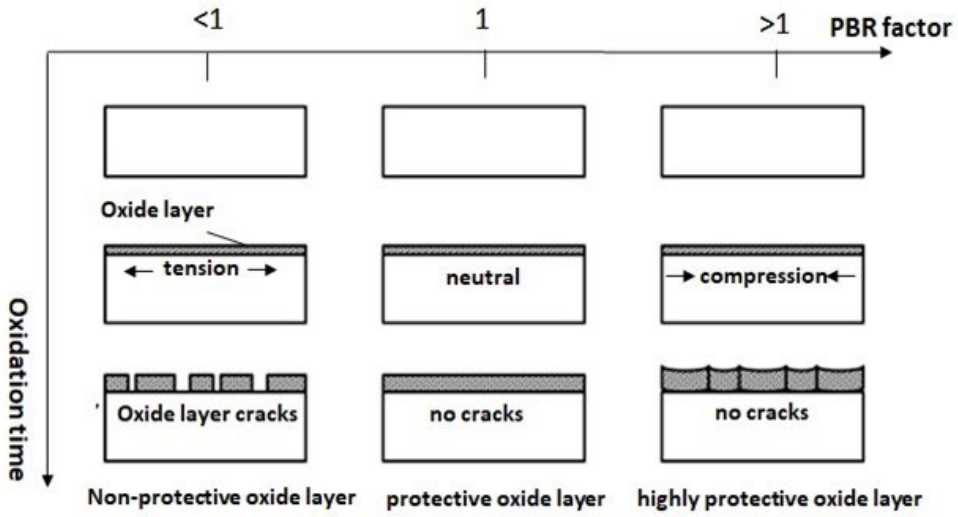

Fig.2 - The PBR explanation of the high temperature oxidation behavior of different metals and their oxides in correlation with porous or non-porous oxide film developed by air oxidation.

The Pilling-Bedworth (PBR) ratio between the molar volume of oxide concerning the molar volume of metal is an indicator to evaluate either tensile or compressive stresses developed in the oxide layer [5]. For PBR < 1, tensile stresses form and cause the oxide layer cracking. Emley [6] found that up to 450 °C, magnesium forms a protective layer, but above 450°C, it becomes porous and non-protective. The time to ignition depends on the magnesium alloy composition [8,9]. The protective gases used in the magnesium industry form a dense protective layer on Mg melt. A recent approach is to add unique alloying elements to improve the ignition resistance. Additions of small amounts of Be, Al, and Ca [6] enhanced the oxidation resistance of solid Mg alloy near the melting point and that the alloy could be melted in the air if the oxide skin on the ingot was not broken. Sakamoto et al. [10] verified that the oxide film on the Mg–Ca consists of CaO surface thin layer, and just below this layer, a mixture of MgO–CaO exists below this layer. To date, the main reason for this protective effect from Ca-O is not clarified. One prominent hypothesis embraces the PBR rule, the higher thermodynamic stability of Ca-O added oxide layer and the kinetics of the diffusion and reaction of Mg ion at and trough the oxide layer formed by the mixture of MgO and CaO the large volume of CaO might compensate for the shrinkage due to MgO formation [11]. Consequently, the compositions of the Mg alloys can be used to improve the ignition and oxidation resistance of Mg alloys. Among possibilities, the ECO-Mg (Environment COnscious magnesium) alloy system based on CaO addition is available on the market [12].

Following the urgent need to find new eco-compatible solutions to process Mg with a drastic reduction of the carbon footprint, reduction of total GHGs emitted over product cycle of Mg cast parts would be challenged by

elimination of protective gases during the cast part manufacturing (protective gases is still used for master alloy production).

EXPERIMENTAL PROCEDURE

A commercial Eco-Mg series alloy AZ91D with a nominal composition of 8.5% Al, 0.75% Zn, 0.3% Mn, Fe and Ni below 0.001%, and Mg as a balance modified with 1.5%CaO provided by Korea Institute of Industrial Technology was employed as experimental material. The as-cast microstructure when supplied in ingot and it shows usual microstructure of high aluminum content casting magne-sium alloy with coarse structure of α-Mg and the network of eutectic β-Mg17Al12 compound discon-tinuously distributed at the grain boundaries (fig. 3).

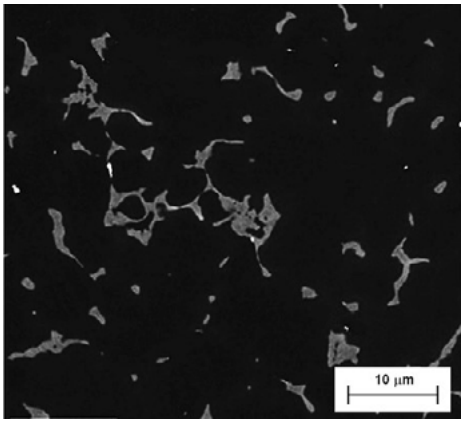

Fig.3 - SEM image of as-cast billet received.

A vertical injection die-casting press machinery in the Advanced Materials Research and Develop-ment laboratories in Brembo facility in Stezzano has been employed for casting the eco-magnesium metal alloy. The machinery is a scale-down replica of the industrial press machinery developed and installed in Brembo foundry during the European CRAL Life project terminated in December 2019.

Tab.1 - Main machine press and cast part dimensioning data.

Machine characteristics		
Injection plunger velocity (two velocity stages available over plunger total stroke)	0,28 (+10%)	m/sec
Plunger total stroke	100	mm
Theoretical locking force	700 (+15%)	kN
Projected complete shot area	135	cm2
Specific pressure on metal (max)	533	kg/cm2
Injection force	200 (+15%)	kN

In table 1 are gathered main machine dimensioning data. The adoption of vertical lay-out was based on main objective of reducing as possible injection plunger stroke in order to target several benefits, such as:

- reducing duration of the injection phase, thus decreasing total cycle time of the process with semisolid metal handling;
- reducing the displacement velocity of plunger during injection in order to reduce turbulence; the maximum injection velocity set in the press machine is 135mm/s, actually around 1 order of magnitude lower than conventional horizontal high pressure die casting machine;
- (thanks to the bottom-up vertical injection layout) reducing total quantity of air to evacuate during injection; this implies it is possible to reduce the maximum injection pressure required for air elimination, resulting in compact size of the machine and consequently low equipment cost.

RESULTS AND DISCUSSION

An AZ91D commercial alloy with the addition of 1.5%CaO compound was tested, avoiding uses of SF6 since it has been banned for die-casting process in Brembo foundry. To that scope, the commercial Eco-Mg AZ91D-1.5CaO has been employed to retard oxidation of magnesium in a molten state with the high risk of burning reaction to start and ignite not self-extinguishable flame.

As the ignition of conventional Mg alloys occurs because of porous MgO surface oxide film at high temperature, CaO added in Mg is thought to solidify with reactive phase formation Mg2Ca, regard-less of CaO contents and process condition [13]. Expressly, during oxidation under an ambient at-mosphere, the Mg2Ca phase on the surface might dissociate by oxygen to form on the molten metal layer directly exposed to air because of porous MgO [13]. This way, a thick, continuous, and protec-tive oxide film consisting of CaO and MgO forms isolating metal baths from the atmosphere. It is reported by Kim et al. l. [13] the 1.5 mass %CaO added AZ91 Mg increased at 615°C, thus about 300°C compared to conventional AZ91D alloy.

Due to the low quantity of magnesium to cast in press machine and its poor heat capacity (substance with a low heat capacity, will heat and cool quickly), to avoid incomplete filling of such a complex cavity, it was necessary to increase the melting temperature in the stationary furnace up to 700°C. That allowed to maintain the final pouring temperature above 630°C when poured in the pre-heated injection chamber within the range 220-250°C. Therefore, the alloy was overheated in a closed fur-nace in air, but for over 10 minutes, it exhibited early ignition problems, safely controlled by using protective flux with CaF powders. Therefore, the other test campaign was devoted to reducing the stationary furnace's oxygen content to eliminate the use of any type of fluxes to protect the molten bath from oxidation.

The ultimate solution was found by mounting a cap that covered the furnace by a hermetic seal for insufflation of a small quantity of nitrogen; insufflation of nitrogen limited the oxygen content inside the furnace and created slight internal overpressure to avoid fresh oxygen to be introduced from outside.

Due to the revised stationary furnace equipment, the molten magnesium alloy was safely maintained in overheating conditions for a prolonged time (up to 1 hour during casting tests). No ignition prob-lems occurred during a few minutes (not more than 2 minutes) of fresh air exposure of the overheated magnesium necessary for the following steps: a) dosing the proper volume of metal by the use of a second pre-heated dosing refractory crucible, b) final pouring of proper magnesium alloy volume into the hot injection chamber.

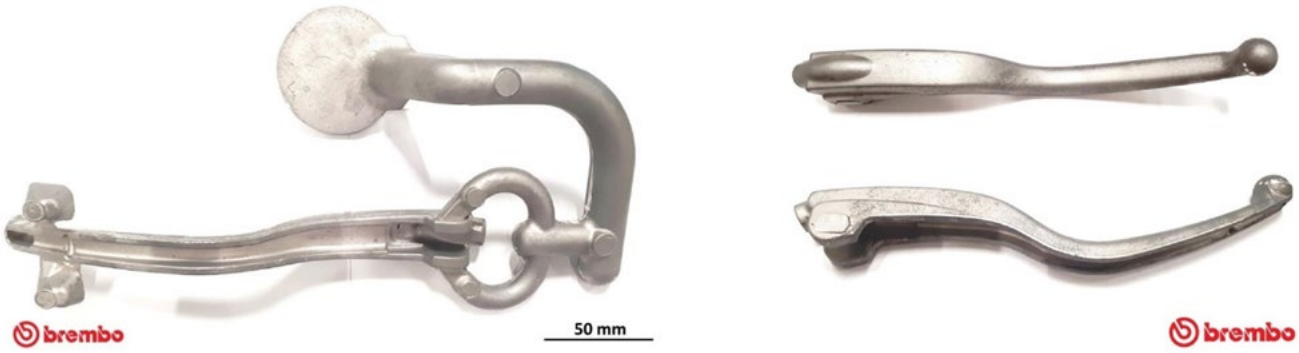

(a) (b)

Fig.4 - a) The die-cast brake leverage with in-gate channels and sprue; b) die-cast brake leverage after re-moving sprue and in-gate channels.

In fig. 4a is shown the prototype of the magnesium brake leverage produced by no GHG die-casting process as die-cast with in-gate channels and sprue. The same is in Fig.4b after cut of channels and sprue, with a non-finished surface, to be mounted on bench test for mechanical testing and valida-tion, in ongoing phase in Brembo mechanical testing laboratories.

CONCLUSIONS

A vertical high-pressure die-casting process was performed with an AZ91D-CaO added magnesium alloy to manufacture the first prototype of magnesium brake leverage without using highly environ-mentally impacting protective gases usually employed in casting conventional magnesium. A net re-duction of 32% weight has been obtained compared to the current aluminum-made part. The pro-cess route employed has been successfully conducted safely in the air, thanks to very compact cycle time. This preliminary test campaign puts some promising premise to the affordable cover gas-free die-casting process by such results. Furthermore, the possibility of processing commercial Eco-Mg system alloys in the air in a compact and low-cost press machine that can work for Mg and Al alloys is an interesting perspective for increasing machine occupancy, one key economic aspect to consid-er in industrial manufacturing processes.

ACKNOWLEDGMENTS

This work uses results produced by the CRAL project (http://www.cralproject.eu/en), co-funded by the European Commission within the LIFE+ Programme. Authors thank support provided by Europe-an Commission for supporting project dissemination activities. This work reflects only the authors' views. The Community is not liable for any use that may be made of the information contained there-in.

REFERENCES

[1] EU Regulation (EU) No 517/2014.
[2] S. Ramakrishnan et all., "Global warming impact of the magnesium produced in China using the Pidgeon process," Resources, Conservation and Recycling, Volume 42, 1: 49–64, 2004.
[3] D'Errico, F., Ranza, L. "Guidelines for the market competitiveness of sustainable lightweight design by magnesium solution: a new Life Cycle Assessment integrated approach", Paper presented at the 72nd Annual World Magnesium Conference, Vancouver, Canada, 17–19 May 2015.
[4] H.E. Friedrich, et all., "Solutions for Next Generation Automotive Lightweight Concepts Based on Material Selection and Functional Integration", Magnesium Technology 2018, The Minerals, Metals & Materials Society, 343–348, 2018.
[5] N. B. Pilling, R. E. Bedworth, "The oxidation of metals at high temperatures", J. Inst. Met, 29: 529–591, 1923.
[6] E. F. Emley, "Principles of magnesium technology" Pergamon Press, Oxford, New York, 1966.
[7] G. C. Wood, "High-temperature oxidation of alloys", Oxidation of Metals, 2:11–57, 1970.
[8] F. Czerwinski, "Oxidation Characteristics of Magnesium Alloys", JOM, 64 (12):1477– 1483, 2012.
[9] Y. M. Kim, et all., "Key factor influencing the ignition resistance of magnesium alloys at elevated temperatures", Scripta Materialia, 65(11):958 – 961, 2011.
[10] M. Sakamoto, et all., "Suppression of ignition and burning of molten Mg alloys by Ca bearing stable oxide", Journal of Materials Science Letters, 16 (12):1048-1050, 1997.
[11] S.H. Ha et all., "Effect of CaO on oxidation resistance and microstructure of pure Mg", Materials Transactions, 49(5) 1081-1083, 2008
[12] S.K. KIM and J. H. SEO, "Magnesium-based alloy for high temperature and manufacturing method thereof", US Patent 8,808,423, 2014.
[13] J.K. Lee, S.K. Kim, "Effect of CaO Addition on the Ignition Resistance of. Mg-Al Alloys", Materials Transactions, Vol. 52, 1483-1488, 2011.

Evaluation of the use of foundry sand cores on solidification and on the characteristics of structural castings: a comparison between organic and inorganic cores and validation with simulation

A. Mantelli

In recent years, the interest in more sustainable and green production has led to searching for new processes and materials to be used especially in foundries. An example is given by the increasing use of inorganic cores instead of organic ones to produce complex and structural aluminum alloy components. The great advantage is related to the reduction of the emissions of toxic substances (such as formaldehyde and phenol), making the working environment healthier. Despite this, the information about the characteristics of this type of materials with inorganic binders is still very low. For this reason, this paper aims at characterizing inorganic cores, especially evaluating the thermal properties of these materials and estimating how they exchange heat with aluminum. Additionally, a comparison between the inorganic and organic sand cores was done in terms of thermal properties. Moreover, in order to evaluate their influences on the alloy solidification and, consequently, on the quality of the casting, properties obtained from the components made with the two different sand cores were analyzed by hardness and tensile tests as well as microstructural analysis. Finally, the measured thermal properties of the inorganic cores were implemented in the casting simulation software ProCAST®. The good agreement between the simulation and the experimental data demonstrated how it is important to know the correct properties of the inorganic sand cores and, in general, the accurate data of the materials to obtain reliable output.

KEYWORDS: FOUNDRY, SAND CORES, GRAVITY CASTING, NUMERICAL SIMULATION, ALUMINIUM;

INTRODUCTION

Foundries play a very important role in the industrial sector, since it is possible to obtain very complex and performing components with a relatively simple production processes and low costs. Among the main casting techniques, gravity casting represents an interesting method to produce structural elements used especially in the transportation field.

Obtaining large-sized pieces with complex and hollow geometries is possible using the so-called cores. These allow the creation of holes and undercuts inside the castings, limiting or eliminating secondary processing. The cores consist mainly of sand which is made moldable and compact thanks to the addition of binders through distinct processes, depending on the type of the cast metal and

Anna Mantelli
Università degli Studi di Brescia

the final characteristics of the parts to obtain [1].
The sand used and thus the cores must have certain requirements including thermal and dimensional stability, mechanical strength, proper permeability and sterrability. Thermal and dimensional stability is essential since it is necessary to ensure a reduced expansion of the sand particles during the mould filling, resulting in an increase of temperature of the sand due to the heat exchange with the liquid alloy, and during the subsequent solidification with the release of latent heat [2]. On the contrary, excessive expansions, cracks and dilatations of the shape could occur, resulting in a casting with incorrect tolerances and defects. Due to the high pressures created during the casting phase, it is also important to ensure good mechanical resistance in order to prevent the penetration of the metal into the core and to guarantee the correct filling of the mould. The permeability, that is the tendency to let gas pass through, is also fundamental for obtaining porosity-free components. Finally, to ensure that the sand could be evacuated from the component after casting, it is essential that it is easy to be removed through the application of mechanical vibrations, to preserve the dimensions of the piece and avoid any deformation.

One of the main problems of foundries is related to the impact the cores have on the environment, which is significant due to gas emissions and the production of polluting waste. The growing demand by the European Parliament [3] to limit the emissions of toxic substances has therefore prompted companies to explore new alternative processes in order to create a healthier work environment. Especially in the automotive sector, a vehicle is evaluated as low polluting not only when it consumes and emits little on the road, but if it is also built with parts and materials whose production has a low environmental impact. For this reason, many companies have invested in the research of new materials and technological processes to obtain less impacting cores that allow to limit the emissions of harmful substances since most of the contaminants come from the combustion of organic binders used to make the cores [4].

In this regard, core production processes using inorganic binders have been developed in order to replace the cores made with organic resins. Most of the inorganic cores are made with sodium silicate which is obtained by melting at high temperature (over 1300°C) [5] high purity silica sand and sodium carbonate. Furthermore, in recent years, the Cordis process has been growing interest, using two types of binders both based on inorganic substances (Cordis and Anorgit). This type of process guarantees the creation of cores suitable to produce structural components in light alloy.

Among the various advantages in the use of inorganic cores there is certainly the reduction of the release of polluting gases, such as formaldehyde and phenol, since there is no degradation of the polymeric resin. This means that also the final products could be characterized by a lower quantity of porosities inside the castings. Additionally, there is no release of unpleasant odors into the environment. Thanks to the use of inorganic cores, therefore, the air in the foundry is significantly cleaner and this results not only in a more favorable condition for workers but also in a reduction in costs for purification plants. Inorganic systems, especially those using the Cordis binder, cannot burn or degrade at high temperatures (up to about 900°C). This is an advantage as it ensures that the core has a high thermal stability during the casting phase, avoiding possible erosions, penetration of the molten metal and/or geometric deformations. Another important advantage is related to the thermal conductivity, which is particularly high. This is since once dried the system with inorganic binder can be assimilated to a glass, whose conductivity is indeed high. Since the quantity of fumes and gases during casting is reduced with the use of inorganic binders, it is not necessary that the cores have a high permeability which allows to use sands with a finer grain size, compared to those obtained with polymeric resins. This allows obtaining a generally better degree of finish for the castings obtained with these cores. One of the negative aspects of the use of inorganic cores is their tendency to absorb moisture: since water is the only solvent of the binder, the core tries to establish a balance with the external environment resulting in a loss or reabsorption of moisture which can lead the breaking of the core itself [6].

Unfortunately, there are only few studies involving the characterization of Cordis inorganic sand core: the limited availability of experimental data on the properties makes difficult to define these materials, in particular for what concern the simulation of the process. The reliability of a simulation depends on the correctness of the input data, this means that a simulation, in which the inorganic sand

core properties have not been implemented, with the risks of providing results that differ significantly from reality.

For this reason, the aim of this paper is to investigate the characteristics of the inorganic sand cores obtained with Cordis Process evaluating their thermal properties. At first, it was done a comparison between the inorganic and organic sand cores in order to evaluate the different thermal properties. In order to do this, it was studied an automotive component produced in FMB S.r.l. The component was characterized in terms of tensile and hardness tests. To better evaluate the effect of the different cores on the casting solidification, a deep metallurgical investigation was performed by optical and scanning electron microscopes. Also, the secondary dendrite arm spacing (SDAS) was measured. Additionally, simulations of the component were done according to the parameters used during the process and the thermal properties obtained during the experimental phase.

MATERIALS AND EXPERIMENTAL PROCEDURE

The experimental procedure was based on the production of some oil pans (Fig. 1) made of AlSi7Mg0.3 aluminium alloy, using gravity casting process in a permanent mould with two distinct sand cores (organic and inorganic).

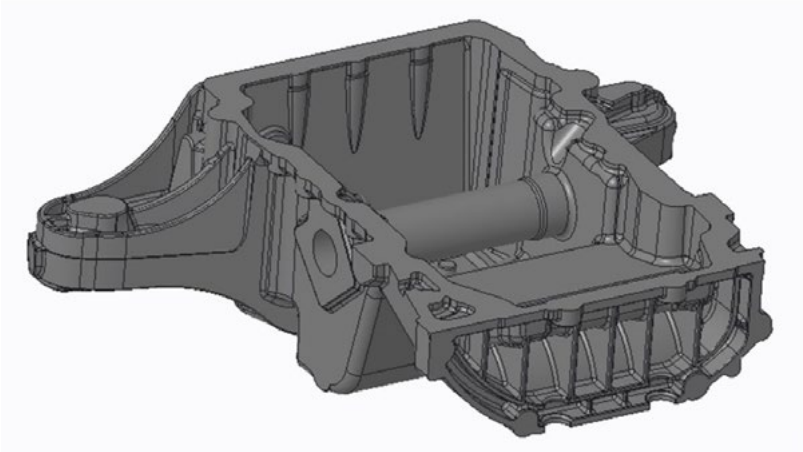

Fig.1 - Oil pan evaluated for the experiment.

As above mentioned, for this study, two types of cores were used: one inorganic and the other organic. The sand cores used to obtain the central tube are showed in Fig. 2: on the left the organic sand core and on the right the inorganic one.

Fig.2 - Organic (left) and inorganic (right) sand core used to obtain the tubular zone of the component.

The inorganic core was obtained through the Cordis process [7], which is a process that can be considered a Hot-Box system but using also hot gassing air. For this reason, metal (steel or cast-iron) core boxes are required, equipped with an adequate heating system. The temperatures of the molds can vary from 120°C, for forming cores with thin sections, up to 200°C, for forming cores with high thickness areas. The binder system consists of two components: Cordis (liquid binder) and Anorgit (additive powder). The correct procedure for preparing the mixture involves dosing the refractory sand into the mixer. The Anorgit powder is then added, and everything is mixed for a few seconds in order to distribute and homogenize the additive with the sand. In the meantime, with appropriate dosing systems, the amount of Cordis to be inserted inside the hopper is prepared. The liquid binder is added and mixed until completely homogenized, which usually takes a few minutes. The simultaneous addition of the powder and liquid parts is to be avoided, as agglomerates that are difficult to homogenize can form. Generally, the percentage of Cordis added is around 1.8-2.5% and it is chosen according to various parameters, including: the type of Cordis, the type and grain size of the refractory sand, the geometry and any mechanics requirements of the core. The percentage of Anorgit instead is around 0.9-1.2%.

The organic core was made with the Croning method, that is a shell-molding technology. The sand used is silica in percentages of about 98%, while the resinous part is around 2%. The latter is made up of phenolic resin of the novolac type (free phenol less than 1%), partially polymerized and lubricated.

After the melting of the aluminium inside the furnace, it moved to the degassing unit in order to reduce the hydrogen content. After degassing, a sample of the alloy was collected to evaluate the hydrogen level. The filling phase was done according to the specifications defined by the company during the production process. All the components obtained were desanded to remove the cores and underwent a T6 heat treatment of solubilization and artificial aging (the proper data, being considerable, is not report). In order to evaluate the casting parameters, various data were acquired to be able to set the simulation with the most accurate process parameters: the times of the casting cycle and the temperatures reached by the mold. Thanks to the identified data and the defined specific heat values of the inorganic core, several simulations were carried out to determine the reliability of the experimental results obtained. Furthermore, three thermocouples were set up inside the inorganic core (Fig. 3) during the production phase, in order to acquire the temperature trend inside them and compare it with the simulation.

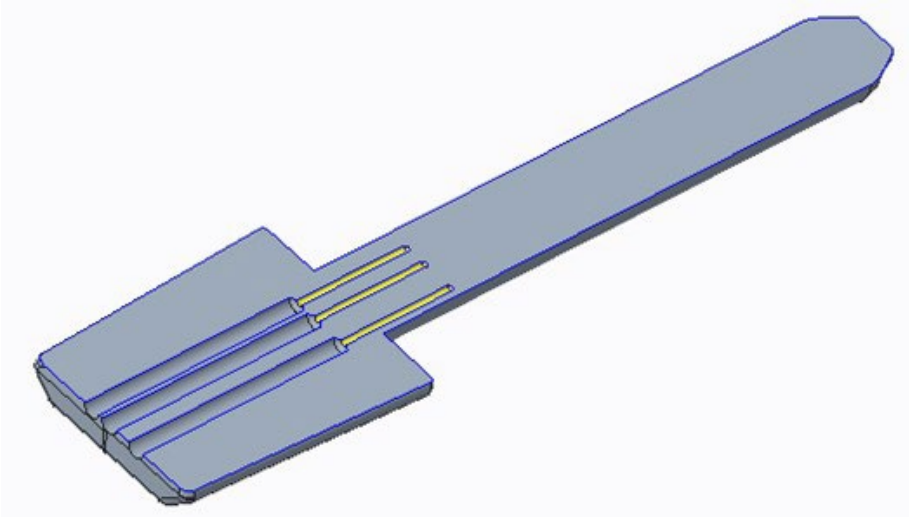

Fig.3 - Core section with the position of the thermocouples.

For this study, three different oil pans were analysed: two were obtained using inorganic sand cores and one using organic sand cores. As said before, one of the most important problems of the inorganic sand cores is the tendency to adsorb moisture. To study this phenomenon, the cores used to obtain one of the oil pans were stocked external to the warehouse: the sand cores absorbed moisture inside and on the surface. This was done in order to determine the influence of the moisture content of the core on the quality of the final components.

Three samples were taken from the tubular zone of the part in order to be able to determine the mechanical properties as it is shown in the Fig. 4. The results will be presented as the average of the three samples.

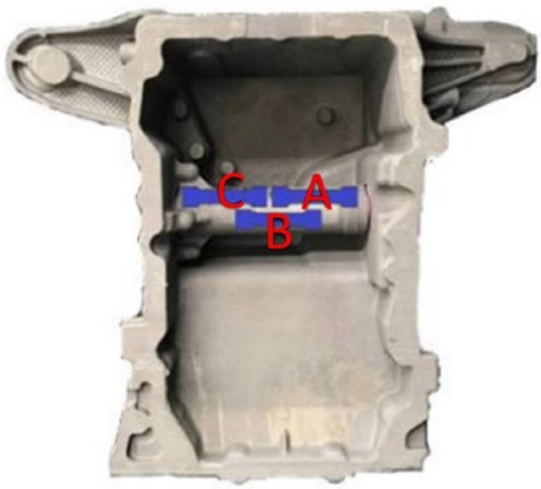

Fig.4 - The three samples taken from the tubular zone named A, B and C.

At first, a thermal characterisation of the inorganic and organic sand cores was carried out in order to compare the materials using the differential scanning calorimetry (DSC). The samples used were 30/40mg and they were kept compact: the sand was not crumbled in order to consider the overall properties of the system. The test was carried out with a DSC/TGA TA Instrument Q600 SDT under argon atmosphere and was performed according to the ASTM C351-92 [8], in particular:

-50°C was reached.
-5 minutes of isothermal at 50°C.
-Heating rate of 20°C/min up to 800°C.
-5 minutes of isothermal at 800°C.

Tensile and hardness tests were carried out on the oil pans and some images from the scanning electron microscope were taken. The measure of the SDAS was obtained using the optical microscope in order to evaluate the microstructure and compared it to the simulation results. The tensile test was done using an Instron machine on rectangular section samples according to the specific defined by the company [9]. The load cell used was 250kN and the strain gauges was long 25mm, as long as the grip length.

The hardness test was carried out using an automatic machine with an indenter of 2.5mm and a force of 612.5N. The sample was kept perpendicular to the indenter for 8 seconds and five surveys were obtained.

Microstructural analysis was performed by using an optical (LeicaDMI5000M) and a scanning electron microscope (LEO EVO 40) and the fracture surfaces of the tensile test samples were evaluated. The images were acquired with different magnifications: 100X, 500X and 2500X.

Finally, optical microscope was used to evaluate the SDAS from the tubular zone, comparing the different oil pans obtained with organic and inorganic sand cores. Three different images were considered for each oil pan with a magnification of 50X and three different dendrites were analysed for each picture.

Subsequently, a series of simulations with inorganic sand

cores was done. In details, the commercial simulation software ProCAST® was used, using a 3D model of 21 elements. A simulation using the properties available in the software database and another one with the thermal properties of the sand cores experimentally measured (specific heat, density and conductivity) were carried out and compared in terms of temperature profiles and SDAS. To check the reliability of the simulation, the microstructural and thermal results were compared with experimentally recorded.

RESULTS

Characterization of the sand core

The DSC test was done according to standard and was carried out in order to determine the specific heat of the organic and inorganic cores. The specific heat [10] was determined according to the relation presented below and reported in the ASTM standard [8]:

$$c_p^{sample} = c_p^{sapphire} \left(\frac{\Delta H_{empty} - \Delta H_{sample}}{\Delta H_{empty} - \Delta H_{sapphire}} \right) \frac{m_{sapphire}}{m_{sample}} \qquad \text{(eq.1)}$$

- cp is the specific heat.
- ΔH the enthalpy difference measured.
- m the mass of the samples used.

The test was conducted at least twice, to obtain more data for statistical purposes, and the average of the results is shown in Fig. 5 (the proper data, being considerable, is not report).

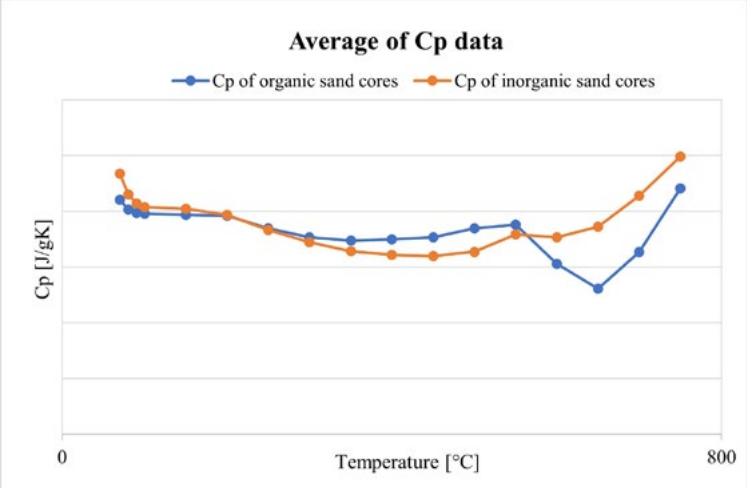

Fig.5 - Average of the tendency of the Cp obtained by organic and inorganic sand cores.

As it can be seen from the data obtained, the curves result similar, although it is possible to observe that the values identified for the specific heat of the organic core are slightly higher. However, there is a significant decrease at higher temperatures: this is related to the decrease in weight of the sample of about 1% that was observed for the organic cores (the analysis was done with the TA program Universal Analysis). It is reasonable to assume that in correspondence of these temperature values, there is a degradation and therefore elimination of the phenolic resin used as binder.

The higher is the value of the specific heat, the higher is the energy (in form of heat) necessary to raise the temperature of the material considered, so long as the specific heat is defined as the quantity of heat necessary to raise, or decrease, the temperature of a fixed quantity of substance by a given value. Since the values found of the specific heat for the inorganic core are lower, in the range

considered, it means that 1g of core, to raise its temperature by 1K, will need a lower amount of energy. In the higher temperature range, however, the trend is reversed, and it is the organic core that needs a lower amount of energy to raise its temperature. During the filling time in the casting phase when the organic core meets the aluminum, the high temperature leads the release of gas due to the degradation of the resin. Cooling is initially rapid but, at lower temperatures, a greater amount of energy will be required in order to allow the continuous temperature increase of the core itself compared to the inorganic one. This implies how the use of inorganic cores allows a greater dissipation of heat and, therefore a higher cooling rate. This is demonstrated evaluating the quantity of heat that the two different core system adsorbed during the heating phase. As it is showed in Fig. 6, the underlying area determines the quantity of heat that the system could absorb during the DSC test. The inorganic sand core could keep a higher value of heat (260.4mJ) compared with the organic sand core (165.4mJ).

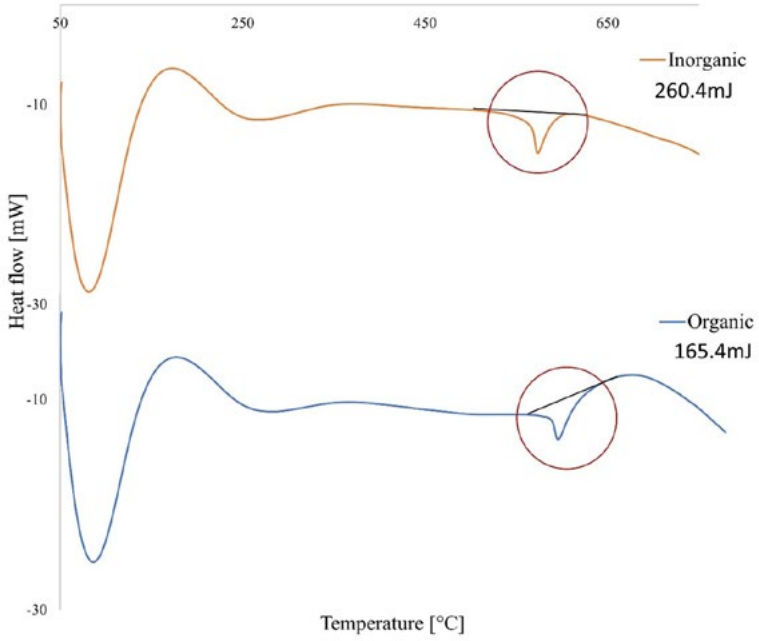

Fig.6 - Heat flow-temperature of the inorganic and organic sand core with the evaluation of the heat absorbed.

This aspect is strictly correlated with the solidification and cooling of the component, since it directly affects the final mechanical properties of the components, especially the elongation A % which it is expected to be better in the components obtained with the use of inorganic cores [6]. In addition, despite the attainment of high temperatures, there is no release of gas (in fact no decrease in weight was recorded during the tests) in the case of inorganic cores, with important consequences from an environmental point of view, regardless of the characteristics of the casting.

Characterization of the oil pans

The results obtained by tensile and hardness tests support the previous considerations. In general, the results show how the properties of the components produced with inorganic sand cores are similar and sometimes also better than those with organic sand ones. In order to identify the different samples, the two oil pans obtained with inorganic sand cores were named 1 and 2 and the one obtained with the organic core was named 3. 1 and 2 differ from the kind of stockage of the sand cores: the inorganic sand cores used for the component 1 did not absorb moisture (no moisture was detected inside and on the surface) instead the inorganic sand cores used for the component 2 absorbed 1% of moisture on the surface and almost 0,25% inside the core.

In Fig. 7 the results of yield strength (Rp0.2), tensile strength (Rm), elongation percentage (A %) and hardness (HB) are summarized.

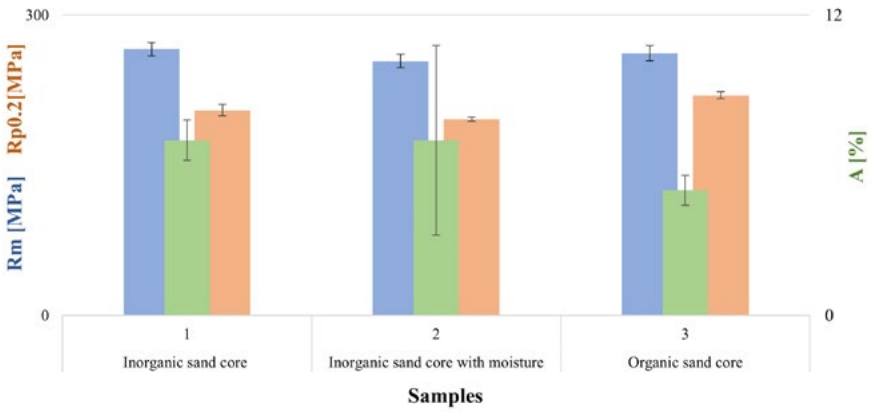

Fig.7 - Graph of the average values of Rm, Rp0.2 and A% obtained from the tensile test of the samples taken from the tubular zone with respective standard deviation.

The results obtained from the tube (average of the three samples A, B, C - Fig. 4) show a higher value of the yield strength in the case of components made with organic cores (part 3), but the difference is not so relevant, since the values obtained are comparable.

Also values of the ultimate tensile strength are very similar comparing the different components. In this case, higher results are obtained for the 1 sample, produced with inorganic sand core, followed by that produced by organic sand core. The dispersion of the results is very low guaranteeing uniformity of performance of the components produced in the three different conditions.

Finally, the percentage elongation results higher for the components made with inorganic cores. The lowest value was recorded instead for the sample 3. Considering the limit that the piece must exceed according to the specifications, it is noted that, with the use of organic cores, we are at the limit of the acceptability range. A remarkable scatter of data can be detected for the component produced with inorganic cores containing moisture, demonstrating the importance of an appropriate storage of this kind of cores.

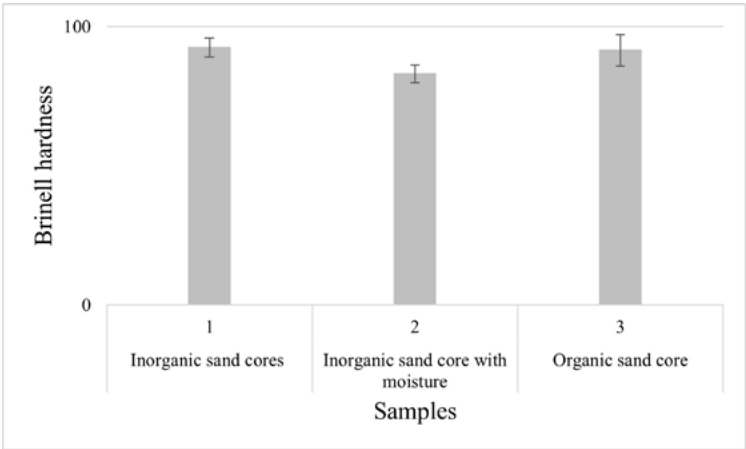

Fig.8 - Graph of the average values of Brinell hardness obtained from the tensile test of the samples taken from the tubular zone with respective standard deviation.

In the Fig. 8 the results of the hardness values are reported. The lowest hardness values were found in the component obtained with inorganic sand cores with moisture: this could be related to the release of moisture during the casting process which, if not properly eliminated through air vents, can lead to the formation of microporosity inside the piece. When the indenter finds a porosity, the material yields providing a lower hardness value. In gene-

ral, the Brinell hardness obtained are comparable among them.
In order to evaluate the fracture mechanism, the fractural surfaces after the tensile test were analyzed by scanning electron microscopy (SEM). From a first preliminary analysis, all the samples showed a ductile fracture as it can be seen from the particularly fibrous and opaque surface. An example, representative of the analyzed surfaces, is reported in Fig. 9 where it is showed the fractured sample 3.

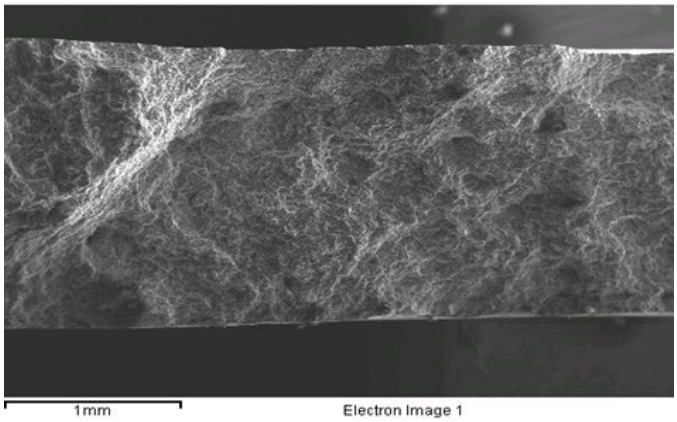

Fig.9 - Fracture surface of the sample 3 which shows a ductile fracture.

In fact, at higher magnifications it is possible to detect the presence of dimples (Fig.10): these are approximately spherical cavities, joined together by thin edges. Inside them, second phases can be observed which however are generally undermined during the tensile test, leaving the multi-cavities empty. Furthermore, their size is similar and homogeneous for all the cavities, as it is a AlSi7Mg0.3 alloy, characterized by second phases that are identical to each other.

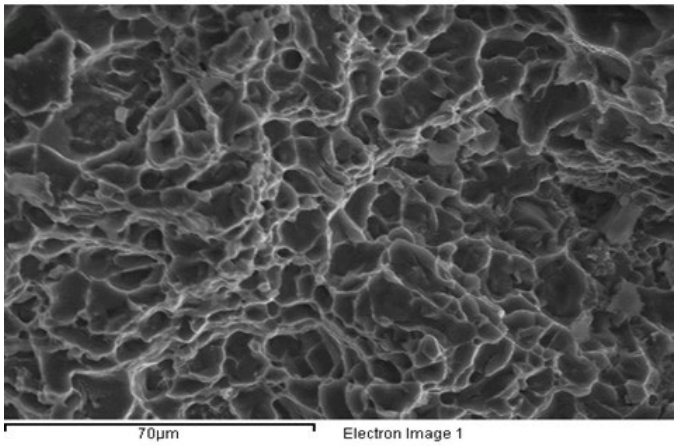

Fig.10 - Dimples on the surface of the sample 1.

In all surfaces it is also possible to observe the presence of porosity both from shrinkage and from gas as it is possible to see in Fig. 11.

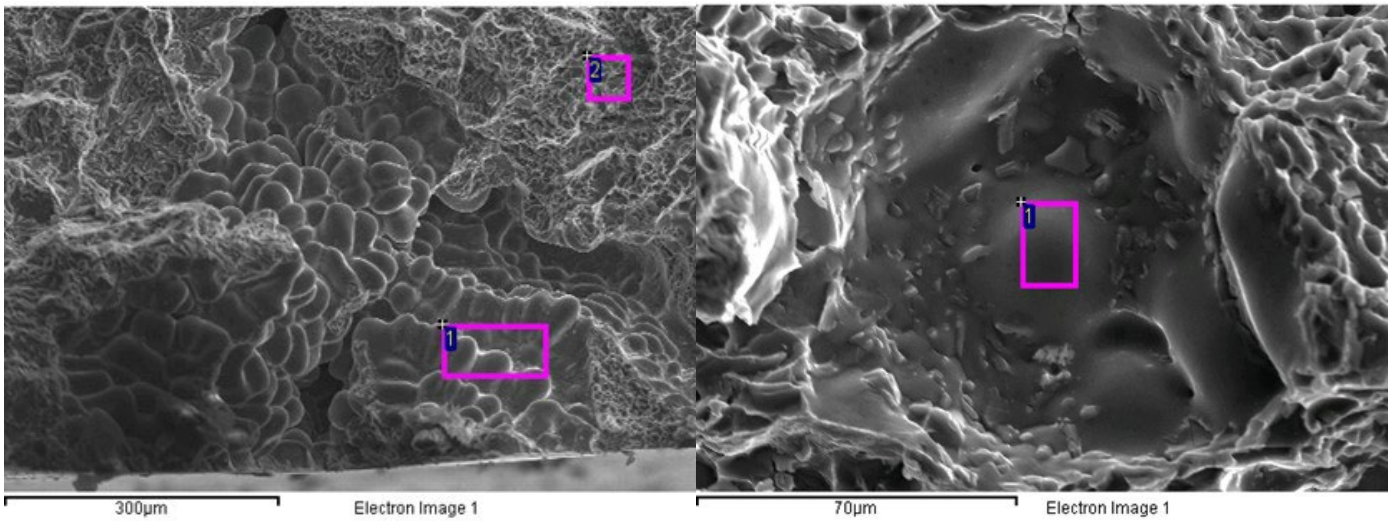

Fig.11 - Examples of porosities due to the shrinkage on the left (sample 2) and to the gas on the right (sample 3).

The particularly rounded shape refers to gas porosity, while the one with a more indented shape refers to shrinkage related defects. The presence of these gas porosity defects may be correlated to various phenomena: release of gas from the organic cores, trapping of air (especially during the filling phase) or, again, humidity released by the "wet" inorganic cores. In these areas, where these porosities are noted, the dendrites are also visible clearly.
Hence, the mechanical tests clearly showed the advantages of the inorganic cores, which guarantee comparable or even higher properties of the cast component combined with no gas emission.

Simulations

It is well known that, to the results of casting simulations depend on the definition of the input parameters and the material properties. However, meanwhile the values of the thermal properties in the ProCAST® database for organic cores are well established (according also to the software house), concerning inorganic cores there are not many data, making the results less reliable. Thus, a set of simulations was conducted, adding the measured thermal properties of the inorganic cores, and their results were compared with experimental data obtained from the instrumented cores (Fig. 3) and from metallographic analyses on the produced parts.
An example of comparison between two simulations and the values recorded by the thermocouples is shown in Figure 12. The red curve shows the simulation done according to the thermal values already present in the database of the software. The blue curve is the final simulation in which all the parameters used were strictly related with the production process. The green one corresponds to the experimentally recorded temperature. They all refer to the point in the core placed at 15mm from the center and at 150mm of depth. As it can be seen, the trend is particularly similar between the final simulation and the experimental curve, whose values result close to each other (more detailed data cannot be reported for confidentiality reason).

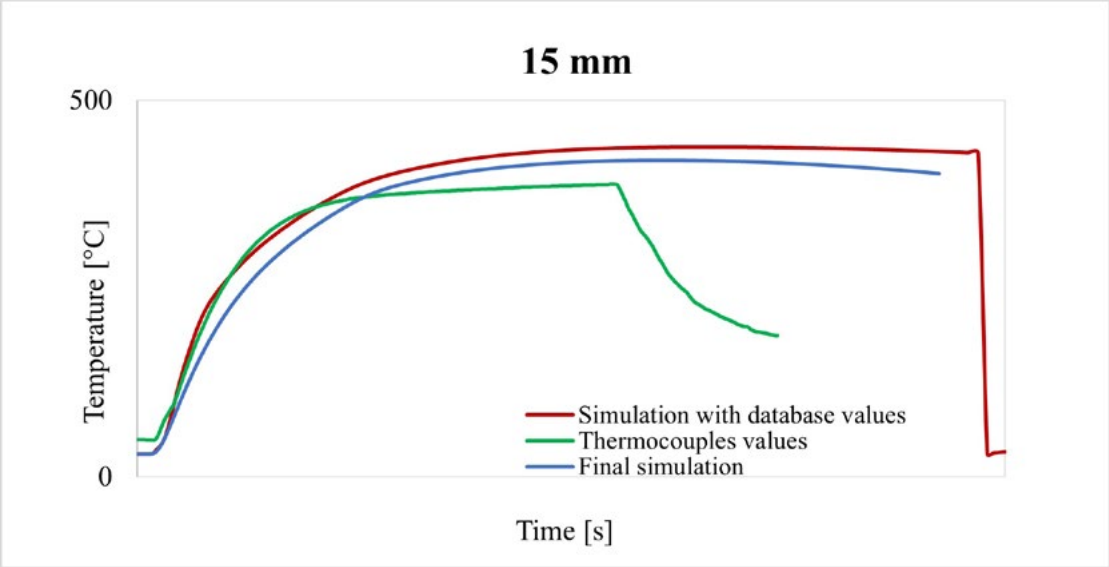

Fig.12 - Trend of the temperatures obtained with thermocouples and with the final simulation inside the inorganic sand core.

This allowed to demonstrate how much the thermal data (especially the specific heat) are important and influential for the final result.
Finally, to further evaluate the reliability of the model, the SDAS was evaluated in the tubular zone. In the Fig. 13 are showed the results obtained from the different oil pans and from the final simulation.

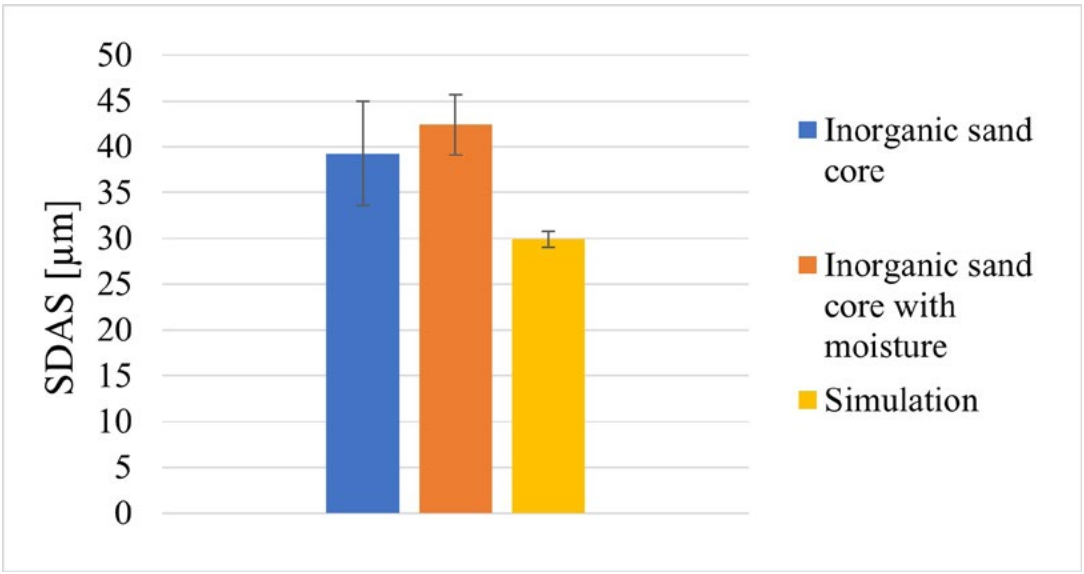

Fig.13 - Values of the SDAS obtained from the tubular zones of the components and the final simulation.

The oil pan obtained with simulation presents the lowest SDAS (30µm), that is however similar to that measured for the component realized with inorganic sand core (39.27±5.73µm). In both cases, the values show a quite fast solidification.
The SDAS from the simulation was evaluated obtaining a high number of nodes in a section of the tube (Fig. 14).

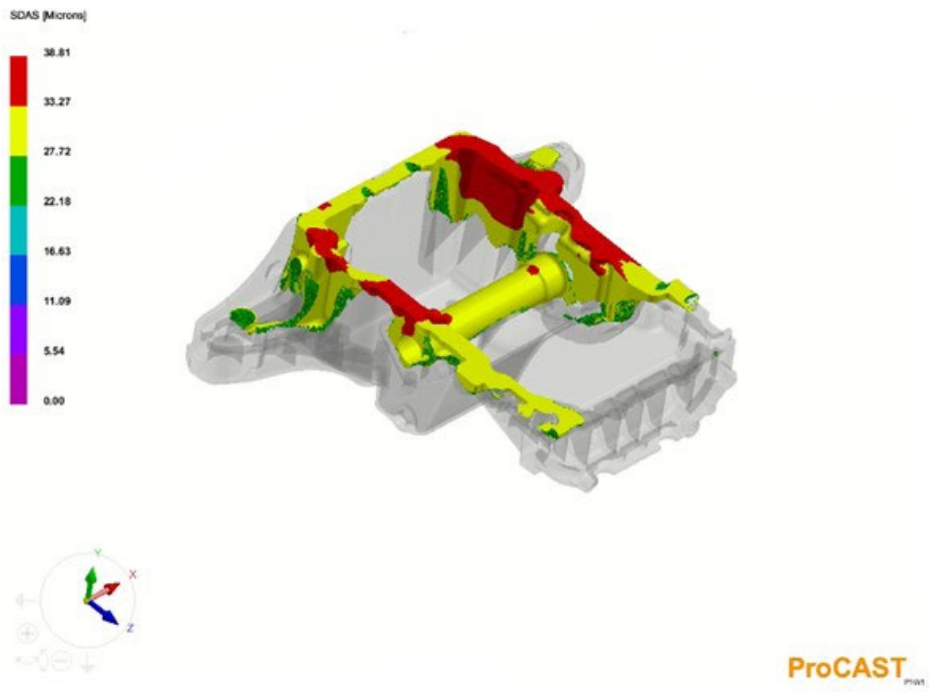

Fig.14 - Evaluation of the SDAS from the final simulation: the coloured zones show the cut-off between 27 and 38μm.

FINAL COMMENTS

The present work was carried out to investigate the thermal properties, in particular the specific heat, of the inorganic cores obtained through the Cordis process, to implement these data in the simulation software, in order to have a more accurate and reliable representation of the solidification of the metal. In fact, performing analyzes by differential scanning calorimetry, it was possible to determine the specific heat value of the inorganic core. It was also possible to assert that the energy requires to increase the temperature of the inorganic system is lower compared with that requires by the organic sand core. In fact, evaluating the energy absorbed by the two kinds of cores during the DSC tests it was shown that inorganic cores allow a higher dissipation of heat and therefore a higher cooling rate.

In order to determine the mechanical properties of the components obtained with the use of the inorganic cores, various mechanical tests were done on samples taken from the tubular zone: tensile, hardness test and scanning electron microscope image acquisition. The values obtained were then compared with those resulting from similar tests but carried out on castings made with organic cores.

The results obtained proved to be better for components realized with inorganic cores as regards the A% and the Rm. In case of the yield (Rp0,2), on the other hand, the values found for castings with inorganic cores were lower. The hardness values appeared to be homogeneous for all the specimens considered. However, it should be noted that the differences found are in the range of tolerance linked to the variability of casting processes, therefore it is possible to affirm that the two modalities, with organic and inorganic cores, are comparable as regards the performance of the casting.

What can be deduced from the images taken with the scanning electron microscope, in correspondence with the fracture surfaces of the samples obtained, is the significant presence, on all the samples analyzed, of gas and shrinkage microporosities, in the area corresponding to the tube. The defects with a particular spherical shape can be related to gas porosity and can be associated to the degradation of the resin during the casting phase or to air entrapment during the filling phase. The release of gas from organic cores was also demonstrated through thermo-gravimetric analyzes conducted on samples, which have shown weight loss, not detectable in the case of the

inorganic ones.
It was also conducted a microstructural analysis in order to evaluate the SDAS on the component obtained with the organic cores. In particular, the results showed a quite small SDAS, synonymous of a fast solidification.
Finally, the identified data of specific heat were essential for the correct setting of the simulations of the casting process. The results obtained with the simulations are similar to the experimental data, demonstrating the reliability of the measured thermal properties of the inorganic cores implemented in the commercial simulation software of mold filling and casting solidification.

ACKNOWLEDGMENTS

I would like to thank FMB S.r.l. for the support and the carrying out of the experiments, ECOTRE Valente S.r.l. for the setting up of the numerical simulations, AQM S.r.l. and Dr. Lorenzo Montesano from University of Brescia for the mechanical tests in laboratory and Prof. Annalisa Pola for the constant support during the project.

REFERENCES

[1] F. Czerwinki, M. Mir and W. Kasprzak, "Application of cores and binders in metal casting," International Journal of Cast Metals Research, pp. 129-139, 2015.
[2] L. Iuliano, Manuale della fondera, 2007.
[3] Parlamento europeo e del consiglio, Direttiva 2010/75/UE relativa alle emissioni industriali (prevenzione e riduzione integrate dell'inquinamneto), 24 novembre 2010.
[4] S. Saetta, F. Maria Di, V. Caldarelli and S. Tapola, Improve the use of natural resources: inorganic binders in iron and steel foundries case of the green foundry life project, 2019.
[5] J. R. Brown, Foseco Non-Ferrous Foundryman's Handbook, Butterworth-Heinemann Ed. 11, 2011.
[6] A. Fortini, M. Merlin and G. Raminella, "A Comparative Analysis on Organic and Inorganic Core Binders for a Gravity Diecasting Al Alloy Component," International Journal of Metalcasting, giugno 2021.
[7] C. Mingardi, Processo Cordis, Presentation in Vicenza, 2014.
[8] A. E1269-11, Standard Test Method for Determining Specific Heat Capacity by Differential Scanning Calorimetry, 2018.
[9] Normativa UNI EN ISO 6892-1, Metallic materials -Tensile testing-, 2020.
[10] M. J. O'Neill, Measurement of specific heat functions by differential scanning calorimetry, 1966.

Influenza dell'impiego di anime in sabbia sulla solidificazione e sulle caratteristiche finali di componenti strutturali: un confronto tra anime organiche ed inorganiche e validazione attraverso la simulazione

Negli ultimi anni, il crescente interesse verso produzioni più sostenibili e green ha portato alla ricerca di nuovi processi e materiali, come, ad esempio, il diffuso impiego nelle fonderie delle anime in sabbia con legante inorganico rispetto a quelle con legante organico per ottenere componenti strutturali in lega di alluminio. Il grande vantaggio è legato soprattutto alla riduzione delle emissioni di sostanze tossiche, come formaldeide e fenolo, presenti nei leganti di tipo organico. Nonostante questo, le informazioni circa le caratteristiche delle anime inorganiche sono ancora molto scarse e, per tale ragione, il presente lavoro si propone di caratterizzare questo tipo di materiale, valutandone le proprietà

termiche e le modalità di scambio di calore con l'alluminio. È stato inoltre effettuato un confronto con le proprietà delle anime organiche e sono state comparate le proprietà meccaniche dei componenti realizzati con le due diverse tipologie di anime. Infine, le proprietà misurate delle anime inorganiche sono state implementate nel software di simulazione ProCAST®: il buon accordo tra la simulazione ed i dati reali ha dimostrato come sia importante conoscere le corrette proprietà dei materiali per ottenere risultati affidabili.

"Lavoro vincitore del Premio Aldo Daccò 2021 ex aequo con il lavoro "Utilizzo di un sistema di ispezione ottica automatica atto al rilevamento dei difetti di colata continua basato su algoritmi di Machine Learning per l'analisi dell'incidenza delle marche di oscillazione su bramme di acciaio inossidabile austenitico AISI 316L e 316LI", che verrà pubblicato sul numero di aprile 2022".

Design and analysis of various cooling conditions of an aluminium wheel mold

edited by: O.Özaydin, Y. Çatal, A. Y. Kaya

During low pressure casting of aluminum alloy wheels, the cooling conditions affect the mechanical properties directly. Cooling of wheel mold is conducted by an air, water, or mist cooling system. These coolants flow in the cooling channels within the mold to reduce temperature of mold to obtain directional solidification. During the solidification of aluminum alloy wheels, directional solidification starts on outer flange area, continues toward inner flange area, and finishes on spoke and hub areas. Directional solidification helps to reduce risk of material defects in the wheel. One way to ensure directional solidification is modelling cooling channel geometries with a CAD program and then analyzing the cooling effects by a casting simulation software. The aim of this study is to develop a complex design with an amorph cooling channel to obtain a high surface area, hence a higher cooling performance while also keeping the producibility in focus. A 'complexity in design' and 'producibility' are contrary terms in traditional manufacturing methods, on the other hand, non-traditional manufacturing methods such as additive manufacturing can be used to obtain geometrical complexity and together with producibility. In this study, different cooling geometries were modelled and then analyzed. During design iterations, various cooling channels with higher surface areas were considered. After casting simulation, temperature in pre-selected areas, UTS (Ultimate Tensile Strength), YS (Yield Strength) and Elongation (ε%) values of simulated wheels are obtained, and designs are compared.

KEYWORDS: ALUMINUM ALLOY WHEELS, CASTING SIMULATION, COOLING CHANNELS, LPDC, MOLD;

INTRODUCTION

It is common to find aluminum alloys used in many industries due to their lightweight and castability. Automotive and aviation industries are common users of aluminum alloys. With the help of aluminum alloys have the obvious advantage of being easy to cast, various casting techniques have developed for the purpose of improving the soundness and productivity of the outputs and continue to be developed [1]. There are many examples of product such as automobile wheels that manufactured by casting. Automobile wheels can be produced by low pressure die casting technique (LPDC). Since the LPDC technique is profitable if large number of productions will be made. On the other hand, permanent molds can be used in low pressure die casting and it provides relatively fast cooling with the help of cooling channels (cooling circuits). Heat is transferred from the cast metal to the die and ultimately to the environment in that process [2,3].

The cooling stage is significantly important for casting products. If it can be controlled, it would alter the microstructure of the product in a better way. So, the cooling directly influence the mechanical properties. Higher cooling rates can help the modifying eutectic silicon into fibrous

Onur Özaydin*
Department of Research and Development, Cevher Wheels, İzmir, Turkey

Yiğit Çatal, A. Yiğit Kaya
Department of Research and Development, Cevher Wheels, İzmir, Turkey

branched morphology and determine the porosity size in A356 alloys. It allows even large castings to solidify quickly, thereby reducing grain segregation and improving grain refinement. It also provides lower cycle times. However, it is not always easy to increase cooling rate. The cooling rate can be changed by coolant, cooling channel design, mold material, etc. and for the purpose of enhancing a best possible quality, everything must be optimized [4,5,6]. In a case the only variable is coolant, even only cooling channel design and coolant (water and air usually used) could significantly alter the cooling rate. Also, water as a coolant provides better cooling efficiency comparing the air in that case [7].

Considering the advantage of calculation times with developing computer technology, numerical simulation technology becomes playing a crucial role in optimizing those cooling parameters. To improve the performance of aluminum alloy LPDC wheels, computer simulation is widely used. Using numerical simulation, the results indicate that casting filling parameters are optimized, and the evolutionary process of casting filling predicted in the study of Zhang L. et al. [8]. The number of cooling inlets and outlets and the pressure of the cooling channel can affect the flow rate in LPDC. The affect can be seen by using computational fluid dynamics software [9]. The software also helps to spot the areas that have possibly casting defects like porosity and give an opportunity to understand defect formation with different casting scenarios. Thus, it could be possible to optimize the parameters in a short time to obtain an almost defect-free casting [10,11,12]. In addition, due to the nature of heat transfer, the change in wall thickness also affects the cooling efficiency. It causes different mechanical properties on different parts of the product. This affair must be considered while cooling channels are designed. The increase in the surface area of the cooling channels can provide a more effective cooling. The purpose is to direct conduction heat transfer away from the molten metal and to solidify it as rapidly as possible. It is difficult to carry out conduction cooling on targeted areas during this process since the solidifying molten metal naturally shrinks away from the mold. In many products like an automobile wheel, directional solidification cannot take place naturally because of its complex geometry with different parts such as the hub, spokes, and the rim. Therefore, it can be controlled by a cooling channel [13]. Numerical and experimental studies were made in recent years and thanks to these studies important results have been achieved. In addition to the geometry and mass flow rate, the cooling water temperature and flow rate are also factoring that influence the quality of the formed region according to some studies [14]. Using different mold materials can change the mold temperature as well as cooling conditions [15].

In this study, the automobile wheel was produced by low pressure die casting using a numerical simulation. To notice the effect of cooling channel design in the solidification stage, four different cooling channels were designed. Then, these designs were defined in the numerical software. Also, air and water as a coolant were used for observing a difference for each design.

EXPERIMENTAL

The experimental study started with the designing new cooling channels. Four different cooling channels were drawn by using CATIA V5 as seen in Fig. 1. Then, defined geometric model of the automobile wheel and its mold parts were imported into the Magmasoft commercial casting software. After choosing the AlSi7Mg0.3 alloy and H13 steel for die casting as material data from the Magma database, each design was run with choosing the coolant data water and air. Eventually, in the result section, these 8 cases compared with each other.

Design 1

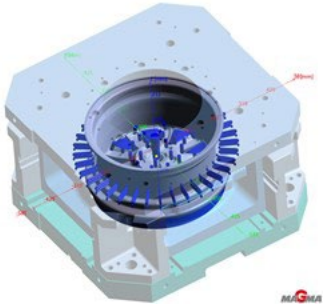

Design 2

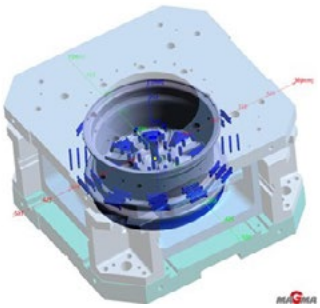

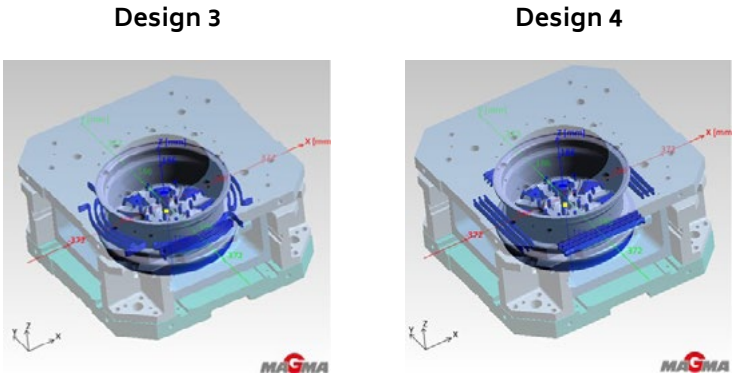

Fig.1 - Four different cooling channel designs.

Tab.1 - Comparison of designs with different coolants.

RESULTS

COOLANT DESIGN	AIR	WATER
Design 1	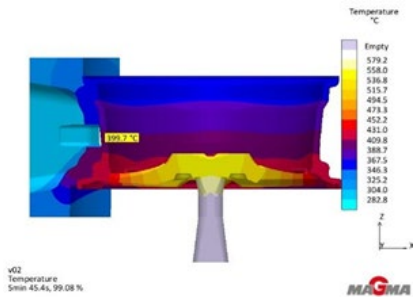 (399.7°C)	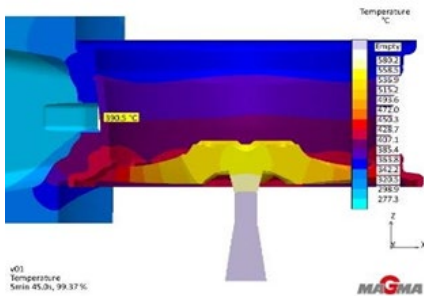 (390.5°C)
Design 2	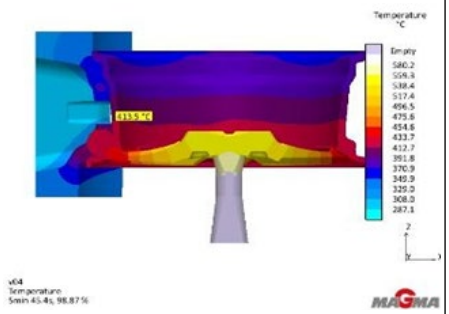 (413.5°C)	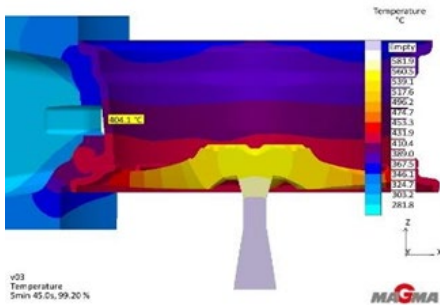 (404.1°C)
Design 3	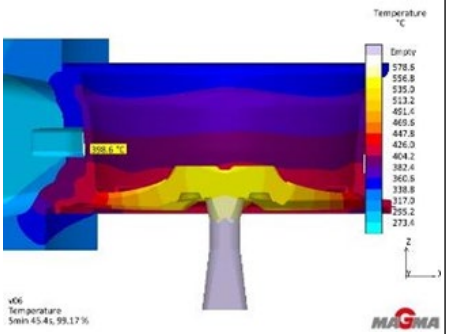 (398.6°C)	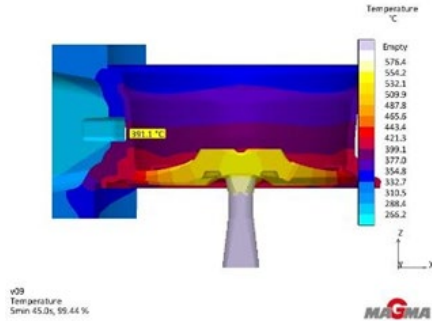 (391.1°C)

Design 4	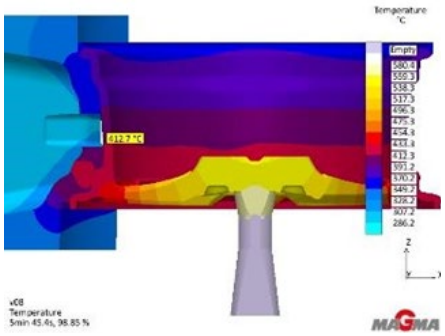 (412.7°C)	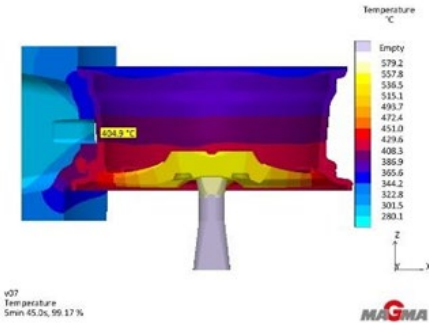 (404.9°C)

CONCLUSIONS

Mechanical properties like UTS (Ultimate Tensile Strength), YS (Yield Strength), and elongation (ε%) values of simulated wheels were obtained as well as temperature (°C) values for each design.

Tab.2 - Mechanical properties of all designs.

COOLANT	WATER				AIR			
Design	#1	#2	#3	#4	#1	#2	#3	#4
Temperature [°C]	390.5	404.1	391.1	404.9	399.7	413.5	398.6	412.7
YS [MPa] (Yield Strength)	102.93	101.72	101.87	101.69	101.63	101.15	101.54	101.21
UTS [MPa] (Ultimate Tensile Strength)	187.85	180.67	181.50	180.51	180.16	177.57	179.66	177.88
Elongation [%]	5.67	5.23	5.28	5.22	5.19	5.04	5.16	5.06

Water is a better option to cool a mold faster for each design as expected. Design 1 and design 3 are more effective coolant than design 4 and design 2. UTS is the most affected feature compared to the YS and Elongation for each case.

The best UTS, YS, and Elongation value achieved in design 1 water cooling case (187.85 MPa, 102.93 MPa, 5.67%).

But generally, it was observed that YS and elongation values were not affected by designs and coolants like UTS values.

The range of YS values differed between 100 MPa and 103 MPa for each case and the range of Elongation values were almost 5% and 6%.

REFERENCES

[1] Campbell J.: Complete Casting Handbook: Metal Casting Processes, Metallurgy, Techniques and Design 236-276, 2015.
[2] Sara M.: Quantification of Cooling Channel Heat Transfer in Low Pressure Die Casting, The University of British Colombia, 2014.
[3] Chen K., Chiu Y., Wang S.: Analysis of Cooling Conditions of A356 Aluminum Alloy Rim Low-pressure Casting, 978-1-60595-416-5, 2017.
[4] Sui D, Cui Z., Wang R., Hao S., Han Q.: Effect of Cooling Process on Porosity in The Aluminum Alloy Automotive Wheel During Low-Pressure Die Casting. International Journal of Metalcasting, 2015.
[5] Zeng Y., Yao Q., Wang X.: The Effect of Air Gap Between Casting and Water-Cooled Mold on Interface Heat Transfer Coefficient, Materials Science Forum. ISSN: 1662-9752, Vol. 893, pp 174-180, 2017.
[6] Chen R., Shi Y., Xu Q.: Effect of Cooling Rate on Solidification Parameters and Microstructure of Al-7Si-0.3Mg-0.15Fe Alloy. Transactions of Nonferrous Metals Society of China (English Edition), 2014.
[7] Ozaydın O, Catal Y.: Evaluation of Cooling Channel Design and Coolants of an Aluminium Alloy Wheel Mold Using Casting Simulation, 5th International Conference on Engineering and Natural Science, Italy, 2019.
[8] Zhang L., Li L., Zhu B.: Simulation Study on the LPDC Process for Thin-Walled Aluminum Alloy Casting, Materials and Manufacturing Processes, Materials and Manufacturing Processes, 2014 Nov 25.
[9] Yavuz H., Ertugrul O.: Numerical Analysis of the Cooling System Performance and Effectiveness in Aluminum Low-Pressure Die Casting, International Journal of Metalcasting, March 2020.
[10] Reilly C., Duan J., Yao L., Maijer D.M., Cockcroft S.L.: Process Modeling of Low-Pressure Die Casting of Aluminum Alloy Automotive Wheels, JOM, Vol. 65, No. 9, DOI: 10.1007/s11837-013-0677-1 2013 July 16.
[11] Guofa M., Xiangyu L., Kuangfe W., Hengzhi F.: Numerical Simulation of Low Pressure Die Casting Aluminum Wheel, China Foundry, 1672-6421(2009)01-048-05, Vol. 6 No.1, Feb 2009.
[12] Fan P., Cockcroft S., Maijer D., Yao L., Relly C., Phillion A.: Examination and Simulation of Silicon Macrosegregation in A356 Wheel Casting, Metals 2018,8, 503; doi:10.3390/met8070503 2018 June 9.
[13] Velluvakkandi N.: Developing an Effective Die Cooling Technique for Casting Solidification, School of Engineering Auckland University of Technology July 2009.
[14] Gemici Z.: Development of A Cooling Die Used in Plastic Pipe Processing: Numerical And Experimental Analysis, Journal of Thermal Engineering, Vol. 4, No. 4, Special Issue 8, pp. 2096-2116, Yildiz Technical University Press, Istanbul, Turkey, June, 2018.
[15] Wenzl C.: Structure and Casting Technology of Anodes in Copper Metallurgy, Montanuniversität Leoben, Sep 2008.

La Metallurgia Italiana
International Journal of the Italian Association for Metallurgy

The new biocide regulation - their impact and innovative sustainable solutions for casting lubricants

edited by: U. Schmidt-Freytag, A. Kelly

Due to new biocide regulations, since May 2020 the commonly used chloromethylisothiazolinone/methylisothiazolinone (CIT / MIT) mixtures have been subject to stricter labeling. By introducing a new generation of biocides, Henkel has improved the biostability of its release agents and lubricants for the die casting industry. In addition to an optimised antimicrobial effectiveness, the new biocide also meets the new criteria thus avoiding stricter labeling.

KEYWORDS: BIOCIDE, CASTING, LUBRICANTS, SUSTAINABILITY, REGULATION;

INTRODUCTION: THE NEW BIOCIDE REGULATION

In order to better control the environmental compatibility, especially in the area of wastewater management, changes have recently been made to the classification of biocidal compounds. With the 13th "Adaptation to Technical Progress" (ATP) according to the "Classification, Labeling and Packaging" (CLP) Regulation (EU Regulation No. 2018/1480), effective since May 1, 2020, the chemical substance mixture CIT / MIT [CAS 55965-84-9] (CS 2513 + CS 36854) is subject to a change in the multiplication factor (M-factor change) from 10 to 100. The latter depends on the acute toxic effect on aquatic organisms. For Europe, this means that for all products that contain at least 0.025 percent of these substances, the labeling will be changed to H410 / H411 (toxic to aquatic organisms with long-lasting effects) (Tab. 1). Furthermore, they must be marked with GHS 09 (pictograms dead fish, dead tree).

For Germany further regulations mean that formulations with these biocide types are reclassified to the highest water hazard class – class 3. As a result, much stricter guidelines apply to the handling and storage of such substances. In the case of release agents and lubricants for die casting foundries, numerous preservation systems are affected by these changes in the law. The new ordinance and the associated environmental, health and safety controls pose major challenges for many customers of Henkel AG & Co KGaA leading them to seek sustainable alternatives.

Ulrike Schmidt-Freytag, Andrew Kelly
Henkel AG & Co KGaA, Germany

BIOZIDE-TYPE	LABELLING 2019	LABELLING FROM MAY 2020
CIT / MIT-mixtures		
Henkel Biozide "N-version"		

ISOTHIAZOLINONES – DESCRIPTION

Isothiazolinones are heterocyclic compounds (Fig. 1) that play an important role as biocides. Five derivatives are used to a significant extent:

- Methylisothiazolinone (MIT, MI)
- Chloromethylisothiazolinone (CMIT, CMI)
- Benzisothiazolinone (BIT)
- Octylisothiazolinone (OIT, OI)
- Dichloroctylisothiazolinone (DCOIT, DCOI)

Isothiazolinones are usually used as preservatives against microorganisms (bacteria, fungi) in water-based systems such as dispersions, emulsions and solutions. With their bactericidal and fungicidal effect, they protect shower products, shampoos, cosmetics, cleaning agents, paints and adhesives from microbial decomposition and are the standard solution in the areas of die casting and aqueous metal forming products. Further areas of application are slime control in paper production, rot protection of cooling and process water, the antimicrobial treatment of textiles and use as a wood preservative. The CMIT / MIT and MIT / BIT mixtures are most frequently used in products for die casting.

In addition to the desired effect, killing or controlling the growth of microorganisms, isothiazolinones also have undesirable effects. They have a high aquatic toxicity, and some derivatives (especially CMIT) can cause skin sensitization in humans through direct contact or via the air.

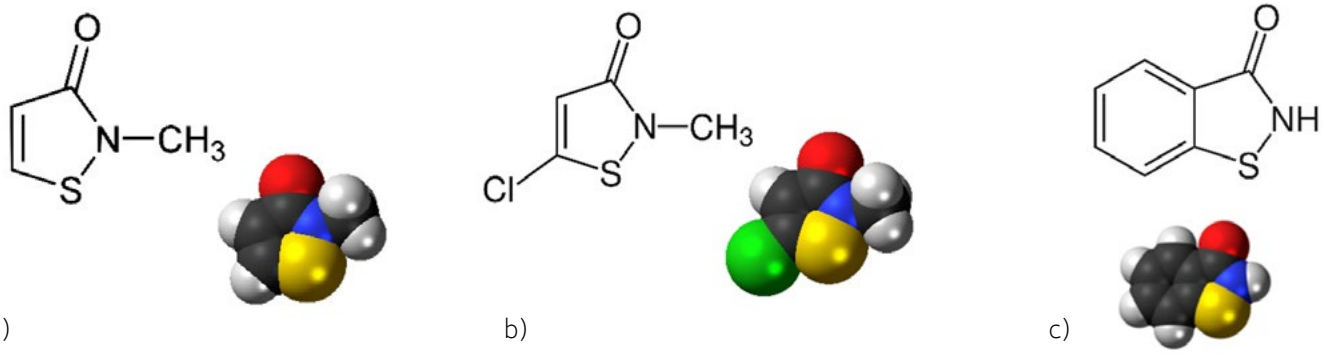

Fig.1 - Chemical structur of a) Methylisothiazolinone (MIT), b) Chlormethylisothiazolinone (CMIT), c) Benzoisothiazolinone (BIT).

HENKEL'S SUSTAINABLE APPROACH

In order to support the sustainability goals of our customers, new conservation systems have been evaluated and implemented, subject to stringent product requirements. On the one hand, they have to be robust enough to prevent bacterial growth during storage, central dilution and application of the product, while at the same time maintaining product stability. Many modern biocides, while offering excellent protection, cannot meet these requirements because their ionic nature is incompatible with

most emulsion systems. An ideal biocide for emulsion application is typically non-ionic while providing sufficient biocidal activity.

As a result of extensive research and development, Henkel was able to successfully identify and approve new active ingredients. The formulations meet the strict new environmental criteria and accordingly avoid the stricter labelling. As has been confirmed by laboratory tests and industrial applications, the new type of biocide has no negative influence on the form, function and stability of the release agent and lubricant foundry products. It is already used in industry for series production and has proven to be even more effective in terms of biostability compared to the old CIT / MIT technology. With the standard biocide, the critical number of bacteria is already reached after 6 weeks of stress test. The formulation with the new biocide, on the other hand, remains below the critical value even after 10 weeks (Fig. 2), which indicates better biostability. The critical value is where the number of bacteria in the stress test reaches at least 106. Experience has shown that with such a high bacteria count number there is a risk of biofilm formation in practical use. Another advantage of the newly introduced biocide is the improved biostability when using hard water (Fig. 3).

The general rule for the biostability of Isothiazolinones is that it decreases when the products are used in lime-containing water and that the time it takes for the critical number of bacteria to form noticeably increases in the stress test with demineralized water. If you now compare the standard biocides with the new products, you can clearly see that they are less sensitive to water hardness and therefore represent a better alternative here too.

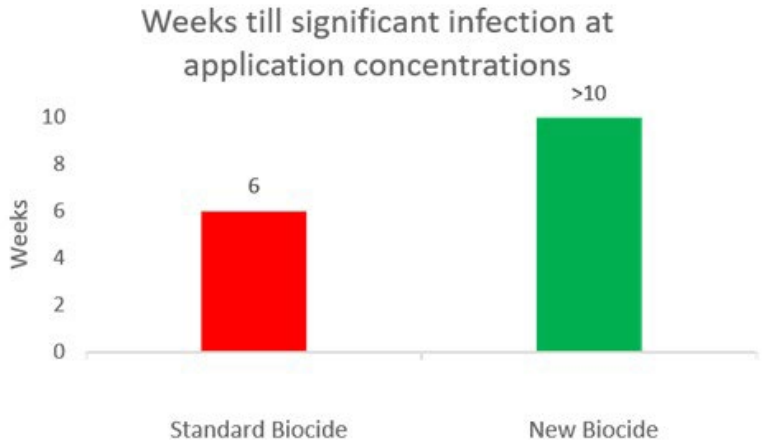

Fig.2 - Comparison of bacterial growth between a product containing a standard biocide and the new biocide (diluation ratio 1:80).

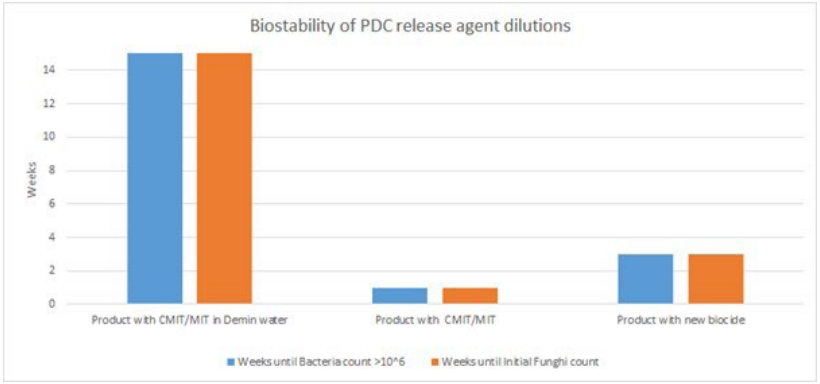

Fig.3 - Comparison of bacteria and funghi-growth in hard and de-mineralized water.

CONCLUSION

The regulation for the classification of several biocides has recently been adjusted. In the case of auxiliary products for the die-casting industry, many industry-standard preservation systems are affected by these legislative changes. Across Europe, the reclassification of chronic M-factors has resulted in products having to be labeled with the "dead fish / dead tree" label. In addition, legislation in Germany has resulted in many products and raw materials being assigned a higher water hazard class.

The stricter environmental, health and safety controls pose great challenges for many customers. With the introduction of the new generation of biocides, we can not only avoid stricter labeling of our foundry products, but also significantly improve their antimicrobial effectiveness and achieve increased biostability even in hard water.

La Metallurgia Italiana
International Journal of the Italian Association for Metallurgy

Applications of automotive lean production tools on die casting industry

Ü. Ayyildiz

It is seen that waste-free processes created by lean manufacturing techniques provide advantages in competitiveness. According to those observations and advantages of it, usage of lean production tools which is already used in automotive world gets wider during last years in metal casting industry. In fact, one of the important step is applying this lean production tool before ındustry 4.0. In order to do this, companies must systematically operate the Man, Machine, Method and Material components called 4M. This harmony can be likened to the gearwheel of a watch. The main purpose is to ensure that the clock performs its task regardless of whether or not each wheel is large or small. All productivity targets are planning and commissioning to ensure gearweel working properly. The whole of this compliance is called the system. The correct identification, fast control and access information were required to system work properly. A simple but effective follow-up and identification format has been created to meet the customer needs of the process. This form is also defined as the main chain link that connects all the lean production tools. This main chain is called "Process Requirement Tablo". In this study, the contribution of a simple but effective table to the production system was observed.

KEYWORDSS: AUTOMOTIVEM, LEAN MANUFACTURING, DIE CASTING, INDUSTRY 4.0, PROCESS REQUIREMENT;

INTRODUCTION: NEED OF PRODUCTION SYSTEM IN DIE CASTING INDUSTRY

In the researches, the concept of lean manufacturing techniques has become widespread with the Toyota production system and it has been observed that the companies have become more systematically more efficient with the implementation of the applications. It is seen that waste-free processes created by lean manufacturing techniques provide advantages in competitiveness. According to those observations and advantages of it, usage of lean production tools which is already used in automotive world gets wider during last years in metal casting industry. In fact, one of the important steps is applying this lean production tool before Industry 4.0. In order to do this, companies must systematically operate the Man, Machine, Method and Material components called 4M. This harmony can be likened to the gearwheel of a watch. The main purpose is to ensure that the clock performs its task regardless of whether or not each wheel is large or small. All productivity targets are planning and commissioning to ensure gearweel working properly. The whole of this compliance is called the system. Prometal has experien-

Ümmet AYYILDIZ
Prometal Hafif Metaller Döküm San., R&D Center, Bursa, Turkey

ce more than 20 years in die casting industry. Prometal was able to provide this experience as mold technology and machine dominance, but had difficulty providing the same experience thoughout the supply chain. In fact, it is known by business people that this situation does not belong only to Prometal, which is a common problem of the sector and businesses. There is a large working area and increasing request in diecasting industry especially for zamac and aluminium enjection. Investments in machinery and materials have provide Prometal to grow steadily since its foundation. In this growth process encountered in every business, the work of 4M, which we call the system, was getting harder in direct proportion to the growth. The deficiencies in the system during growth and the increase in the disrupted parts of the supply chain due to these deficiencies cause serious problems for the customer.

ZERO ERROR ZERO ACCIDENT

In casting companies; machinery, raw materials and molds can be supplied easily with capital power. It is seen that the first thing to do for entry into the casting industry is to bring this trio together, and it still continues to be seen in many companies. It is an attractive trio that is readily available if you have the capital and is deemed sufficient to set up the process. However, when we start production, many problems arise and are expected to arise. But there is a very serious risk involved! Loss of customers...

The constant change of the operator using the machine, the production numbers that cannot be completed on time due to the operation or operations that the operator skips on the machine and the mold and does not know, and the deteriorated production plan creates great chaos. This chaos causes accumulated balance problems and loss of customers as a result. This loss is very difficult to recover. Because they fall into the situation of factories with bad performance in their customer portfolio. This situation is experienced in every business, but the risks increase according to the size of the customer portfolio. Of course, in order to eliminate this situation and to ship the product on time, organizations and opportunities focus on producing parts in terms of logistics. Efficiency is being ignored and overtime is increasing rapidly even though customer orders are not increasing. In order not to experience this situation, the number of operators will increase and the automation process, which is Industry 3.0, will be ignored. As customers expect ZERO DEFECTS by completing system installations that take 10-15 years in their own structure, quality standards will increase and previously accepted errors will be defined as rejection. In this case, bad scores come from quality ratings in addition to logistics ratings. Systemlessness would have reached an unsustainable point.

These events were seen within Prometal and the need for a system installation, like many companies, started to be emphasized by the senior management. Within this system requirement and board, the company management declared 2018 as the year of transformation. It is obvious that the lean production system should be established in the casting sector as well as in the automotive and other sectors. Prometal quickly took steps in this direction for competitiveness and sustainability and decided to present its strong machinery, molds and knowledge to customers within a system.

APPLICATION OF LEAN MANUFACTURING IN PROMETAL

First of all, it was emphasized that the lean system is not a transformation project to be carried out within 1 year by outsourcing, but that lean transformation is a cultural transformation, it will be a process that will take many years and the support of the top management is absolute. For this reason, it was first started by appointing a leader with the right person policy for the right job. The change studies started rapidly and as a result of long-term studies, it was determined that there were noticeable improvements in quality first.

In this successful ongoing transformation, dozens of tools and behavioral management methods have been used and these methods continue to be used increasingly. One of the first starting points was the use of the process requirements table, which is one of the cogwheels of the clock, which is one of these transformation tools.

Correct identification, fast control and access information are required for the system to work properly. A simple but effective tracking and identification format has been created to meet the customer needs of the process. This form

is also determined as the main chain link that connects all lean production tools. The name of this ring was PRT/ Process Requirements Table (Fig.1). This form has been arranged to be used within the company in casting processes. Since there was more than one group of people and work in the company, it was necessary to collect them systematically and for this purpose, it was foreseen to create the concept of work area. The concept of work area has been defined as the most basic work station. If there is a person, the jobs that that person does and the stations (machine, area, etc.) where these jobs are performed are given the postal definition.

TABLE OF PROCESSING REQUIREMENTS AND USAGE

Date of Update	PROCESS REQUIREMENTS TABLE						
Work Area Number:	NAME OF THE OPERATION						
Operation Performed by the Machine	Operations Performed by the Operator (Cyclic, Frequency, Abnormality)	Quality Characteristics Impact Expectations on the Output Product Functional characteristics -Customer Expectations-	Standard Terms Reference Conditions Necessary to Ensure Quality Tools	Environment	Input Product	Necessary Warnings	Required Technical Competencies

Fig.1 - PRT (process requirements table).

Date of Update

Indicates the date the form was last updated. Work area documents are living documents. The intention here is that it can be constantly updated and its content can be changed.

The most common causes of change:
- Change in the number and form of operations
- Changes made after a quality analysis in the work area
- Changes due to KAIZEN activities to improve work area
- Change in tools used in work area

Work Area Number

It is used for addressing work area and ordinary numbering can be done according to the request of the business.

Common numbering methods:
- 10-20-30 ... shaped like
- 100-200-300 ... shaped like

In case of intermediate work area, intermediate numbering is used.
- 10-15-20-25 ... shaped like
- 100-150-200 ... shaped like

Work Area Name

It is the designation given to the work station.

Operations by Machinery, Device and Automatic Systems

The job defined in the work area can be performed by machine only or human only, or human-machine can perform operations together. In this section, operations pertaining to the machine, device or automatic system are defined in both operating states.

The use of a macro expression by grouping provides a disadvantage in the time management phase of the works. Therefore, as far as possible, every phase that undergoes

permanent deformation on the product should be defined as an operation.

Operations Performed by The Postal Operator (Serial jobs, frequency jobs, PPS activities...)

All activities performed by the existing human being in the working area are written in a sequential manner.

Two main groups are considered here:
• Activities in the stream
• Non-flow activities

All activities done by the person in charge of the mail are first tracked. During this follow-up, the employee is asked to take notes of all the work he has done. Any work with this note is sorted and observed on the spot (1).

Important Note (1)

How to perform all operations performed by both machine and human should also be standardized. At Prometal, we carry out this work using the standard operation sheet and thus, we provide the link of the process requirements table with other lean production tools.

While all the defined jobs are described in detail with the standard operation sheet (SOF), the issues to be considered during the execution of that job, customer special requests, important key points that may have a negative impact on quality, cost, time, environment or occupational safety if not done are defined in the next column.

Here, activities in the flow, ie operations that have a direct impact on the product, are often written. However, the frequency activities, which we call non-flow and mostly for the operation of the system, are skipped. However, it should be noted that the performance of activities that affect the product in the flow is directly related to the accurate and complete definition of the non-flow activities.

Examples of non-flow activities:
• Filling the oil drum at the beginning of each shift
• Lubrication of the mold at each machine stop
• Autonomous maintenance activity
• Cleaning the machine
• Anomaly notification
• Filling out the work area document
• Notification of relevant persons in case of abnormality
• Filling the suggestion form

Key Points for Product and Process, Customer and Business

"Operations Performed by Machinery, Device or Automatic Systems" and "Operations Performed by Operator (Serial jobs, frequency jobs, PPS activities ...)" defined in the first two columns on the Process Requirements Table (PRT), are defined as key points that are effective in terms of product, process, customer and business.

The key point concept is defined as the issues that cause harm in terms of quality, cost, time, environment or work safety when not applied to the business or personnel.
This part should be taught very well, especially to the employees. It is very important to make sure that it is learned and to verify that it is understood in certain periods.

The first two lines in the PRT are the subjects that should be emphasized during the training of a new employee in the field of word.

Standard Requirements for Performance and Quality

It has been deemed appropriate to define the basic process characteristics in order to meet the customer demands in the work areas and to eliminate the waste afterwards. If this definition is missing, the equipment in the work area cannot be controlled, the human resources unit cannot be connected to the system when a new operator is needed, and 5S cannot be made for visual and financial management.

In the absence of this section, instead of the management of period and processes according to the standard, a variable management model comes into play according to the wishes and competencies of the people.

Tools Used

In the process requirement table, the operations and activities performed by machine and human in the first two stages are defined.

When you do not define the equipment required for the operations in a working area, it cannot be said that the operation is carried out at the desired time with the desired quality and efficiency. In such a case, the sorting activity, which is the first step of the 5S activity, is not performed correctly. In such a case, the sorting activity, which is the first step of the 5S activity, cannot be performed correctly. The decision-making mechanism is left to the individual to distinguish the equipment and material required in the work area from the unnecessary. With this incomplete definition, it is a fact that there is a risk of serious occupational accidents, even experienced. This situation is explained as follows.

In the three-shift system, when the operator working at the injection machine is putting the part into the mold, because of the tight fit;

1.The shift operator pre-places the part in the mold and starts the injection activity by hitting it with a metal hammer

a. Since the metal hammer is not defined, the use of unnecessary equipment increases the cost and carries a safety risk.

b. By hitting the part with a metal hammer, the risk of geometric deformation of the part on the mold increases.

c. There is a risk that the part will go to the customer as a quality defect and be recalled.

d. In case the hammer accidentally hits the mold surface, it causes deformation on the mold, resulting in cost loss.

e. A defined area is required for the hammer.

2. The shift operator pre-places the part into the mold and places it by hitting it with the help of the same part. In this case;

a. There is a risk of deformation of both the part in the mold and the part used for striking.

b. The piece is used out of purpose by using a hammer.

c. There is a risk of occupational accident due to the risk of being cut in the hand while using the hammer.

3. The shift operator pre-places the part into the mold and presses it down to make sure it fits with just his hand

These activities are carried out in this way during the period when there is no PRT (Process Requirements Table). However, thanks to PRT, the operations to be performed by the operator in the work area are specified and the equipment, if any, to be used for these operations are defined in the "tools used" step.

In this way, we can define and monitor the tools and equipment that should be in a work mail during the project period. Thanks to this definition, there are no missing tools and equipment in occupational safety risk analysis, and we make the first step of 5S activities according to this definition. Thanks to this column, the process requirements table provides the information and standard that other lean production tools need.

Required Environmental Conditions

It has been observed that environmental conditions are the subject that is often neglected while performing operations in the process. In the quality control work area, the operator performs visual control. In this visual inspection, it has been determined that the light intensity of the environment is important so that the operator can make a healthy control on the part. Excessive light intensity will tire the operator, and insufficient light will deteriorate the control quality. While starting the lean transformation, these standards did not form an idea about how the environmental conditions should be.

The process requirements table is prepared separately for each work area.

As environmental conditions:

- Ventilation
- Audio
- Ergonomic conditions
- Cleaning
- Definitions are made.

Figure 2 shows the sample form for lighting. With this definition, the occupational safety risks of the business area are minimized and it is possible to create a risk-free process that will respond to quality standards and customer requests.

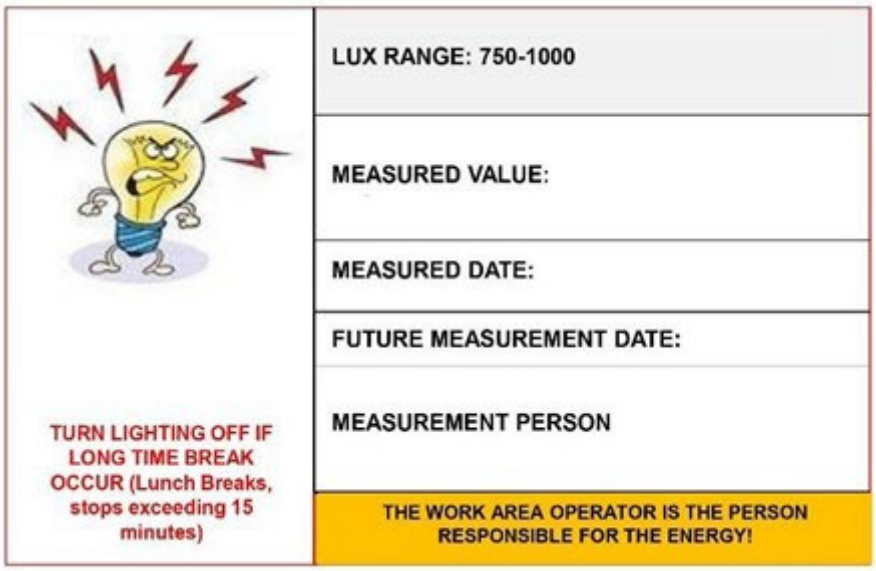

Fig.2 - Work Area Lighting Standard.

Process Inputs

Basically, each process is created in the "input - processing - output" logic. Thanks to PRT, by defining the inputs, 5S, which is a visual management tool, was made more effective and the quality level on the product was increased. This situation is explained as follows.

CNC machined parts are sanded. However, this type of sandpaper is not defined anywhere. For this reason, the sanding sand depth may vary and quality problems are experienced on the product depending on this variability. However, this is an entry for that workspace and must be defined. However, in the current system (before the lean production system), there is no section where this is defined.

By defining the type of sandpaper (600 grit diameter 75) in the process inputs section of the process requirements table, quality problems are prevented and stock follow-up becomes possible.

As another case, there is the "human" factor as the input of the work area. However, although this person is directly affected by the quality and efficiency of the work done in that work area, it is undefined in many organizations. The activities to be performed by the machine and human defined in the process requirements table and the basic features sought in the human profile to manage the equipment to be used are defined in this section.

For example:

- 20-35 age range
- Vocational high school graduate
- Just woman
- Height below 1.90
- Maximum weight of 100 kg

Thanks to this definition, it is ensured that human resources find suitable personnel for the job and that polivalence studies are managed more effectively.

Required Warnings During Working In the Working Area

In the work area, the points to be considered for the customer and efficiency are defined both in the operations performed by the machine and the operations performed by the operator while the operator is performing his activities.Thus, customer protection activities for each operation are defined, ready to be taught and made available for inspection.

Examples for this part:

- Pieces should not be left untidy during breaks
- The parts should not be mixed on the table
- Only plastic hammer should be used in the work area
- Part temperature must be at least 25 degrees

Basic Competencies Of The Operator

He explained its importance as 4M in the process. In this 4M, one of the two most important subjects that we can-

not buy with money is "human".

It is essential that the employee who will ensure efficiency in the work area and fulfill the customer requests can perform the activities specified in the transaction requirements table, and that the information and trainings that the employee who will observe the standard conditions and fulfill the requirements must have.

Thanks to this definition, the trainings to be given and the competencies to be gained should be defined before placing an operator in a work area. With this definition, the trainings that should be prioritized in the annual training plans of human resources have been determined. At the same time, the follow-up of the basic and compulsory trainings that should be given to the employees, especially the laws numbered 4857 and 6331, and the giving of the trainings are made easier to monitor.

Examples of basic competencies that the operator should have:

- Work area risk analysis
- Ergonomic activities in the workplace
- Visual management in the work area 3S+2S
- Workplace regulations
- Workplace training

Relation of Processing Requirements Table with Prometal Production System Tools

The senior management had a full determination that the first condition for competitiveness was the necessity of system installation by increasing productivity at Prometal. These studies are carried out in large corporate enterprises in 10-15 years, accompanied by large investments and organizations.

If these studies are not considered as a whole, it will reveal a single-ring chain and its effectiveness will be weak. For this reason, firstly, the transaction requirements table was prepared and its integration with other tools was ensured.

Fig.3 - Relation of Process Requirements Table with Prometal Production System Tools.

CONCLUSION

When all these substances were applied in the enterprise, it was observed that there were noticeable improvements in quality. Thanks to the serious reductions in the 8D analyzes made by the quality unit due to the decreasing complaints, the stress decreased and the motivation increased. A 50% improvement in quality in the first 7 months continues as a zero error in a 1-year period as a result of the studies that were commissioned and continued. On the one hand, the company has experienced improvement in quality, and the quality level of seat belt parts, which are of great importance for human life, has been appreciated by the customer and paved the way for new investments and collaborations. Thanks to the tools and systems commissioned during the development of the system, serious improvements were experienced in logi-

stics and production processes, and the balance problem decreased from 200% to 0.0001%.

As a result of these studies, customer satisfaction was observed in customer visits and business volume growth was achieved by obtaining high (VDA...) scores in supplier audits carried out before new projects.

ACKNOWLEDGEMENT

With the establishment of PPS (Prometal Production System) by taking the decision to establish a system for the high quality and efficiency expected by the customers instead of contract manufacturing activities in such a high competitive environment; Endless thanks to Burak AZMAN, the General Manager of Prometal, and the management staff, who strengthen the competitiveness of the enterprise, protect and increase employment, increase turnover and foreign currency inflow to our country through the acquisition of new customers with sustainability.

La Metallurgia Italiana
International Journal of the Italian Association for Metallurgy

Suction system from the self-induced mold cavity (Venturi)

F. Tonolli

Our suction system's goal is to be a valid and more simple alternative to the application of traditional vacuum system. We generate a depression in the mold cavity using the movement of air developed by the metal entering in the mold. We have designed a particular auxiliary channel directly connected to the inlet metal in the mold. The metal inlet in the mold pushes the air in this channel in a Venturi striction to increase the air speed to ultrasonic values. This develops a pressure reduction in the expander and in the connected mold cavity. In this way we experience a suck effect from mold cavity. The Venturi valve can be applied to both hot and cold chamber.

KEYWORDS: SUCTION, VACUUM, VENTURI, POROSITY;

INTRODUCTION

System layout

The particularity of our system (Fig. 1) consists essentially in an auxiliary channel (A) for the generation of compressed air. This channel is directly connected to the inlet point of the mold and to the section reduction (C) to generate the Venturi effect. With this section reduction we observe an acceleration of air speed to ultrasonic values, and then a pression reduction in the expander. This expander is directly connected to the mold cavity by a suction channel (B) and for this we can suck air from the cavity.

Obviously, we need to let out the air from the mold. For this we need a chill vent (C) in the end position. The auxiliary channel is nothing else that a container of air that we push to the Venturi restriction to generate a complete Venturi effect.

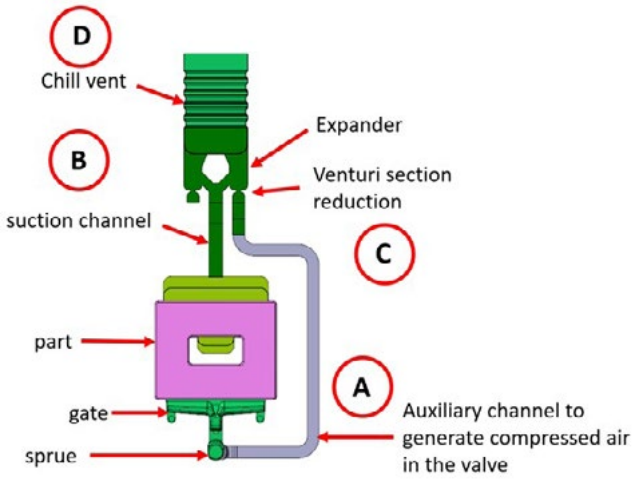

Fig.1 - System layout.

F. Tonolli
TF, Villa Carcina, Italy

The principle upon the valve is based is the principle of energy conservation for a fluid.

$$p + \frac{1}{2}\rho v^2 = cost$$

As the speed increase the pressure decrease (the geodetic term is negligible).
Key aspect of design: the metal must reach the expander after we have filled the cavity. When the metal reach the expander the suction phenomenon ends

FEATURES

Follow some characteristic of this system:

1. Reduction of pressure in the cavity
2. Reduction of porosity in the die part
3. Easier to fill 'shaded' areas with respect to the molten metal flow
4. Gradual generation of vacuum in the cavity
5. No need of external equipment (suction pumps)
6. Fully calibrated on the application
7. If properly designed, it is foolproof

From the comparison with passive or active systems (vacuum) the Venturi valve places in the between.

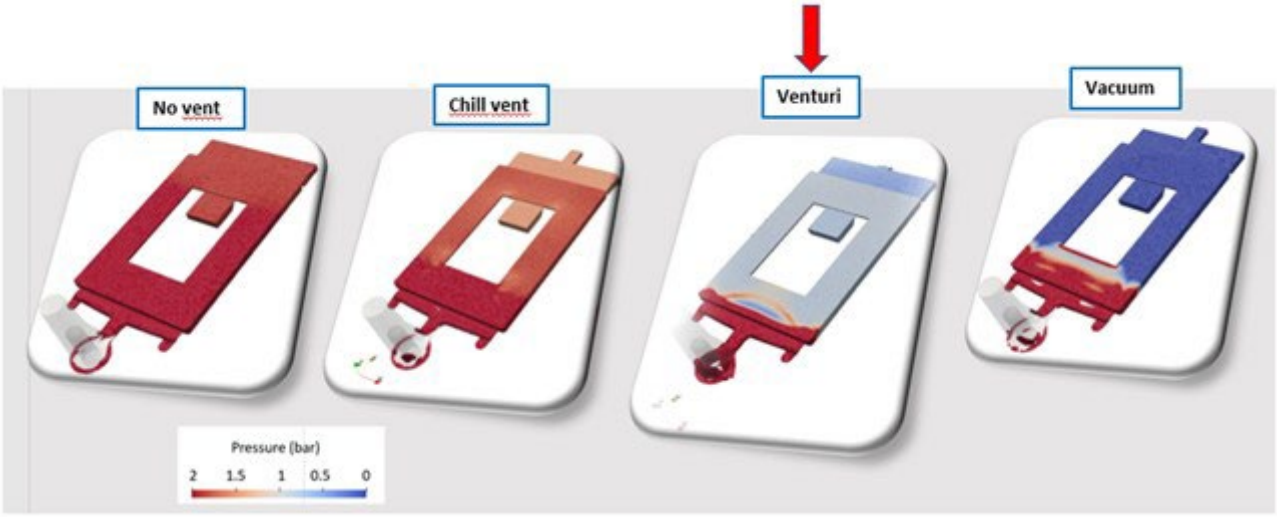

Fig.2 - Comparison with other technology (air pressure in cavity).

The venturi system is worse of a vacuum system but better of any other passive system (Fig 2).

VACUUM GENERATION

Since the vacuum is generated by the metal entering in the mold, the aspiration effect increases as the mold is filled. Small aspiration at the beginning, big at the end.
In the follow pictures you can see as at the beginning we must compress the air inside the auxiliary channel (Fig. 3). For this we experiment a delay with little depression in the starting stage. After this the system starts to work and the air pression inside the mold cavity (in comparison to passive system) decreases (Fig 4 and 5).

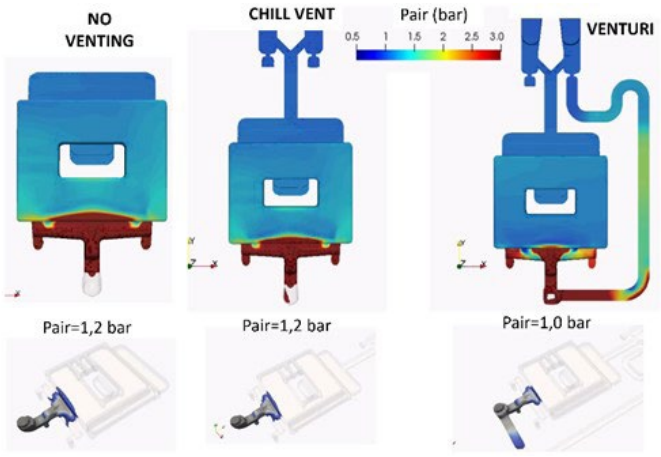

Fig.3 - Starting stage of filling (air pressure in cavity).

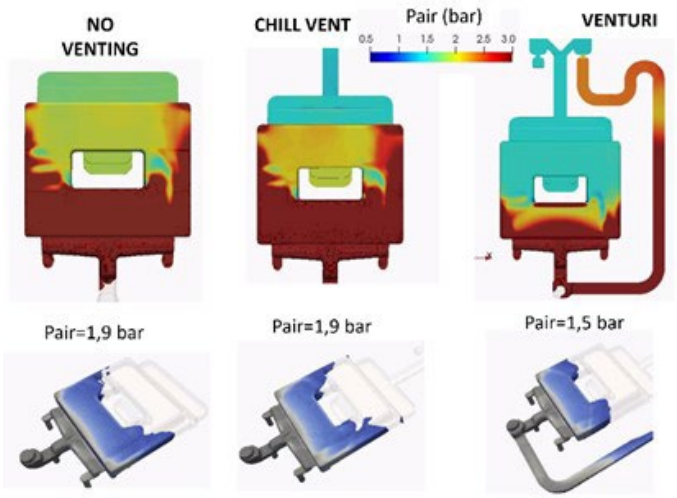

Fig.4 - Middle stage of filling (air pressure in cavity).

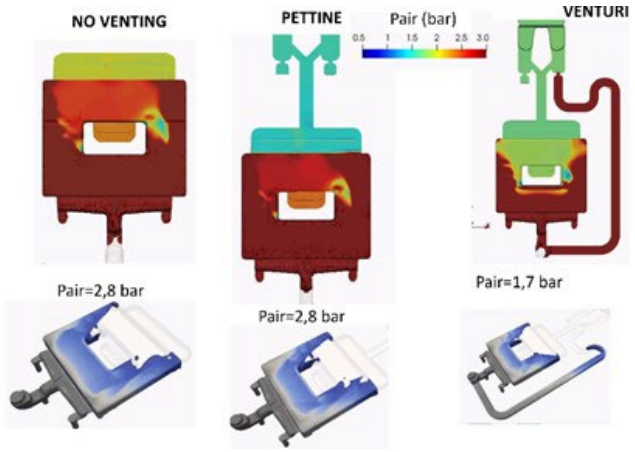

Fig.5 - Final stage of filling (air pressure in cavity).

In table 1 we have a summary of the delta air pressure in mold cavity for different filling stage.

Tab.1 - Venturi pressure reduction VS filling phase.

filling phase	Delta pressure
Start filling	-200 mbar
Half filling	-400 mbar
End filling	-1100 mbar

Valve design – APPLICATION

The box design of valve is geometric compatible to the standard vacuum valve on the market. To overcome the variability represented from the auxiliary channel that can come from left or from right we have designed a double valve (Fig. 6-7). This valve can also be used to maximize the aspiration using a double configuration (Fig. 8). Different measures are available for different cavity volumes.

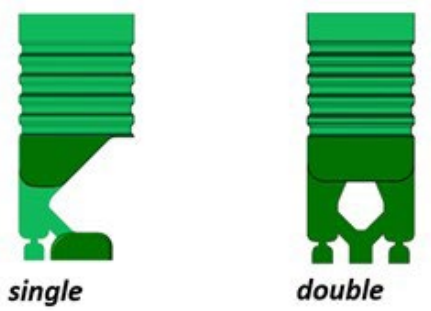

Fig.6 - Single and double valve layout.

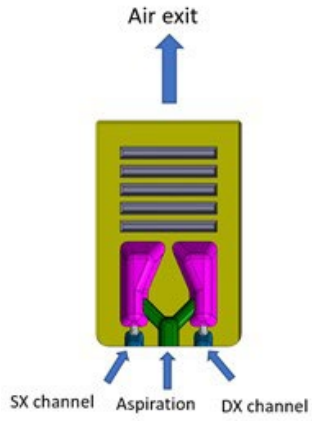

Fig-7 - VDouble valve description.

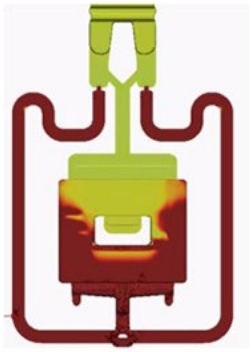

Fig.8 - Double Venturi application layout.

CASE STUDY

To test the Venturi system we have made many virtual test with numerical simulations in comparison with practical sampling either in cold and hot chamber. Interesting results are obtained for finned parts like a heatsinks where the filling is first in the thickness and after in the fins. These results are very close to the use of vacuum system (Fig. 9). Another test was made with Zamak in which we can clearly see the different flow in the part using or not using the Venturi valve (Fig. 10)

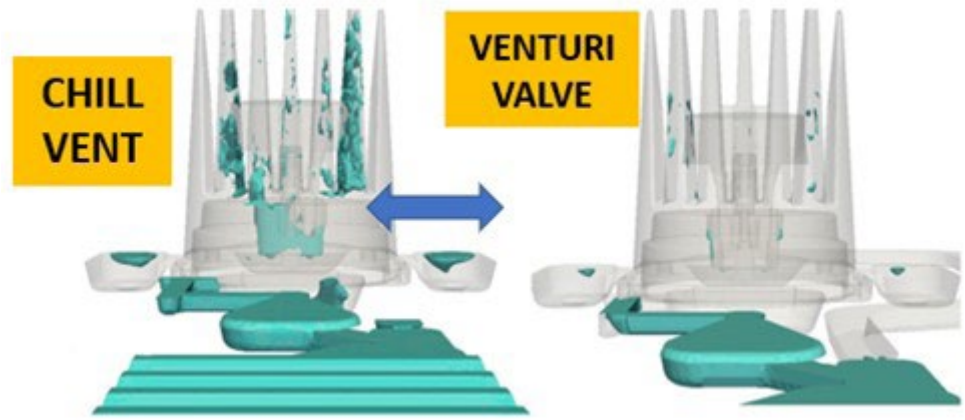

Fig.9 - Entrapped air without and with the use of Venturi valve.

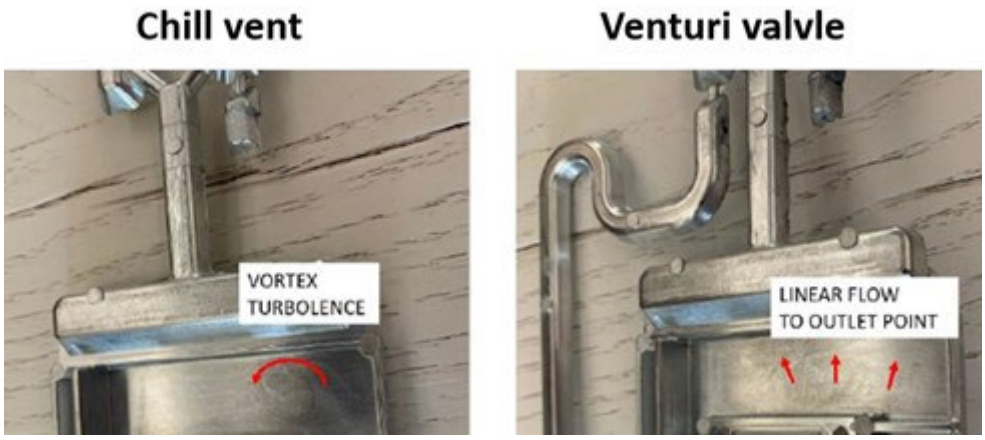

Fig.10 - Flow in real casting (ZAMAK).

REFERENCES

[1] Tonolli Francesco, inventor 'Stampo di formatura' Application Number PCT/IB2021/062327

premio ALDO DACCÒ

L'AIM è lieta di indire il bando per l'edizione 2022 del prestigioso **Premio Aldo Daccò**, con l'obiettivo di stimolare i tecnici del settore e contribuire allo sviluppo e al progresso delle tecniche di fonderia e di solidificazione con memorie e studi originali.

L'Associazione invita tutti gli interessati a concorrere al **Premio "Aldo Daccò" 2022**, inviando a mezzo email il testo di memorie inerenti le tematiche fonderia e solidificazione, unitamente al curriculum vitae dell'autore concorrente, **entro il 30 giugno 2022**.

Saranno presi in considerazione e valutati i lavori riguardanti le varie tematiche di fonderia e di solidificazione, sia nel campo delle leghe ferrose che in quello delle leghe e dei metalli non ferrosi.

Il premio, pari a **Euro 5000 lordi**, è offerto dalla **Fondazione Aldo e Cele Daccò**, istituita dalla signora Cele Daccò, recentemente scomparsa, per onorare la memoria del marito Aldo Daccò, uno dei soci fondatori dell'AIM e suo encomiabile Presidente per molti anni.

Le memorie verranno esaminate da una Commissione giudicatrice designata dal Consiglio Direttivo, il cui giudizio sarà insindacabile.

Nel giudicare, la Commissione terrà conto, in particolar modo, dell'originalità del lavoro e dell'argomento in relazione alla reale applicabilità dei risultati. Non sono ammesse candidature da chi abbia già ottenuto riconoscimenti, anche per lavori diversi, dalla Fondazione Aldo e Cele Daccò.

Le memorie premiate e quelle considerate meritevoli di segnalazione, potranno essere pubblicate sulla rivista La Metallurgia Italiana.

La cerimonia di premiazione avrà luogo in occasione del 39° Convegno Nazionale AIM, che si terrà a Padova nei giorni 21-23 settembre 2022.

Per informazioni e candidature:

ASSOCIAZIONE ITALIANA DI METALLURGIA
Via Filippo Turati 8 · 20121 Milano
Tel. +39 02-76397770 · +39 02-76021132
E-mail: info@aimnet.it
www.aimnet.it

La Metallurgia Italiana
International Journal of the Italian Association for Metallurgy

In memoria di Cecilia Monticelli

Cecilia Monticelli, Professore Associato di "Corrosione e protezione dei materiali metallici" presso il Centro Studi Corrosione e Metallurgia "A. Daccò" dell'Università di Ferrara, è venuta a mancare il 22 febbraio scorso, all'età di 64 anni. Nonostante la grave malattia, ha continuato a seguire le attività di ricerca e didattica fino agli ultimi giorni, senza far mancare mai il suo prezioso supporto al gruppo di ricerca.

Dopo la laurea con lode in Chimica presso l'Università degli Studi di Ferrara, nel 1981, ha preso servizio come Ricercatrice Universitaria presso il Centro di Studi sulla Corrosione "A. Daccò" dell'Università di Ferrara. Ha trascorso alcuni anni in rinomati centri di ricerca ed in industrie del settore (MTA, UMIST, Sulzer) dove ha avuto modo di arricchire le sue competenze professionali. Dal 1° novembre 2001 ha ricoperto il ruolo di Professore Associato di "Scienza e Tecnologia dei Materiali". Ha formato generazioni di studenti e ricercatori, dedicandosi con passione all'attività didattica, inizialmente per il Corso di laurea in Ingegneria dei Materiali e poi per quella in Ingegneria Meccanica dove, negli ultimi anni, è stata docente del corso di "Corrosione e protezione dei materiali metallici". È stata per diversi anni socia AIM, molto partecipe e attiva nel Comitato Tecnico Corrosione. Tra le diverse iniziative, cui ha prestato il suo importante contributo, citiamo l'organizzazione delle Giornate Nazionali di Corrosione e Protezione del 2015 a Ferrara.

Eventi AIM / AIM events

CONVEGNI

27° CONVEGNO NAZIONALE TRATTAMENTI TERMICI – Genova, 26-27 maggio 2022
http://www.aimnet.it/tt.htm

ESSC & DUPLEX 2021 - 11TH EUROPEAN STAINLESS STEEL CONFERENCE SCIENCE & MARKET & 8TH EUROPEAN DUPLEX STAINLESS STEEL CONF. & EXHIB. – Bardolino (Verona), 15-17 giugno 2022
http://www.aimnet.it/essc.htm

39° CONVEGNO NAZIONALE AIM – Padova, 21-23 settembre 2022
http://www.aimnet.it/nazionaleaim

ROLLING 2022 - 12th INTERNATIONAL ROLLING CONFERENCE – Trieste, 26-28 ottobre 2022
https://www.aimnet.it/rolling-12/

IWSQ 2022 - 2ND INTERNATIONAL WORKSHOP ON SURFACE QUALITY OF CONTINUOSLY CAST PRODUCTS – Bergamo, 1-2 dicembre 2022
https://www.aimnet.it/iwsq-2.htm

CORSI E GIORNATE DI STUDIO

Giornata di Studio LE OPPORTUNITA' REGIONALI PER LO SVILUPPO DI UN ECOSISTEMA CIRCOLARE NEL SETTORE METALLURGICO – Milano c/o Regione Lombardia, 27 aprile

Corso DIFETTOLOGIA NEI GETTI PRESSOCOLATI: METALLIZZAZIONI - 3 maggio – webinar FaReTra

Corso ADDITIVE METALLURGY – 4-10-17-24 maggio – webinar FaReTra

Giornata di Studio SVILUPPO TECNOLOGICO DEGLI IMPIANTI DI PRODUZIONE A CALDO DI VERGELLA DI ALTA QUALITÀ PER USI SPECIALI – Lecco c/o Caleotto, 5 maggio

Corso Modulare METALLOGRAFIA – ibrido – Milano, 31 maggio, in modalità webinar 7-8-9-14-15-28-29 giugno, 5-6 luglio, 13-14-15 settembre

Corso modulare FONDERIA PER NON FONDITORI – maggio/giugno – webinar FaReTra

Giornate di Studio GETTI PRESSOCOLATI PER APPLICAZIONI STRUTTURALI – Brescia, giugno

Seminario TRASMISSIONI NELL'AUTOMOTIVE: DALL'ACCIAIERIA AL PROCESSO DI PALLINATURA – Modugno, (Bari) c/o Magna, 16-17 giugno

Corso MICROSCOPIA ELETTRONICA IN SCANSIONE – SEM - III Edizione– Milano, Lecco, 21-22 giugno

Corso TRIBOLOGIA INDUSTRIALE – ibrido – 22-23 giugno e Modena, 29-30 giugno

Giornata di Studio ANALISI INFORTUNI – giugno

SCUOLA DI METALLURGIA DELLE POLVERI – Imola c/o SACMI, 5-6 luglio

Metallurgy Summer School SURFACE ENGINEERING OF METALS – Bertinoro (FC), 24-27 luglio

Corso MASTER PROGETTAZIONE STAMPI – itinerante, settembre/ottobre/novembre/dicembre

Giornata di Studio LEGHE PER ALTA TEMPERATURA PRODOTTE CON TECNOLOGIE ADDITIVE – Firenze (c/o Baker Hughes), 15 settembre

Giornata di Studio MICROSCOPIA ELETTRONICA APPLICATA ALLA FAILURE ANALYSIS – Padova, 20 settembre

Per ulteriori informazioni rivolgersi alla Segreteria AIM, e-mail: info@aimnet.it, oppure visitare il sito internet www.aimnet.it

Giornate di Studio CEMENTAZIONE VS NITRURAZIONE – Provaglio d'Iseo c/o Gefran, settembre
Corso PROVE NON DISTRUTTIVE – ottobre

Giornata di Studio RIVESTIMENTI E ADDITIVE MANUFACTURING – Milano, novembre

Giornata di Studio DALLA SCELTA ALLA REALIZZAZIONE DI COMPONENTI TRATTATI TERMICAMENTE: COME EVITARE PROBLEMI TECNICI E CONTRATTUALI? – novembre

Giornata di Studio TECNICHE DI CARATTERIZZAZIONE DEI MATERIALI – Vicenza, novembre

www.aimnet.it

FaReTra (Fair Remote Training) - FORMAZIONE E AGGIORNAMENTO A DISTANZA

Modalità Asincrona (registrazioni)

Corso METALLURGIA PER NON METALLURGISTI

Giornata di Studio PRESSOCOLATA IN ZAMA

Giornata di Studio LA SFIDA DELLA NEUTRALITÀ CARBONICA

Corso itinerante METALLURGIA SICURA

Corso modulare TRATTAMENTI TERMICI

Corso modulare I REFRATTARI E LE LORO APPLICAZIONI

Corso GLI ACCIAI INOSSIDABILI 11ª edizione

Corso FAILURE ANALYSIS 11a edizione

Giornata di Studio PERFORMANCE E DEGRADO DEI MATERIALI METALLICI UTILIZZATI IN CAMPO EOLICO: CAPIRE PER PREVENIRE

Giornata di Studio DIFETTI NEI GETTI PRESSOCOLATI: POROSITA' DA GAS

Corso PROVE MECCANICHE

Corso di base LEGHE DI ALLUMINIO

Giornata di Studio GREEN ECONOMY E ASPETTI AMBIENTALI PER L'INDUSTRIA DEI RIVESTIMENTI

Giornata di Studio IL CICLO DI FABBRICAZIONE DI UNA VALVOLA. NORMATIVE, PROGETTO, ACCIAIO, FUCINATURA COLLAUDO

Corso CORROSIONE PER NON CORROSIONISTI

Giornata di Studio TECNOLOGIE DI FORMATURA DELLE ANIME IN SABBIA PER GETTI IN LEGA LEGGERA

L'elenco completo delle iniziative è disponibile sul sito: www.aimnet.it
(*) In caso non sia possibile svolgere la manifestazione in presenza, la stessa verrà erogata a distanza in modalità webinar

Comitati tecnici / Study groups

CT AIM / ASSOFOND – FONDERIA (F)

(riunione telematica del 18 gennaio 2022)

Manifestazioni in corso di organizzazione

- Il CT discute delle figure accademiche e professionali cui affidare le lezioni del primo modulo del corso "Fonderia per non fonditori". Vengono messi a punto alcuni dettagli e discussi gli argomenti da inserire, tra cui una lezione sulla simulazione e sull'interpretazione critica dei risultati ottenuti. Si decide che al termine del corso gli iscritti dovranno sostenere un test per ottenere un attestato di partecipazione. Si valuterà anche la possibilità di ottenere crediti formativi. Un gruppo ristretto si incontrerà per stabilire gli ultimi dettagli del programma. Il corso si svolgerà a maggio/giugno 2022.

Iniziative future

- Una GdS sulle resine e i loro aspetti legati all'ambiente si potrebbe organizzare entro giugno 2022 se i produttori saranno disponibili e daranno indicazioni sugli argomenti da trattare.
- Bonollo, coordinatore del corso di "Metallografia delle ghise", informa che non è ancora stata stabilita la data di inizio del corso.

CT TRATTAMENTI TERMICI E METALLOGRAFIA (TTM)

(riunione telematica del 10 febbraio 2022)

Notizie dal Comitato

- Il presidente Petta informa che è mancato l'ing. Daniele Franchi, uno dei membri storici del CT TTM, molto presente e attivo in tante iniziative. Petta ricorda che Franchi era un pioniere nei collegamenti con le associazioni consorelle di AIM e collaborava a mantenere vivi i rapporti. Il Presidente e tutto il CT sono vicini alla famiglia. Silvia Roggero, che lavorava insieme a Franchi, esprime i ringraziamenti della famiglia e dell'azienda per tutte le manifestazioni di cordoglio ricevute.
- L'ing. De Feo sostituisce ufficialmente l'ing. Bellino per la Air Liquide nel comitato.

Manifestazioni in corso di organizzazione

- La GdS sullo shot-peening - coordinatore Morgano – si terrà presso Silco a Rivalta (TO) a fine aprile 2022 in presenza. Morgano ha preparato una bozza di programma e aspetta le conferme da parte dei relatori. La locandina sarà disponibile ai primi di marzo.
- "Convegno Nazionale Trattamenti Termici" (Genova, 26 e 27 maggio 2022): tutto è confermato. Bassani si sta interessando della parte logistica, compresa la cena sociale. Il programma scientifico, come già definito, sarà separato dalle presentazioni dell'area espositiva. Bassani mostra la locandina, praticamente pronta, con lo schema delle sessioni nelle due aree, e la piantina della zona del Congresso: ci sono spazi ampi, con un corner per le presentazioni degli espositori – non chiuso – e subito accanto alla zona degli stand c'è la sala per le presentazioni scientifiche.
- L'inizio del "Corso di Metallografia" è fissato a giugno 2022 come per i corsi precedenti. Petta vorrebbe organizzare questo corso con didattica in webinar ed esercitazioni o parte pratica in presenza presso un'azienda strutturata in maniera tale da supportare questa attività. Si istituisce un comitato ristretto per coordinare e ristrutturare il corso partendo dal programma della edizione precedente, sia per i temi delle lezioni che per i nominativi dei docenti. Ci sarà anche una parte dedicata ai trattamenti dei metalli leggeri, per la quale di solito interviene il CT ML. Petta vorrebbe far fare l'introduzione del Corso al dr. Bavaro, coordinatore di tutte le precedenti edizioni.
- Il seminario "Trasmissioni nell'automotive: dall'acciaieria al processo di pallinatura" – coordinatori Morgano e Rosso – si terrà il 16 e 17 giugno 2022 a Modugno (Bari) presso Magna. Non c'è nessuna variazione di programma e tutto è confermato. La Rivista di Metallurgia pubblicherà una intervista con il CEO del plant Magna, che servirà anche a lanciare la manifestazione.

Iniziative future

- La GdS "Cementazione e nitrurazione" si terrà presso Gefran (Provaglio di Iseo – BS) a fine settembre/inizio ottobre 2022. Il programma prevede le presentazioni seguite da una visita allo stabilimento. Il programma sarà definito anche prendendo spunto da precedenti giornate organizzate da AIM sullo stesso tema. Bassani richiede una bozza della locandina per la prossima riunione.
- GdS "Il Mondo Industrial - aspetti metallurgici e metodologie di controllo": il coordinatore Fabio Massa non ha per ora comunicato novità circa la possibile data, dipendente dalla disponibilità di Iveco CNH per ospitare la manifestazione.

- Seminario congiunto con CT Metallurgia delle Polveri e Tecnologie Additive (2022–data da definire): anche su questa manifestazione non ci sono novità per le date, che dipendono dalla disponibilità delle due aziende ospitanti. Aspettiamo fine marzo per vedere se i vincoli attuali decadono.
- Si decide di organizzare tra ottobre e novembre 2022 una manifestazione dal possibile titolo: "Dalla scelta alla realizzazione di componenti trattati termicamente: come evitare problemi tecnici e contrattuali" – coordinatori Vicario, La Vecchia, Cusolito. Si discute dei possibili argomenti da trattare.

CT METALLURGIA FISICA E SCIENZA DEI MATERIALI (MFM)

(riunione telematica del 11 febbraio 2022)

Consuntivo di attività svolte

- Il presidente Bassani riferisce sugli esiti della GdS "Il ruolo dei materiali nell'economia dell'idrogeno" - coordinata da Cabrini del Comitato Corrosione, in collaborazione con i Comitati di Metallurgia Fisica e Materiali per l'energia e tenuta in modalità webinar. La manifestazione ha avuto un notevolissimo successo di pubblico (184 iscritti) e ha raccolto una buona soddisfazione da parte del pubblico che ha risposto ai questionari di soddisfazione: in particolare sono state apprezzate la qualità della docenza e l'organizzazione. È emerso l'interesse per ulteriori approfondimenti, ad esempio relativamente all'interazione dell'idrogeno con i materiali ottenuti da processi additive.

Manifestazioni in corso di organizzazione

- Tuissi e Vedani presentano il corso "Additive Metallurgy", che si svolgerà online in quattro mezze giornate nelle date 27/4, 4/5, 11/5, 18/5, ciascuna con 4 inteventi più il tempo per domande e discussione. Gli argomenti del corso saranno focalizzati principalmente sulle proprietà dei materiali metallici prodotti per additive piuttosto che sugli aspetti tecnologici. I temi delle giornate saranno: solidificazione e microstrutture, trattamenti termici (precipitazione e rilascio delle tensioni residue), proprietà meccaniche e correlazione con le microstrutture, effetto su proprietà metallurgiche dei processi "non-beam" (filo, arco).
- Montanari relaziona sull'organizzazione della "Metallurgy Summer school" (24-27 luglio a Bertinoro), dedicata all'ingegneria delle superfici metalliche. La locandina dell'evento è già pronta e a breve sarà resa pubblica.
- Paola Bassani relaziona sull'organizzazione del corso "Microscopia elettronica in scansione per Metallurgisti - SEM" che si terrà in presenza tra la seconda metà di giugno e la prima di luglio. Le date esatte verranno decise sulla base della disponibilità delle sedi ospitanti e dei relatori. Il corso comprenderà un adeguato tempo dedicato alla tecnica EBSD, a cui si sarebbe voluto dedicare un evento specifico.

Iniziative future

- Casati e Vedani comunicano che la Giornata di Studio sui "Materiali funzionali", già prevista a settembre 2021 e rinviata, è tuttora in standby ed aggiornamenti saranno forniti nel corso della prossima riunione.
- Il coordinatore Montanari prevede che il corso di base "Solidificazione" si potrà tenere a marzo 2023.
- Montanari e Varone relazionano sull'organizzazione della Giornata su "Caratterizzazione dei materiali", prevista per fine novembre 2022 a Vicenza con la collaborazione di Bonollo. La bozza del programma è ancora da definire e verrà presentata durante la prossima riunione.
- Montanari, Tuissi e Vedani discutono della possibilità di organizzare un'iniziativa sui materiali metallici biodegradabili, che in passato non era stato possibile realizzare per il limitato numero di gruppi che opera sull'argomento. Montanari nota che l'interesse biomedico per i materiali metallici biodegradabili è in aumento e che si potrebbe coinvolgere un'azienda per coprire gli aspetti industriali. Sia Bassani che Montanari concordano che si potrebbe organizzare un evento con un approccio multidisciplinare non esclusivamente metallurgico.

CT ACCIAIERIA (A)
CT FORGIATURA (F)

(riunione telematica congiunta del 23 febbraio 2022)

Notizie dal Comitato

- Il presidente Mapelli informa che Engris Ceccaroli, dopo molti anni di attiva partecipazione al CT, ha rassegnato le dimissioni.
- Il presidente Rampinini informa che il congresso Internazional Forgemasters Meeting è stato assegnato ufficialmente all'Italia e sarà

organizzato da Federacciai (sezione Fucinati) e AIM nella tarda primavera del 2024. Rampinini presenta un elenco di temi di acciaieria e forgiatura a cui i membri del CT sono invitati ad aggiungere le loro idee.

Manifestazioni in corso di organizzazione

- Rampinini conferma l'intenzione di organizzare la GdS "ITER experience for new DTT Enea Fusion Reactor" in presenza nell'autunno 2022.
- Mapelli informa che probabilmente ad aprile si svolgerà un evento in presenza di mezza giornata dedicato al preridotto: oltre ad un paio di interventi sull'uso di idrogeno come riducente all'interno dei preriduttori, parteciperanno DRI d'Italia, ECCO che si occupa di studi sull'impatto ambientale e Patrizia Toia, Europarlamentare e Vicepresidente della Commissione per l'industria, la ricerca e l'energia (ITRE).

Iniziative future

- Dai questionari di soddisfazione della GdS "Il ruolo dei materiali nell'economia dell'idrogeno" è emersa la richiesta di organizzare una manifestazione sull'uso degli acciai (forgiati e da fusione) nell'ambiente idrogeno oil&gas, evidenziandone i limiti di applicazione. Rampinini e Lissignoli ritengono il tema interessante e porteranno una possibile scaletta per la prossima riunione.

CT METALLI E TECNOLOGIE APPLICATIVE (MTA)

(riunione telematica del 02 marzo 2022)

Iniaziative future

- Il coordinatore Stella, con il presidente Loconsolo, ha preparato una prima scaletta di sette interventi per la GdS sulla sostenibilità ambientale nel campo delle costruzioni civili. I possibili relatori sono in fase di definizione, tanto da poter arrivare a fissare lo svolgimento della giornata per l'autunno 2022.
- La GdS "Utilizzo leghe di nichel in saldatura" rimane in stand-by: si potrebbero prendere in considerazione altri partner industriali. Una decisione sarà presa alla prossima riunione.
- La GdS "Trattamenti per la rimozione del piombo per il riciclo degli ottoni" al momento è da ritenere sospesa anche a causa di alcuni aspetti tecnici controversi tra i vari produttori.
- Per la manifestazione sui metalli nel settore automotive non ci sono novità, ma il tema sarà tenuto in considerazione.

CT PRESSOCOLATA (P)

(riunione telematica del 17 febbraio 2022)

Manifestazioni in corso di organizzazione

- La GdS "Difettologia nei getti pressocolati: metallizzazioni" – coordinatrice Pola – è stata definita come programma e come relatori. La locandina è stata distribuita. La manifestazione si terrà in webinar nella mattinata del 3 maggio 2022.
- Il corso "Getti Strutturali" – coordinatori Pola e Valente – si svolgerà in presenza in due giornate, di cui la prima già definita presso IDRA in data 15/06/22, mentre la seconda sarà definita a breve.

Iniziative future

- GdS "Sostenibilità nella fonderie HPDC": il presidente Parona e il coordinatore Bonollo provvederanno a rivalutare questa GdS, a contattare i potenziali relatori e a presentare una bozza di programma entro la prossima riunione.
- Il Master di progettazione "Stampi" si svolgerà tra settembre e dicembre 2022 in modalità itinerante. Le location, il programma dettagliato e i relatori sono in fase di definizione.
-

CT CORROSIONE

(riunione telematica del 11 febbraio 2022)

Consuntivo di attività svolte

- Il corso di "Corrosione per non corrosionisti" in collaborazione con il CT Controllo e Caratterizzazione Prodotti si è svolto il 24 e 25 novembre 2021. Bassani conferma che, nonostante non siano stati compilati i questionari di valutazione, si sono ricevuti commenti positivi sull'iniziativa.

- Per quanto riguarda la GdS sul ruolo dei materiali nell'economia dell'idrogeno, tenutasi il 27 gennaio in collaborazione con altri CT, Bassani fa vedere i risultati molto positivi emersi dai questionari e comunica che ci sono stati 165 partecipanti collegati online, concludendo così che la GdS ha avuto un grande successo.

Manifestazioni in corso di organizzazione

- La 15° edizione delle "Giornate Nazionali sulla Corrosione e Protezione" si svolgerà nel 2023 presso il Politecnico di Torino, sperabilmente in presenza. Si valutano le tempistiche di ricezione delle memorie per poterle pubblicare in tempi stretti sulla Rivista di Metallurgia: il riferimento è l'edizione del 2017 quando però la scadenza per l'invio dei riassunti era stato fissato a dicembre dell'anno precedente il Congresso.

Iniziative future

- Si discute a lungo del Corso di "Tecniche elettrochimiche per lo studio della corrosione", che comprende anche l'illustrazione delle più comuni tecniche di indagine. Bellezze e Balbo illustrano la bozza di programma precisando che il corso sarà principalmente indirizzato a dottorandi e magari esteso ad assegnisti e neo-ricercatori. Si potrebbero organizzare esercitazioni sperimentali, didatticamente molto utili, che però richiedono una sede universitaria con ampi laboratori e postazioni di prova multiple, oppure una unica postazione da cui il docente potrebbe illustrare le esercitazioni. Gli altri dettagli saranno fissati nel gruppo di lavoro che era già stato costituito.
- Bolzoni osserva che si dovrebbe riprendere in considerazione il corso modulare di corrosione "tradizionale", storicamente proposto in seno all'AIM e che non viene organizzato da un po' di tempo. La discussione sarà ripresa alla prossima riunione del CT C.

CT AMBIENTE E SICUREZZA (AS)

(riunione telematica del 24 febbraio 2022)

Notizie dal Comitato

- Come sempre, i membri del CT si scambiano informazioni circa esperienze o insegnamenti che possano essere utili. Si è parlato attività sul tino a volta aperta, confrontando i vari approcci per definire le attività necessarie da svolgere in sicurezza. Alcuni membri del CT hanno raccontato di incidenti avvenuti nella loro azienda e dei conseguenti provvedimenti presi con lo scopo di evitare che si possano ripetere.

Iniziative future

Sicurezza

- Si decide di organizzare una GdS sull'analisi degli infortuni occorsi. Saranno coinvolti enti esterni neutrali (INAIL, Vigili del Fuoco) e un avvocato per presentare le ultime novità legali in tema di sicurezza. Un gruppo di lavoro preparerà una bozza di locandina.
- Ambiente
- La GdS "Le opportunità regionali per lo sviluppo di un ecosistema circolare nel settore metallurgico", organizzata con AFIL, si terrà presso Regione Lombardia a Milano in aprile 2022: si stanno definendo i partecipanti alla tavola rotonda.

CT AIM / ASSOFOND – FONDERIA (F)

(riunione telematica del 28 febbraio 2022)

Manifestazioni in corso di organizzazione

- Il presidente Caironi legge l'ultima revisione della bozza del programma del corso "Fonderia per non fonditori", che avrà una durata di 28 ore. I presenti accolgono con favore la nuova versione, sostenendo che il corso ha così assunto una struttura coerente con gli obiettivi ed i destinatari per cui è stato pensato. Si discute di alcuni dettagli relativi alle lezioni relative alle normative sui getti. Il corso si potrebbe svolgere tra maggio e giugno 2022.

Iniziative future

- Bonollo, coordinatore del corso di "Metallografia delle ghise", contatterà Bassani per definire una data di svolgimento del corso.
- La GdS sulle resine e i loro aspetti legati all'ambiente ha per ora suscitato una risposta limitata tra i produttori di resine. Si decide di coinvolgere nell'iniziativa anche altri esperti per ottenere un sufficiente numero di presentazioni.

Normativa / Standards

Norme pubblicate e progetti in inchiesta (aggiornamento all'8 marzo 2022)

Norme UNSIDER pubblicate da UNI nel mese di febbraio 2022

UNI EN ISO 2566-2:2022
Acciaio - Conversione dei valori di allungamento - Parte 2: Acciai austenitici

UNI EN ISO 2566-1:2022
Acciaio - Conversione dei valori di allungamento - Parte 1: Acciai al carbonio e basso legati

UNI EN 17415-3:2022
Tubi di raffrescamento - Sistemi bloccati di tubi singoli per reti di acqua fredda interrati - Parte 3: Gruppo valvola in acciaio realizzato in fabbrica per tubo di servizio in acciaio o plastica, isolamento termico in poliuretano e guaina esterna in polietilene

UNI EN 17415-2:2022
Tubi per teleraffrescamento - Sistemi bloccati di tubi singoli per reti di acqua fredda interrati - Parte 2: Raccordi di tubi di servizio in acciaio o plastica realizzati in fabbrica, isolamento termico in poliuretano e guaina esterna in polietilene

UNI EN 10264-2:2022
Filo di acciaio e relativi prodotti - Filo di acciaio per funi - Parte 2: Filo di acciaio non legato trafilato a freddo per funi per applicazioni generali.

Norme UNSIDER pubblicate da CEN e ISO nel mese di febbraio 2022

ISO 16573-2:2022
Steel — Measurement method for the evaluation of hydrogen embrittlement resistance of high-strength steels — Part 2: Slow strain rate test

ISO 15211:2022
Steel sheet, twin-roll cast, zinc-coated by the continuous hot-dip process, of structural quality and high strength

ISO 15208:2022
Continuous hot-dip zinc-coated twin-roll cast steel sheet of commercial quality

ISO 15179:2022
Hot-rolled twin-roll cast steel sheet of structural quality and high strength steel

Progetti UNSIDER messi allo studio dal CEN (Stage 10.99) – febbraio 2022

prEN 12560-1 rev
Flanges and their joints - Gaskets for Class-designated flanges - Part 1: Non-metallic flat gaskets with or without inserts

prEN 1514-1 rev
Flanges and their joints - Dimensions of gaskets for PN-designated flanges - Part 1: Non-metallic flat gaskets with or without insert

Progetti UNSIDER in inchiesta prEN e ISO/DIS – febbraio 2022

prEN – progetti di norma europei

prEN ISO19901-5
Petroleum and natural gas industries - Specific requirements for offshore structures - Part 8: Marine soil investigations (ISO/DIS 19901-8:2021)

prEN ISO 13704
Petroleum, petrochemical and natural gas industries - Calculation of heater-tube thickness in petroleum refineries (ISO/DIS 13704:2021)

prEN ISO 12736-1
Petroleum and natural gas industries - Wet thermal insulation systems for pipelines and subsea equipment - Part 1: Validation of materials and insulation systems (ISO/DIS 12736-1:2021)

prEN ISO 12736-2
Petroleum and natural gas industries - Wet thermal insulation systems for pipelines and subsea equipment - Part 2: Qualification processes for production and application procedures (ISO/DIS 12736-2:2021)

prEN ISO 12736-3
Petroleum and natural gas industries - Wet thermal insulation systems for pipelines and subsea equipment - Part 3: Interfaces between systems, field joint system, field repairs and prefabricated insulation (ISO/DIS 12736-3:2021)

prEN ISO 19905-3
Petroleum and natural gas industries - Site-specific assessment of mobile offshore units - Part 3: Floating units (ISO 19905-3:2021)

prEN ISO 19905-1
Petroleum and natural gas industries - Site-specific assessment of mobile offshore units - Part 1: Jack-ups (ISO/DIS 19905-1:2022)

prEN 1092-3
Flanges and their joints - Circular flanges for pipes, valves, fittings and accessories, PN designated - Part 3: Copper alloy flanges

prEN 1759-3
Flanges and their joints - Circular flanges for pipes, valves, fittings and accessories, Class designated - Part 3: Copper alloy flanges

prEN 1759-4
Flanges and their joints - Circular flanges for pipes, valves, fittings and accessories,

Class designated - Part 4: Aluminum alloy flanges

prEN 15542
Ductile iron pipes, fittings and accessories - External cement mortar coating for pipes - Requirements and test methods

prEN 17800
Life cycle cost (LCC) and Life cycle assessment (LCA) for ductile iron pipe systems

prEN ISO 16808
Metallic materials - Sheet and strip - Determination of biaxial stress-strain curve by means of bulge test with optical measuring systems (ISO/FDIS 16808:2021)

prEN ISO 3785
Metallic materials - Designation of test specimen axes in relation to product texture (ISO/DIS 3785:2022)

prEN ISO 14556
Metallic materials - Charpy V-notch pendulum impact test - Instrumented test method (ISO/DIS 14556:2022)

prEN 10278
Dimensions and tolerances of bright stainless and other cold drawn steel products

ISO/DIS – progetti di norma internazionali

ISO/DIS 24139-2
Petroleum and natural gas industries — Corrosion resistant alloy clad bends and fittings for pipeline transportation system — Part 2: Clad fittings

ISO/DIS 21826-1
Iron ores — Determination of total iron content — EDTA photometric titration method — Part 1: Microwave digestion method

ISO/DIS 19905-1
Petroleum and natural gas industries — Site-specific assessment of mobile offshore units — Part 1: Jack-ups

ISO/DIS 19901-8
Petroleum and natural gas industries — Specific requirements for offshore structures — Part 8: Marine soil investigations

ISO/DIS 14556
Metallic materials — Charpy V-notch pendulum impact test — Instrumented test method

ISO/DIS 12736-1
Petroleum and natural gas industries — Wet thermal insulation systems for pipelines and subsea equipment — Part 1: Validation of materials and insulation systems

ISO/DIS 12736-2
Petroleum and natural gas industries — Wet thermal insulation systems for pipelines and subsea equipment — Part 2: Qualification processes for production and application procedures

ISO/DIS 12736-3
Petroleum and natural gas industries — Wet thermal insulation systems for pipelines and subsea equipment — Part 3: Interfaces between systems, field joint system, field repairs and prefabricated insulation

ISO/DIS 3785
Metallic materials — Designation of test specimen axes in relation to product texture

Progetti UNSIDER al voto FprEN e ISO/FDIS – febbraio 2022

FprEN – progetti di norma europei

FprEN ISO 10113
Metallic materials - Sheet and strip - Determination of plastic strain ratio (ISO/FDIS 10113:2019)

ISO/FDIS – progetti di norma internazionali

ISO/FDIS 24200
Petroleum, petrochemical and natural gas industries — Bulk material for offshore projects — Pipe support

ISO/FDIS 23991
Irrigation applications of ductile iron pipelines — Product design and installation

ISO/FDIS 13503-3
Petroleum and natural gas industries — Completion fluids and materials — Part 3: Testing of heavy brines

ISO/PRF 11257
Iron ores for shaft direct-reduction feedstocks — Determination of the low-temperature reduction-disintegration index and degree of metallization

ISO/FDIS 4968
Steel — Macrographic examination by sulfur print (Baumann method)

39 aim convegno nazionale

Padova, 21-23 settembre 2022

www.aimnet.it/nazionaleaim

AIM annuncia la **39a edizione del proprio Convegno Nazionale**, che avrà luogo nel settembre 2022 a Padova, in concomitanza con le celebrazioni degli 800 anni dell'Università. Il Convegno Nazionale AIM è l'iniziativa di riferimento per tecnici d'azienda, ricercatori e accademici che lavorano in campo metallurgico. L'edizione 2022 del Convegno acquista un particolare significato alla luce della ripresa post-pandemica e del ruolo sempre più strategico e trasversale che le discipline metallurgiche giocano nell'ambito della transizione ecologica, della mobilità sostenibile, dell'economia circolare, delle performance sempre più elevate richieste a qualsiasi componente meccanico.

Gli interessati a presentare memorie tecniche/scientifiche dovranno inviare **entro il 31 marzo 2022**, il titolo della memoria, i nomi degli autori ed un breve sommario. Maggiori informazioni sono disponibili sul sito dell'evento: **www.aimnet.it/nazionaleaim**

Organizzato da

ASSOCIAZIONE ITALIANA DI METALLURGIA

in collaborazione con

1222·2022 800 ANNI — UNIVERSITÀ DEGLI STUDI DI PADOVA — dtg — DIPARTIMENTO DI INGEGNERIA INDUSTRIALE

con il patrocinio di

AMAFOND — ASSOFOND ASSOCIAZIONE ITALIANA FONDERIE — 33 bimu fieramilano — FONDAZIONE UCIMU